REPORT
193

A SEISMIC INTERPRETATION OF THE BROOME PLATFORM, WILLARA SUB-BASIN AND MUNRO ARCH OF THE CANNING BASIN, WESTERN AUSTRALIA

by Y Zhan

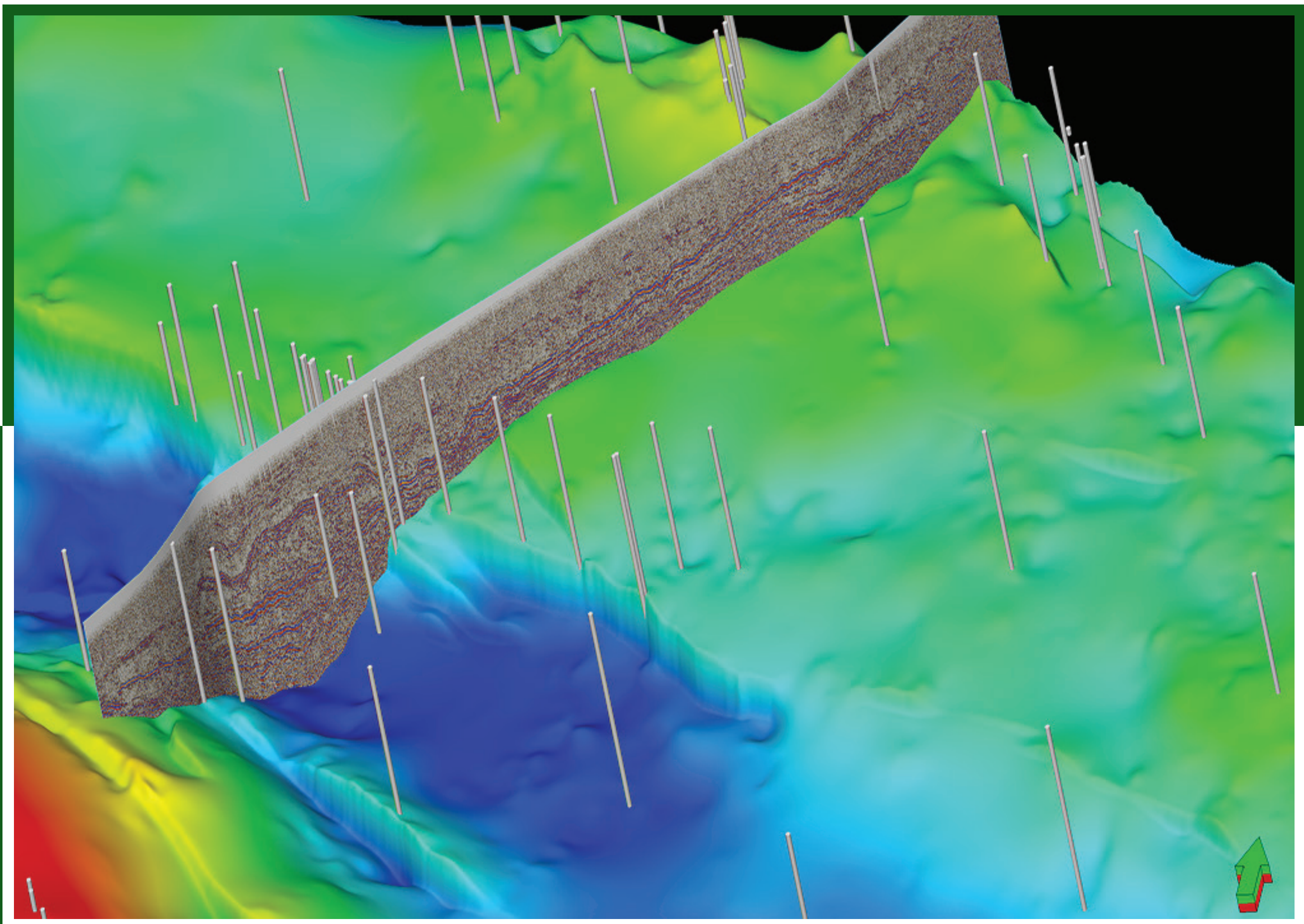

Government of Western Australia
Department of Mines, Industry Regulation and Safety

Geological Survey of Western Australia

Government of **Western Australia**
Department of **Mines, Industry Regulation and Safety**

REPORT 193

A SEISMIC INTERPRETATION OF THE BROOME PLATFORM, WILLARA SUB-BASIN AND MUNRO ARCH OF THE CANNING BASIN, WESTERN AUSTRALIA

by
Y Zhan

PERTH 2019

Geological Survey of Western Australia

MINISTER FOR MINES AND PETROLEUM
Hon Bill Johnston MLA

DIRECTOR GENERAL, DEPARTMENT OF MINES, INDUSTRY REGULATION AND SAFETY
David Smith

EXECUTIVE DIRECTOR, GEOLOGICAL SURVEY AND RESOURCE STRATEGY
Jeff Haworth

REFERENCE
The recommended reference for this publication is:
Zhan, Y 2019, A seismic interpretation of the Broome Platform, Willara Sub-basin and Munro Arch of the Canning Basin, Western Australia: Geological Survey of Western Australia, Report 193, 43p.

ISBN 978-1-74168-863-4
ISSN 1834-2280

NATIONAL LIBRARY OF AUSTRALIA
A catalogue record for this book is available from the National Library of Australia

Grid references in this publication refer to the Geocentric Datum of Australia 1994 (GDA94). Locations mentioned in the text are referenced using Map Grid Australia (MGA) coordinates, Zone 51. All locations are quoted to at least the nearest 100 m.

Disclaimer
This product was produced using information from various sources. The Department of Mines, Industry Regulation and Safety (DMIRS) and the State cannot guarantee the accuracy, currency or completeness of the information. Neither the department nor the State of Western Australia nor any employee or agent of the department shall be responsible or liable for any loss, damage or injury arising from the use of or reliance on any information, data or advice (including incomplete, out of date, incorrect, inaccurate or misleading information, data or advice) expressed or implied in, or coming from, this publication or incorporated into it by reference, by any person whosoever.

Published 2019 by the Geological Survey of Western Australia
This Report is published in digital format (PDF) and is available online at <www.dmp.wa.gov.au/GSWApublications>.

© State of Western Australia (Department of Mines, Industry Regulation and Safety) 2019

With the exception of the Western Australian Coat of Arms and other logos, and where otherwise noted, these data are provided under a Creative Commons Attribution 4.0 International Licence. (http://creativecommons.org/licenses/by/4.0/legalcode)

Further details of geoscience publications are available from:
Information Centre
Department of Mines, Industry Regulation and Safety
100 Plain Street
EAST PERTH WESTERN AUSTRALIA 6004
Telephone: +61 8 9222 3459 Facsimile: +61 8 9222 3444
www.dmp.wa.gov.au/GSWApublications

Cover photograph: 3D illumination of the seismic interpretation for the Broome Platform and Willara Sub-basin

Contents

Abstract 1
Introduction 1
Regional geology 4
Data description 4
    Petroleum wells and mineral drillholes 4
    Seismic dataset 4
Tectonic elements 8
    Broome Platform 8
    Willara Sub-basin 9
    Munro Arch 10
Seismic interpretation 11
    Top basement (Appendix 3, Maps 1–4) 12
    Top Nambeet Formation (Appendix 3, Maps 5–9) 13
    Top Willara Formation (Appendix 3, Maps 10–14) 19
    Top Goldwyer Formation (Appendix 3, Maps 15–19) 20
    Top and base of Minjoo and Mallowa Salts (Appendix 3, Maps 20–37) 22
    Base Grant–Reeves unconformity (Appendix 3, Maps 38–42) 31
    Fitzroy Transpression unconformity (Appendix 3, Maps 43–46) 32
Discussion and conclusion 34
Acknowledgement 39
References 39

Figures

1. Tectonic elements and seismic lines in the study area 2
2. Petroleum wells and mineral drillholes in the study area 3
3. Stratigraphy of the Canning Basin 5
4. Maps of available seismic data categorized by age and quality 6
5. Seismic line MA69-L in the Willara Sub-basin, before and after reprocessing 7
6. Comparison on the seismic stacking velocity of the same seismic profile (M2-71-V) 9
7. Seismic mis-ties across different seismic surveys 10
8. Erroneous seismic signatures caused by line navigation 11
9. Synthetic seismograms for Parda 1 and Sharon Ann 1 14
10. Synthetic seismograms for Willara 1 and Pegasus 1 15
11. Southwest–northeast seismic interpretation from Pittston SD 1 to East Crab Creek 1 16
12. Southwest–northeast seismic interpretation from Calamia 1 to Mahe 1 17
13. Southwest–northeast seismic interpretation from Munro 1 to Lovells Pocket 1 18
14. Southwest–northeast and northwest–southeast interpreted geological sections 22
15. Seismic interpretation across Calamia 1 and Samphire Marsh 1 23
16. Map of elevation onshore and water depth offshore 24
17. Seismic interpretation across the ABFZ 25
18. Seismic interpretation from Parda 1 to Great Sandy 1 26
19. Seismic interpretation across Pegasus 1 27
20. Well correction from Samphire Marsh 1 to Roebuck Bay 1 28
21. Seismic interpretation in the offshore area 29
22. Seismic interpretation around the present-day salt margins 30
23. Seismic interpretation within the inner area of the salt deposition 31
24. Schematic diagram for salt deposition 33
25. Salt withdrawal and associated structures beyond the present-day salt margin 33
26. Schematic diagram for salt dissolution in the southern Canning Basin 36
27. Modern salt lakes in the southern Canning Basin 37
28. Seismic interpretation in the area affected by salt movements 38

Table

1. Two types of cycles showing lithological and mineralogical composition of the Mallowa Salt 22

Appendices

The Appendices are available on the accompanying zip file

1. Summary of key horizons for petroleum wells and mineral drillholes 43
2. Available seismic surveys in the Broome Platform, Willara Sub-basin and Munro Arch area 43
3. Maps from seismic interpretation 43

A seismic interpretation of the Broome Platform, Willara Sub-basin and Munro Arch of the Canning Basin, Western Australia

by

Y Zhan

Abstract

A number of subsurface faults and horizons, ranging from Top basement to the Mesozoic Fitzroy Transpression unconformity, is mapped for the Broome Platform, Willara Sub-basin, and Munro Arch of the Canning Basin based on integration of data from petroleum wells, mineral drillholes and seismic profiles. Most of west-northwest to northwesterly oriented faults show growth components and displacement in the Ordovician succession but terminate below the Base Grant–Reeves unconformity, representing the initial phase of subsidence in a northwesterly striking orientation. The easterly to east-northeasterly oriented faults generally displace the strata from Ordovician to Permian and are interpreted to have formed during the Carboniferous–Permian extension.

Horizons selected for seismic interpretation can be categorized into three groups: 1) top of the basement and horizons within the Ordovician section; 2) tops and bases of salt intervals; and 3) angular unconformities at the bases of the Permo-Carboniferous and Jurassic successions. The first group of horizons, generally conformable to each other, deepens from the southwest margin of the Willara Sub-basin and Munro Arch towards the northeast and reaches maximum depth just south of the Admiral Bay Fault Zone. The Minjoo and Mallowa Salts within the second group are interpreted to be present in the northeastern Willara Sub-basin, southeastern Broome Platform and most of the Munro Arch. The Minjoo Salt is less aerially extensive compared with the Mallowa Salt within the study area. The two major angular unconformities in the third group are much less faulted and have reduced structural variation compared with the underlying formations, and they shallow inland towards the southeast.

KEYWORDS: Canning Basin, Mesozoic, Paleozoic, seismic interpretation

Introduction

The Broome Platform and Willara Sub-basin have been lightly explored for petroleum and Mississippi Valley-type lead–zinc deposits. Recent interpretations by industry have mostly been conducted within their exploration permits thus were relatively small scale (e.g. Williams and Harvey, 1989; Rudge, 2011). Historical regional mapping of this area, prior to this project, was completed more than 20 years ago (top Ordovician by Iasky et al., 1991; base Grant Group by Taylor et al., 1991; depth to base Phanerozoic by Romine et al., 1994 and Copp, 1994) and requires updates to incorporate new datasets. Since those studies, exploration by the industry and geological investigation by Commonwealth and State Governments has provided a large amount of new data, including wells (e.g. Sharon Ann 1, Robert 1, Looma 1, Olympic 1, Theia 1; Appendix 1) and seismic profiles (e.g. Great Sandy 1998 survey, Commodore East 2011 survey, Canning Coastal 2014 survey; Appendix 2). In addition to the data brought by seismic acquisition, reprocessing has improved the quality of vintage data (e.g. the Thangoo 1984 survey reprocessed in 2004, Willara 1987 survey reprocessed in 2010; Appendix 2) and have added more information to the dataset. The seismic data in the Broome Platform and Willara Sub-basin are of reasonable quality and therefore provide an opportunity for interpretation of some major faults and key stratigraphic horizons.

This Report is the second mapping project for the southern Canning Basin following publication of the Report on the southwestern area (Zhan, 2018). The aim of this project is to delineate the structure and stratigraphy of the Broome Platform, Willara Sub-basin and Munro Arch. The study area (Fig. 1) lies in the VISSCHER, LAGRANGE, MOUNT ANDERSON, MANDORA, MUNRO, MCLARTY HILLS, YARRIE, ANKETELL and JOANNA SPRING 1:250 000 map sheets and geographically spans latitude 18°S to 20.4°S, and longitude 121.1°E to 124.4°E. Through the integration of seismic profiles (Fig. 1), petroleum wells, mineral drillholes (Fig. 2) and surface geological mapping, this Report aims to improve delineation of the regional structural elements and map the key stratigraphic horizons within the southern Canning Basin, including Top basement, tops of key Lower Ordovician formations, tops and bases of two salt intervals (Mallowa and Minjoo Salts), and two pronounced unconformities (Base Grant–Reeves Formation and the Fitzroy Transpression unconformities). The maps generated in this study exclude the Jurgurra Terrace and northern part of Mowla Terrace where the Paleozoic successions and Top basement seismic horizons are severely obscured by poor-quality data.

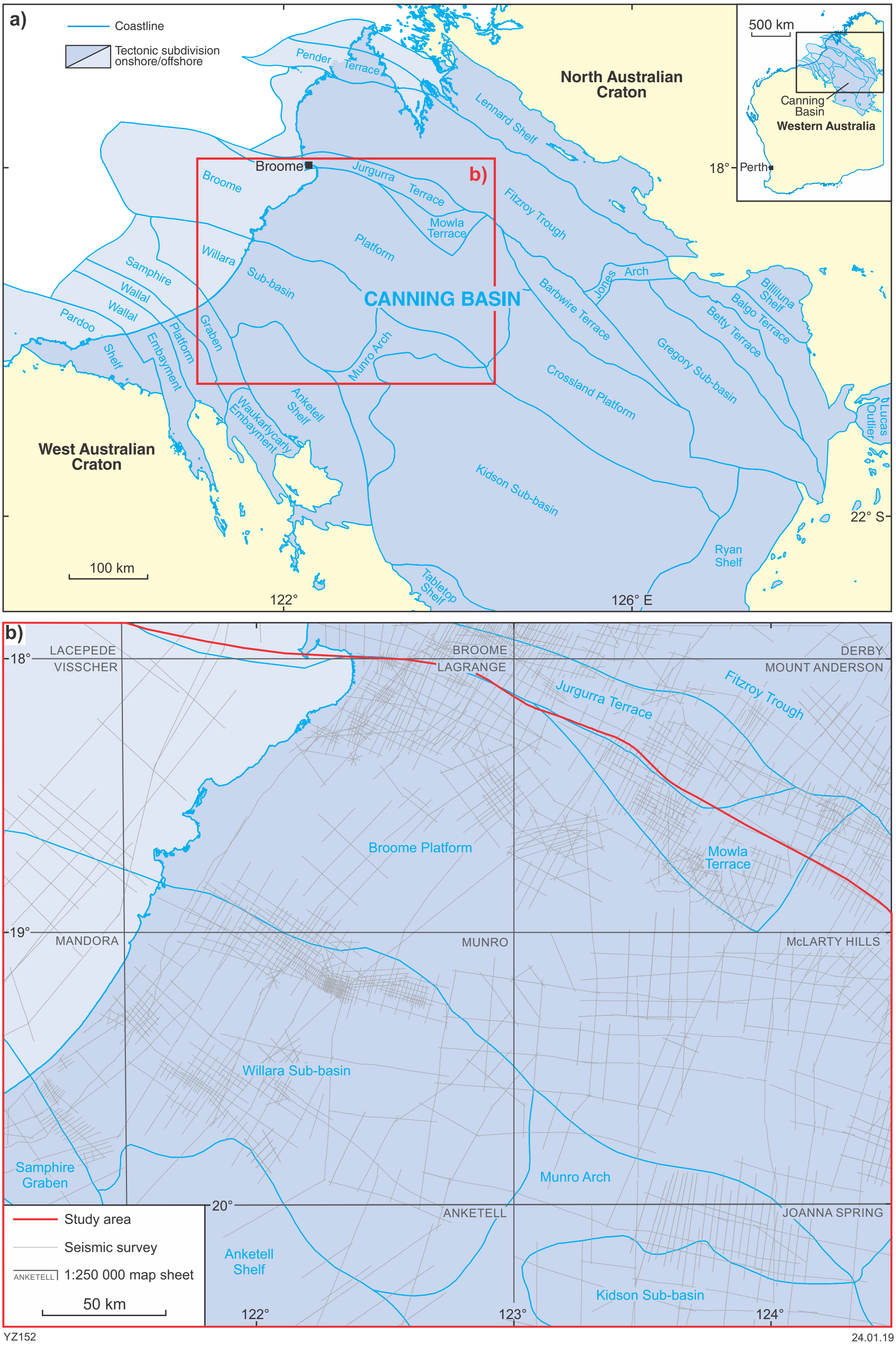

Figure 1. Tectonic elements and seismic lines in the study area: a) tectonic elements of the Canning Basin (GSWA, 2017); b) study area showing 1:250 000 map sheets and distribution of seismic data

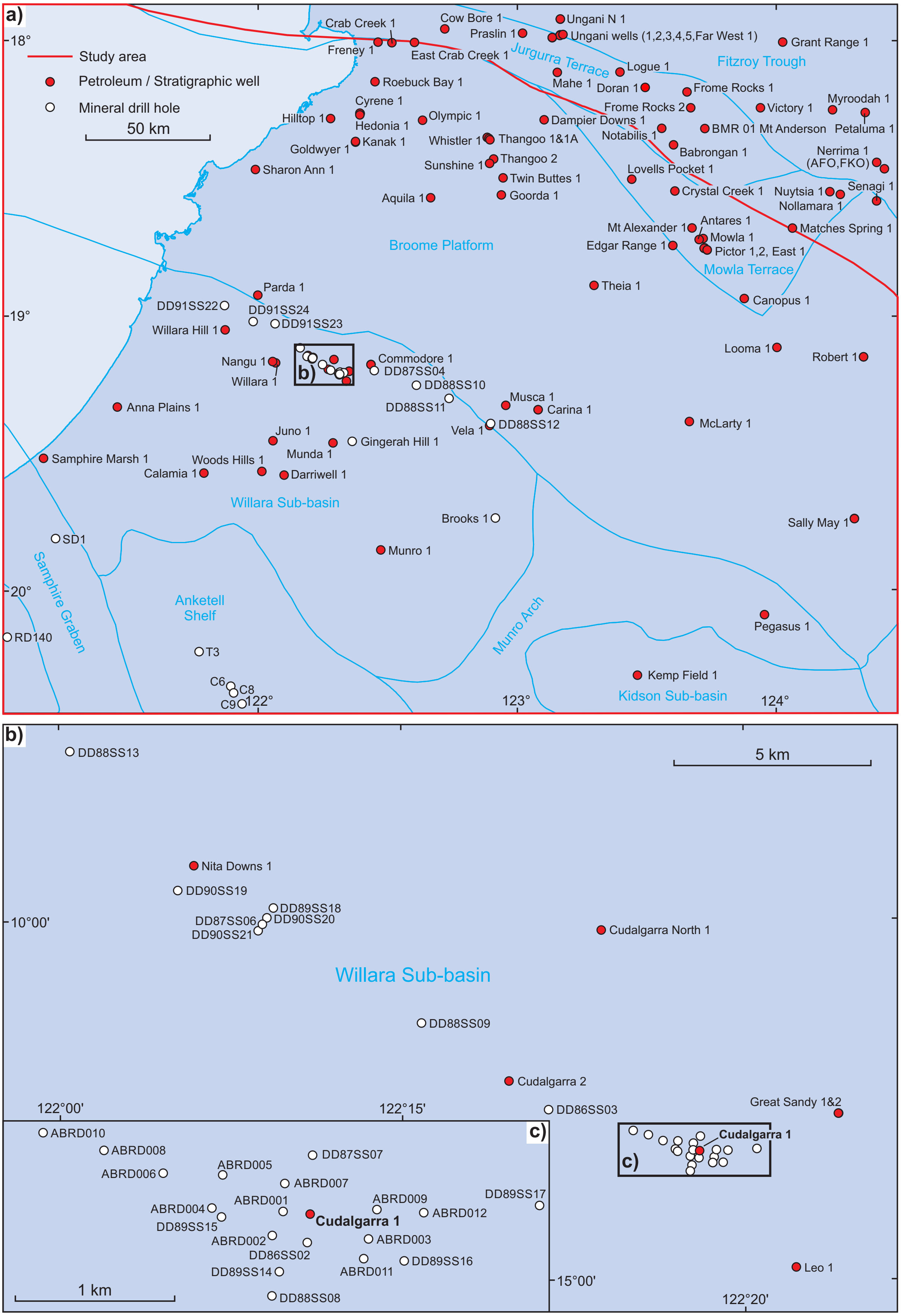

YZ153 05.03.19

Figure 2. **Petroleum wells and mineral drillholes in the study area: a) whole area; b) detail of drilling along part of the ABFZ; c) cluster of mineral drillholes around Cudalgarra 1**

Regional geology

The Canning Basin, a mostly onshore intracratonic basin covering 640 000 km^2, contains an Ordovician to Cretaceous sedimentary succession reaching an estimated thickness of 15 km within the Fitzroy Trough (Forman and Wales, 1981; Kennard et al., 1994). The basin is subdivided into a number of major elements (GSWA, 2017) that include: 1) an elongate northwesterly trending depocentre (the Fitzroy Trough and contiguous Gregory Sub-basin); 2) a mid-basin platform (the Broome and Crossland Platforms); and 3) southern depocentres (the Willara and Kidson Sub-basins). The periphery of the basin is flanked by the contiguous Pardoo – Anketell – Tabletop Shelves to the south, the Lennard – Billiluna Shelves to the north, and the Ryan Shelf to the east.

The stratigraphic framework (Fig. 3) of this study follows that of Haines (2009), Mory (2010), Mory and Haines (2013) and Haines et al. (2013). Based on several major angular unconformities, the Phanerozoic sequence in the Canning Basin has been divided into four megasequences with durations varying from 70 to 100 million years. The Ordovician to Middle Devonian megasequence includes the succession from the Nambeet Formation to the Mellinjerie Limestone respectively and is extensive in the south of the basin although only locally preserved on the Lennard and Billiluna shelves near the northern basin margin. The Middle Devonian to mid-Carboniferous megasequence consists of the Devonian reef complexes, the Fairfield Group and the Anderson Formation which, based on available well intersections, are only present in the northern Canning Basin. The mid-Carboniferous to Triassic megasequence incorporates the succession from the Reeves Formation and Grant Group up to the Erskine Sandstone (Fig. 3), and is laterally extensive across the basin. In general, this megasequence unconformably overlies the Middle Devonian to mid-Carboniferous megasequence in the north and the Ordovician to Middle Devonian megasequence in the south. The Jurassic to Cretaceous megasequence unconformably overlies the mid-Carboniferous to Triassic megasequence and ranges from the Wallal Sandstone to the Anketell Formation. This megasequence has a relatively uniform thickness from north to south, although it generally thins from the coastal area in the west to the middle of the basin in the east. The preserved sedimentary succession within the study area is restricted to parts of three megasequences with ages including Ordovician–Silurian, Carboniferous–Permian and Jurassic to Cretaceous.

Data description

Exploration in the study area has created a wide range of datasets from petroleum wells, mineral drillholes, and potential field and seismic surveys. Hydrogeological bores are not discussed here as most of them are less than 100 m deep and do not intersect the Permian to Ordovician succession. The geological information used in this study is open file and can be accessed from the data repositories of the Geological Survey of Western Australia (GSWA), Western Australian Petroleum and Geothermal Information Management System (WAPIMS) and Western Australian Mineral Exploration Reports (WAMEX).

Petroleum wells and mineral drillholes

Petroleum exploration over the Broome Platform and Willara Sub-basin commenced in the 1950s (e.g. Roebuck Bay 1, Goldwyer 1), and culminated in the 1980s (e.g. Great Sandy 1, Nita Downs 1, Hedonia 1) following oil discoveries on the Lennard Shelf of the northern Canning Basin. To date, more than 50 petroleum wells have been drilled throughout the study area, with most reaching Permian to Ordovician rocks (Fig. 2a; Appendix 1). Some of these wells (e.g. Cudalgarra 1 and 2) in the transitional area between the Broome Platform and Willara Sub-basin intersected base metal mineralization in carbonate rocks at depths greater than 1000 m. Subsequent mineral exploration in this area between 1986 and 2009 included 27 deep drillholes that identified significant high-grade lead and moderate-grade zinc mineralization (Fig. 2b,c; Appendix 1). Most of the petroleum wells and mineral drillholes provide downhole velocity profiles and/or sonic logs, which are used to calibrate the horizons between the Base Jurassic and Top basement onto seismic profiles, as well as constrain the velocity field along with seismic stacking velocity profiles for depth conversion.

The original formation tops from the well completion reports (e.g. Samphire Marsh 1 in Johnstone, 1961 and 1966; Munda 1 in Moyes, 1972; Juno 1 in Royal Resources, 1985a; Woods Hills 1 in Royal Resources, 1985b; Darriwell 1 in Geary and Robbie, 1989) were mainly based on lithology and wireline data thus only provide loose stratigraphic constraints. Since the drilling of these wells, the stratigraphy has been revised during regional studies, incorporating biostratigraphic data when available, to allow a basinwide understanding of depositional history (e.g. Haines, 2009; Mory, 2010). The formation tops (Appendix 1) from those regional studies with integration of best available palynology data provide a more systematic and coherent stratigraphic correlation and thus are used in this study.

Seismic dataset

The seismic data used in this project were mostly acquired between 1960 and 2000. Since then only a small number of surveys have been undertaken and become open file for this study (Appendix 2; Fig. 4a): 1) Athos survey (about 300 km; Buru Energy Ltd, 2011a) along the northern margin of the Broome Platform; 2) Commodore East survey (about 170 km; Buru Energy Ltd, 2011b); 3) Commodore West survey (about 120 km; Rea, 2014) along the northern margin of the Willara Sub-basin; and 4) central part of the Canning Coastal seismic survey (about 240 km; Zhan, 2017) between Samphire Marsh 1 and Roebuck Bay 1. Some nearshore seismic profiles are also included to delineate the structural extension of the offshore portions of the Broome Platform and Willara Sub-basin. Overall, the seismic coverage is patchy with a large number of seismic lines clustered in the area between the two tectonic elements where the grid spacing ranges from 1 to 3 km. However, seismic surveys elsewhere are generally very sparse with an average line spacing around 20 km to the southwest of Goldwyer 1, Aquila 1 and Theia 1 in the central part of the Broome Platform, as well as southeast of Gingerah Hill 1 in the Willara Sub-basin and Munro Arch.

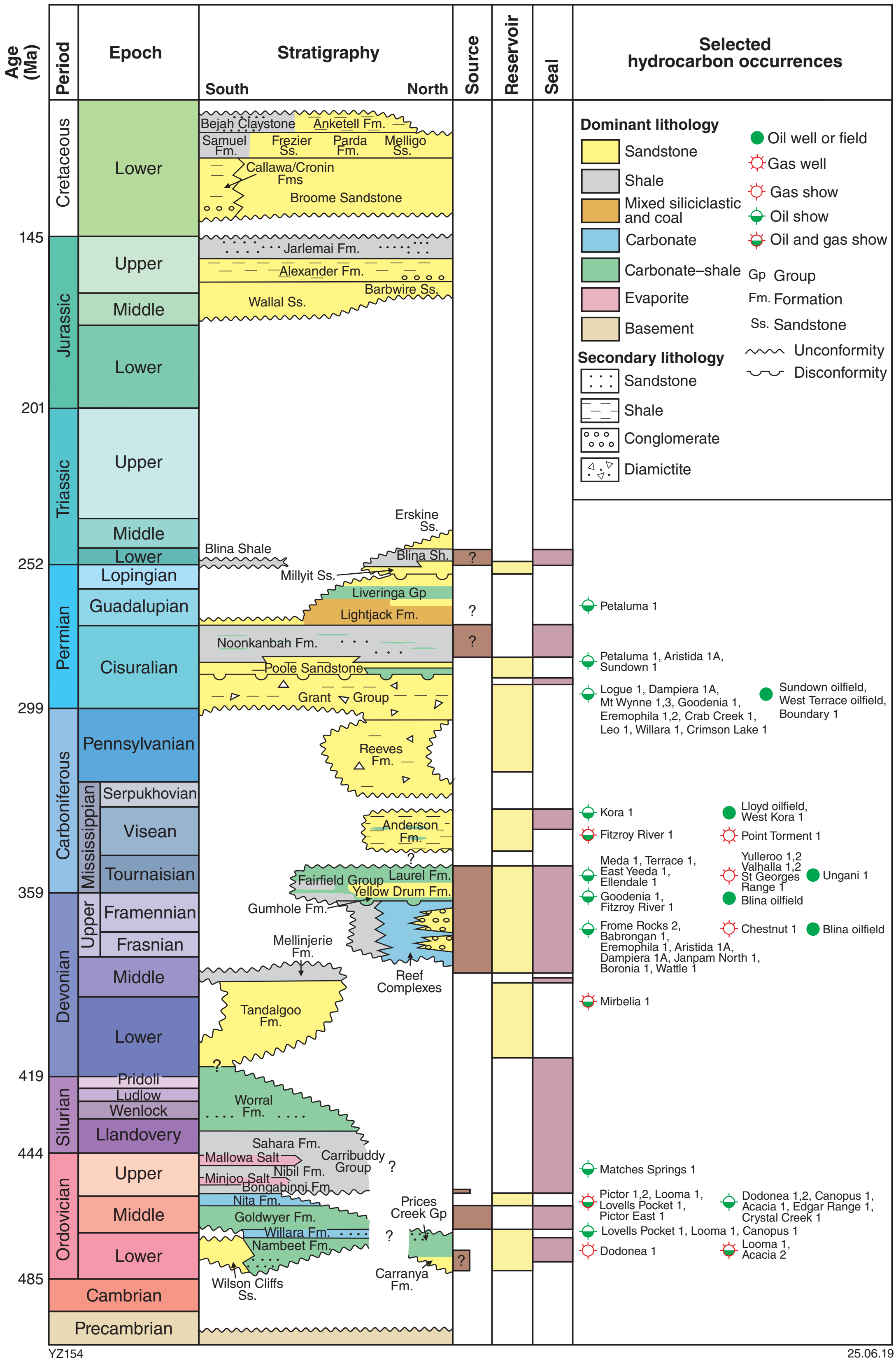

Figure 3. Stratigraphy of the Canning Basin (modified from Haines, 2009; Mory, 2010; Mory and Haines, 2013; Haines et al., 2013)

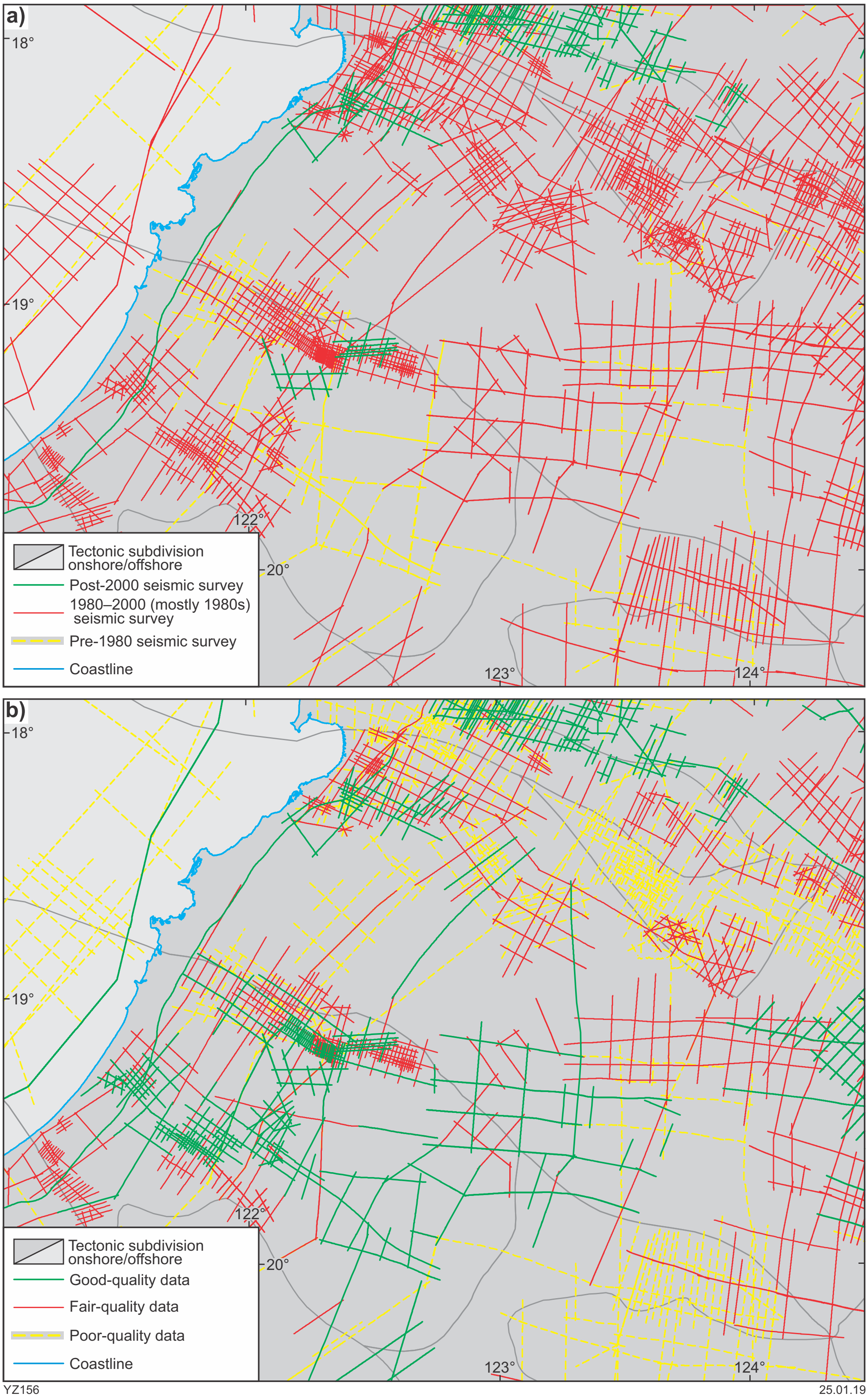

Figure 4. Available seismic data for the study area, shown by: a) age; b) profile quality

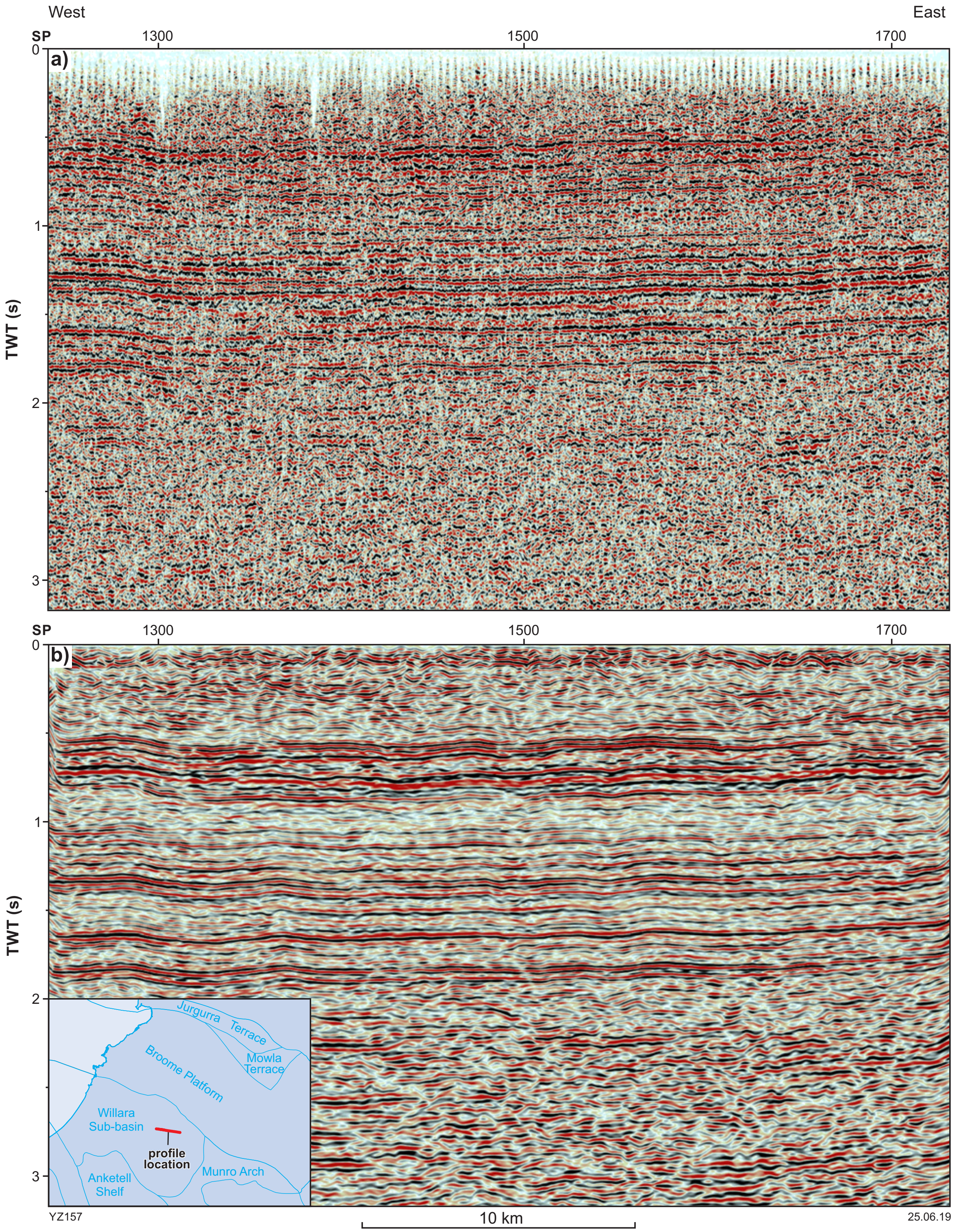

Figure 5. Seismic line MA69-L in the Willara Sub-basin: a) before; b) after reprocessing

Data quality varies from poor to good, and generally has improved in recently acquired surveys mainly due to their higher fold coverage (Fig. 4b; Appendix 2). For example, the S91C, S92C and Great Sandy 1998 surveys show good quality in the southeast of the Broome Platform where the lowermost stratigraphic units and salt tectonics are clearly imaged. By comparison, some vintage surveys, such as Munro R1 1969, Samphire 1970 and BMR Canning Basin 1988, are of insufficient quality in their originally processed versions, although have been significantly improved by seismic reprocessing in recent times (Fig. 5). For some surveys, the improvement by reprocessing is still marginal due to limitations in the original acquisition settings, including folds, source energy types and spread patterns.

The seismic reprocessing provides a different perspective to understand the uncertainties in structure and velocity. Some small structural folds on the originally processed sections were absent after reprocessing, indicating these apparent small-scale structures were probably artefacts caused by static miscorrection or incorrect salt velocity applied during the original processing. These artificial structures may require a certain level of filtering and smoothing to map the horizons. Furthermore, each reprocessing has also led to substantial differences in stacking velocities of the same 2D seismic lines (e.g. Fig. 6). This implies that a combination of stacking velocities from different sources will not reflect true variations of the velocity across different profiles. As a result, well velocity data from both checkshots and sonic logs are more robust than stacking velocities in establishing a velocity field for depth conversion.

The seismic datum across the different surveys varies and requires systematic adjustments before interpretation (Fig. 7; Appendix 2). For example, the 2015 processed data of the Canning Coastal survey has a datum of 200 m above mean sea level (MSL) to preserve the seismic reflections from shallow Mesozoic and Cenozoic strata (DownUnder Geosolutions, 2015). This type of preservation of seismic reflection commonly applies to the surveys farther inland where the surface elevation is much higher than MSL, for example 100 m above MSL used for reprocessing the Munro Arch 1969 survey in 2010, and 200 m above MSL for reprocessing the Great Sandy 1988 survey (Dayboro Geophysical, 2010). Based on their processing datum and replacement velocity, the various original datums have been corrected to a final datum of MSL to enable a consistent seismic correlation across the study area (Appendix 2). This correlation can also help identify some erroneous signatures caused by navigation (Fig. 8), and avoid invalid interpretation of faults on the seismic profiles.

Tectonic elements

Based on the tectonic subdivision of the Canning Basin (Fig. 1), the study area contains a number of mostly northwesterly trending tectonic elements defined by lateral differences in the preserved stratigraphy and structural setting (Hocking, 1994a,b). However, the boundaries of these elements have in the past been loosely constrained due to a lack of data that precluded a systematic interpretation of this area. The present study shows that some of the original boundaries are incorrectly located (Hocking, 1994a,b), thus the tectonic element boundaries labelled on the seismic profiles in this Report do not strictly correspond to their original positions.

Broome Platform

The Broome Platform is the northwest portion of a basement high located in the central part of the Canning Basin. It has also been termed the Broome Ridge (Wells, 1960), Broome Swell (Veevers and Wells, 1961), and Broome Arch (Towner and Gibson, 1983). This northwest-trending platform contains a relatively thin Paleozoic section compared with surrounding tectonic elements: the Jurgurra, Mowla and Barbwire Terraces to the north, and the Willara Sub-basin and Munro Arch to the south (Hocking, 1994a,b).

The interpretation of stratigraphic units on the Broome Platform are constrained by petroleum wells including Goldwyer 1, Sharon Ann 1, Parda 1, McLarty 1, and others. The intersections in these wells indicate that sedimentation on the Broome Platform commenced in the Early Ordovician with a sequence of marine deposits. The Lower to Middle Ordovician sequence generally thins towards the margins of the platform, and includes a basal conglomerate, sandstone and shale unit (Nambeet Formation, up to 350 m thick), a carbonate section (Willara Formation, ~200 to 400 m thick), a shale unit with a middle carbonate member (Goldwyer Formation, ~150 to 400 m thick) and an interbedded limestone, shale and dolomite unit (Nita Formation, up to 200 m thick).

The Upper Ordovician to Silurian sequence thickens towards the southeast of the Broome Platform and is absent in the northwest towards the coast. Well penetrations of this sequence reviewed by Haines (2009) include a thick succession of fine-grained clastic rocks and evaporites interbedded with minor sandstone and carbonate rocks (Carribuddy Group, up to 1050 m thick, consisting of two prominent thick halite units – Mallowa and Minjoo Salts), and an overlying succession of shale and sandstone with interbeds of dolomite and limestone (Worral Formation, up to 265 m thick).

The Permo-Carboniferous sequence unconformably overlies the Lower to Middle Ordovician rocks in the northwest and Upper Ordovician to Silurian sediments in the southeast of the Broome Platform. The overlying sequence ranges from 200 to 500 m in thickness, and mainly includes fluvial to marine glacigene siliciclastic rocks (Grant Group, averaging 350 m thick) and a predominantly deltaic to marine sandstone (Poole Sandstone, up to 100 m thick along the northern margin of the platform).

Younger units resting unconformably on the Permian sequence are mostly Jurassic and Cretaceous in age. This shallow cover includes fluvial to shallow-marine sandstones interbedded with shales and minor carbonate rocks (Wallal Sandstone, Alexander and Jarlemai Formations, Broome Sandstone and other units). Along the strike of the Broome Platform the total thickness of this sequence varies significantly, from approximately 600 m in the northwest coastal area to less than 50 m or even absent inland to the southeast.

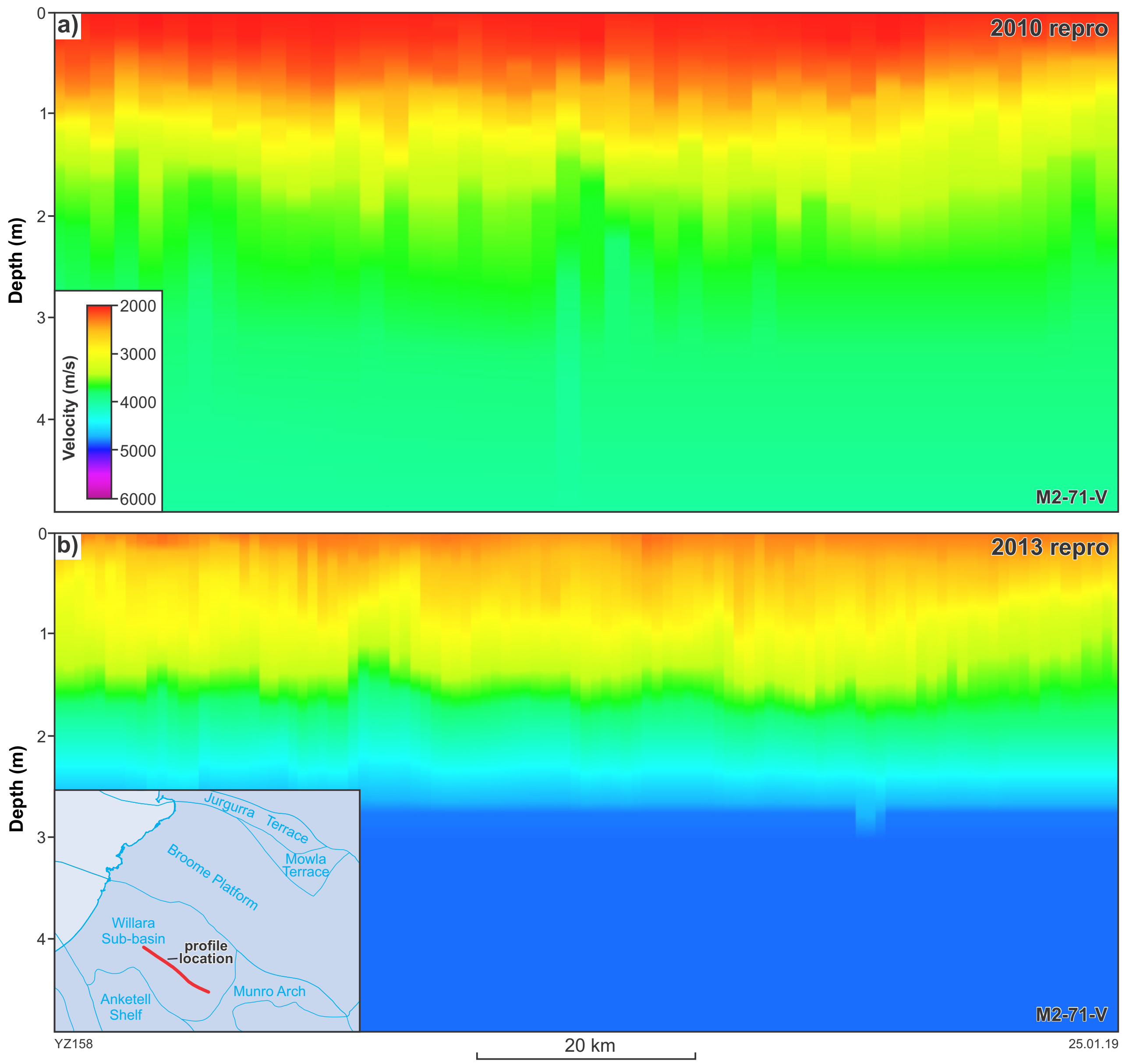

Figure 6. Comparison of seismic stacking velocity within the same colour range along the same seismic profile (M2-71-V) after different reprocessing by: a) Dayboro Geophysical (2010); b) DownUnder Geosolutions (2013). The differences indicate difficulties in merging the stacking velocities from different sources to reflect true velocity trend

Willara Sub-basin

Prior to drilling activities in this region, the Willara Sub-basin was known as the Lagrange Platform based on several southeast-trending Bouguer anomalies (Quilty, 1960; Veevers and Wells, 1961; Flavelle and Goodspeed, 1962). Veevers and Wells (1961) interpreted a slightly deeper basement transitioning from the elevated 'Broome Swell' to the north and 'Samphire Depression' to the south. Following initial seismic reflection and drilling explorations, the name of this tectonic element was revised to the Parda Sub-basin (Dennison, 1964; Williams, 1965; Johnson, 1966b) to signify a relatively deeper basement than the surrounding domains. The name was changed to Willara Sub-basin and recognized as one of the two basement depressions of the southern Canning Basin during further exploration activities (e.g. Moyes, 1972; Schroder et al., 1986) which confirmed a deep basement and a fault boundary to the Broome Platform.

Based on well and drillhole intersections, the Willara Sub-basin is mostly infilled with Paleozoic and Mesozoic rocks overlying basement. This stratigraphy resembles that of the Broome Platform in age and lithology but varies significantly in thickness. The Lower to Middle Ordovician sequence generally thickens towards the northern margin of the sub-basin. Well intersections of this sequence consist of up to ~780 m of Nambeet Formation, ~530 m of Willara Formation, ~740 m of Goldwyer Formation and an average ~100 m of Nita Formation.

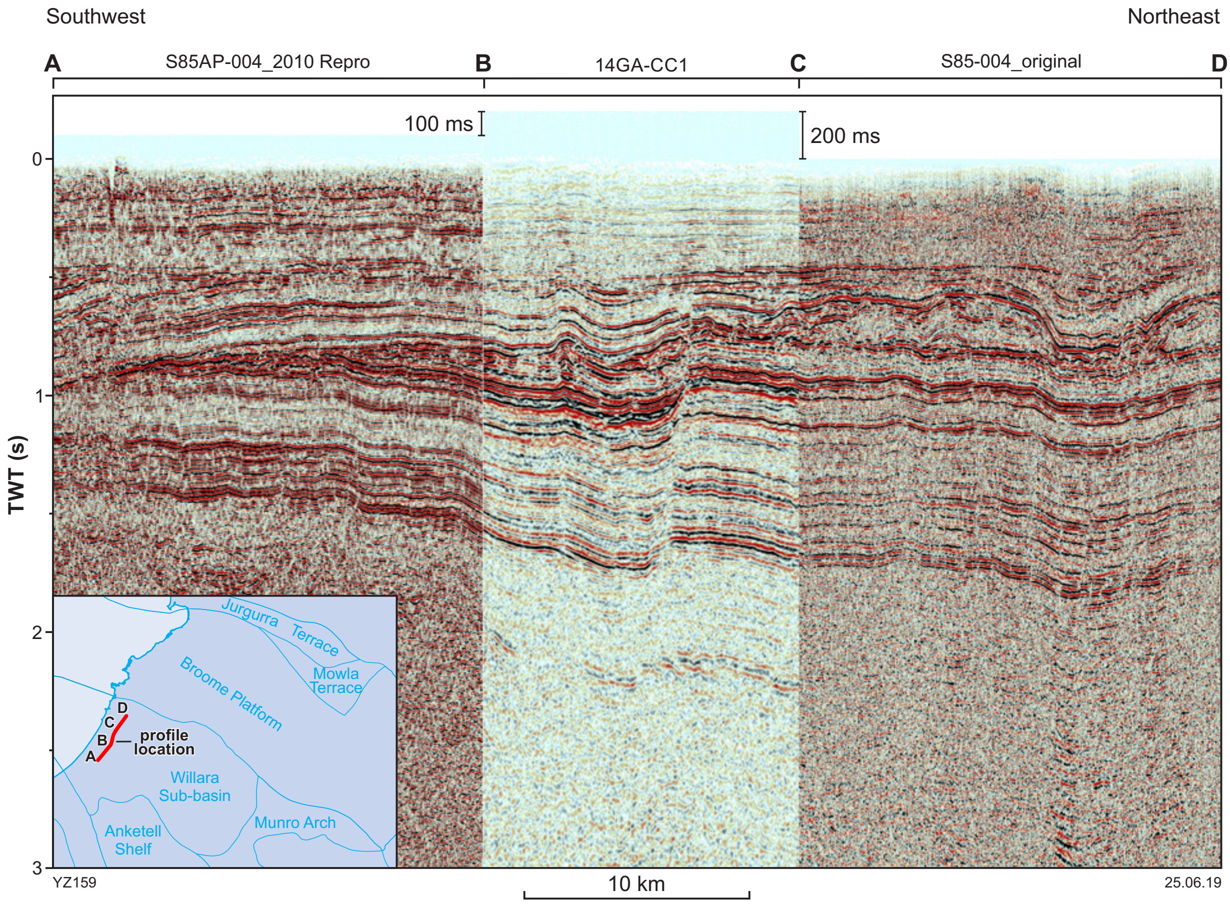

Figure 7. Composite seismic section showing examples of mis-ties across different seismic surveys

The Upper Ordovician to Silurian sequence has been intersected in the southeastern and northern parts of the Willara Sub-basin. Within the Carribuddy Group the lower unit of evaporites, the Minjoo Salt, is relatively thinner (less than 100 m) compared to the upper massive Mallowa Salt (up to 800 m). Both intervals exhibit a sporadic trend in lateral thickness variation probably due to salt mobilization and dissolution. In comparison, the intersections of the Worral Formation conformably overlying the Carribuddy Group are relatively uniform, averaging 150 m thick (Haines, 2009).

The Permo-Carboniferous sequence unconformably overlies the Lower to Middle Ordovician in the west and the Upper Ordovician to Silurian in the east and north. This sequence was generally intersected below 600 m and is restricted to the Grant Group, consisting of interbedded shale and sandstone across the Willara Sub-basin (Mory, 2010; Davies and Dorsch, 1988; BHP-Utah Minerals International Asia Pacific Division, 1988). Its thickness is highly variable, ranging from ~320 to 780 m, presumably influenced by local glacial incision, periodic salt tectonism and post-depositional erosion.

Following the Triassic to Jurassic Fitzroy Transpression (Zhan and Mory, 2013), the depocentre of the Willara Sub-basin shifted to the offshore Canning Basin, with the Jurassic to Cretaceous succession thinning inland to the southeast. The Mesozoic sequence in the Willara Sub-basin mostly includes Wallal Sandstone, Alexander and Jarlemai Formations, and Broome Sandstone, in ascending age order. The well intersections show that this sequence generally thickens from about 230 m in the southeast to ~700 m near the coastal area due to tilting towards the increased subsidence area offshore.

Munro Arch

The name Munro Arch originated from the term Munro Gravity Platform (Flavelle, 1974) that described an area of moderate Bouguer anomaly variations in the middle of the southern Canning Basin. This gravity platform extended across most of the currently defined Broome Platform, Willara Sub-basin, and overlapped the Munro Arch within the central part of an east-trending gravity high (Joanna Springs Gravity Ridge of Flavelle, 1974). The Munro Arch is about 50 km to the southeast of Munro 1 and was poorly defined, as explained by Hocking (1994b), with boundaries following the contour trends of the base of the Grant Group (Taylor et al., 1991) and the top of the Ordovician sequence (Iasky et al., 1991). As opposed to the regional Broome–Crossland Platform, this arch is relatively small scale and was presumed to have elevated basement striking northeast between the Willara and Kidson Sub-basins.

The sedimentary rocks in the Munro Arch have only been intersected in Pegasus 1 in the northeast corner of the arch. The stratigraphic penetration ranges in age from Mesozoic to Early Ordovician with basement not reached at total

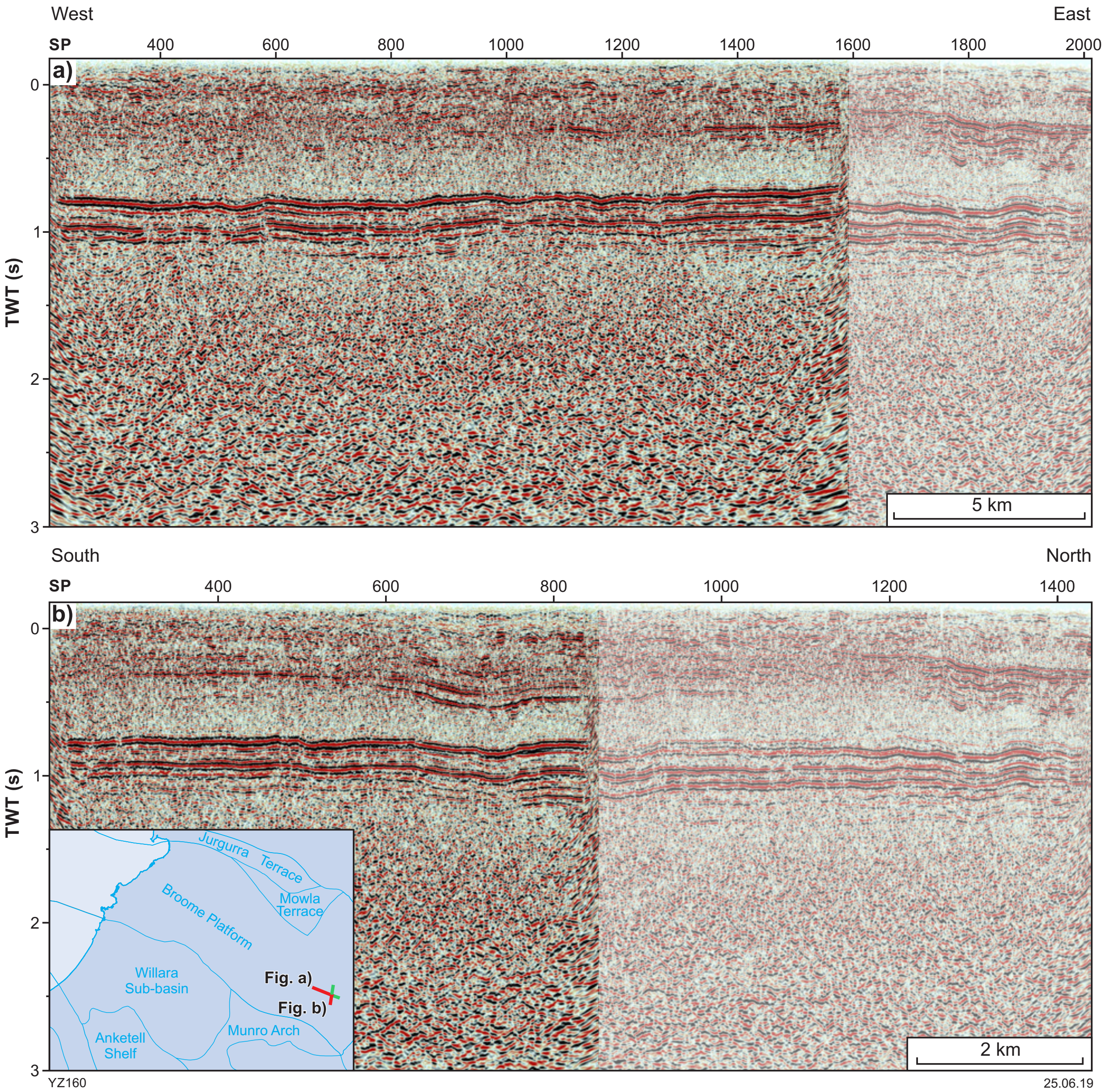

Figure 8. **Erroneous seismic signatures caused by line navigation. The right parts of both sections (displayed in lighter colour) do not belong to the lines and need to be removed for seismic interpretation**

depth (2995 m; Farrelly, 1988). The Lower to Middle Ordovician sequence was around 700 m thick, consisting of Nambeet, Willara, Goldwyer, and Nita Formations which are similar to those in the Willara Sub-basin and Broome Platform. The Upper Ordovician to Silurian sequence includes about 1000 m of the Carribuddy Group, most of which is massive halite of the Mallowa Salt, and about 200 m of the Worral Formation. Overlying this sequence, the Lower to Middle Devonian Tandalgoo Formation (Haines, 2009) and Mellinjerie Limestone (Farrelly, 1988) are about 600 m thick in total and both exhibit relatively uniform lithologies throughout this interval. The Permo-Carboniferous Grant Group unconformably overlies the Lower to Middle Devonian strata and the group consists of mostly sandstone (~200 m thick) and conglomerate (~120 m) below the Mesozoic succession.

Seismic interpretation

The seismic dataset in the study area provides opportunities to map key stratigraphic horizons through interpretation and address the uncertainties in the structural subdivision of the basin. It should be noted that the interpretation is also restricted by patchy and poor-quality seismic data (Fig. 4) and has a varying level of confidence by horizon and area. Fault correlation for each horizon is ambiguous in some areas of sparse seismic coverage.

Ten horizons have been tied to well intersections (e.g. Figs 9, 10), interpreted (e.g. Figs 11–14) and mapped (Appendix 3, Maps 1–46), including Top basement, tops of Lower Ordovician successions, boundaries of two salt intervals (Mallowa and Minjoo Salts), and two pronounced unconformities at the bases of the Permo-Carboniferous Grant Group – Reeves Formation and Jurassic successions. These two unconformities were interpreted by Kingsley and Russell (1989) as key boundaries that separate depositional history into three parts: Early Ordovician to Late Devonian, late Carboniferous to Middle Jurassic, and Middle Jurassic to present day. In the areas of deep pre-Permian erosion, the original upper parts of the Ordovician successions have been removed by the Base Grant–Reeves unconformity, such as incision down as far as the Goldwyer Formation at Hilltop 1, Willara Formation at Olympic 1, and Nambeet Formation at Samphire Marsh 1. In the partially eroded areas, the mapped Ordovician horizons are amalgamated with the Base Grant–Reeves unconformity to delineate the lateral extent of the remnant sections (see Fig. 15 for explanation). The horizons of Minjoo and Mallowa Salts were selected for interpretation based on their petroleum significance as regional seals.

Two-way time (TWT) horizons were converted to depth domain mainly using sonic log and/or checkshot data recorded in wells. As discussed in the data description section, seismic stacking velocity shows significant differences between surveys, or even between different vintages of the same profiles, as a result of being processed separately and with different processing parameters (Fig. 6). This creates great difficulties in reflecting the true velocity variations when merging stacking velocities from different sources. The datum of seismic data has been systematically adjusted to MSL, and surface elevations and bathymetry (Fig. 16; Whiteway, 2009) were taken into account for depth conversion.

Top basement (Appendix 3, Maps 1–4)

The term 'basement' used in this study refers to the Precambrian to Cambrian rocks below the Paleozoic fill of the Canning Basin. The basement intersections commonly include granitic and metasedimentary rocks (Appendix 1), which are calibrated to a zone of low-amplitude chaotic reflections and generally do not exhibit much internal structure. By comparison, the overlying Paleozoic succession is characterized by relatively high-amplitude continuous reflection. Such a strong contrast locally induces more than one reflection in its travel path and multiplicative seismic events add tails to the primary reflection, interfering with the response of the uppermost part of the basement (see basement responses below Parda 1, Hilltop 1 and Hedonia 1 in Figs 11, 17) and increasing the uncertainties in the interpretation. Therefore, Top basement is generally tracked along a strong seismic reflection that is not necessarily the very bottom of the continuous zone of reflectors due to the possibility of reflections from basement beds and multiple reflections.

Willara Sub-basin

The Top basement reflector is generally of reasonable quality, and can be correlated through some localized highly reflective events at the bottom of the layered package. The TWT to Top basement horizon in the Willara Sub-basin ranges from 0.5 s in the southwest to 2.4 s in the northeast (Map 1).

Within the northeastern margin of the Willara Sub-basin the basement has been intersected at 2319 m in Leo 1, although was not reached in deeper Willara 1. The former well is interpreted to be in the footwall of a fault block, thus does not provide a representative depth for Top basement in this area. The northwest portion of the Admiral Bay Fault Zone (ABFZ) is interpreted to consist of at least four parallel northwest-striking faults, each of which has a significant throw at Top basement level. The fault zone extends along strike to the southeast where its geometry changes to a single fault. The depth of Top basement along the strike of the ABFZ ranges from 2.4 s near Willara 1 to 1.3 s about 20 km north of Pegasus 1.

Basement rocks comprising fine- to medium-grained granitic rocks were intersected at Munro 1 (2016 m), Calamia 1 (1671 m) and Samphire Marsh 1 (2015 m) along the southwestern margin of the Willara Sub-basin. These three wells targeting potential petroleum traps in Ordovician rocks were drilled on the footwall of faulted blocks (Figs 12, 13, 15; Maps 1, 3, 4). The fault southwest of Munro 1 (Munro Fault System in Kingsley and Russell, 1989) is interpreted to extend to the southwest of Darriwell 1. This northwest-striking fault also extends to the southeast near the boundary between the Willara Sub-basin and the Munro Arch. It is parallel to the ABFZ in the north and the Anketell Fault in the south, dividing the southeast part of the Willara Sub-basin into two half-grabens both deepening towards the northeast (Fig. 13). The fault adjacent to Calamia 1 (Geary, 1988; Chirit Fault System in Kingsley and Russell, 1989) is believed to have a similar nature to that near Munro 1, dipping to the southwest and displacing the Lower Ordovician above the basement. However, the faults north of Samphire Marsh 1 are interpreted to strike west and dip to the north. These west-trending faults also have younger phases of movement, displacing the strata from Ordovician to Permian.

Across the ABFZ between the Willara Sub-basin and the Broome Platform, Top basement was multiply displaced with three to four major faults downstepping towards the southwest (Fig. 17). The cumulative vertical displacement is believed to exceed 2100 m based on the vertical distance between the Lower Ordovician at total depth in Willara 1 (3903 m) and the basement intersection in Parda 1 (1777 m) with these wells being located on either side of the fault zone. The fault correlation shows that the ABFZ changes strike with a clear bend about 5 km north of Nita Downs 1 (Map 1). This fault segment probably terminates north of Cudalgarra North 1 where another northwest-oriented segment emerges and extends to the southeast.

Broome Platform

The basement intersected in Parda 1 on the southern margin of the Broome Platform comprises weathered gneiss and schist below 1777 m (Williams, 1965). The change in lithology from the overlying sedimentary succession to metamorphic rocks corresponds to a strong reflector with a high-amplitude peak at the bottom of continuous reflections at about 1.1 s TWT (Fig. 18). This strong event in the southwest of the Broome Platform exhibits an overall horizontal trend at a relatively shallow level (1 to 1.5 s, Fig. 18), and locally undulates or is folded along with the overlying reflectors. The apparent deformation shortening the reflectors could either have a geological origin or be a geophysical artefact related to: 1) post-Early Ordovician compression; 2) salt mobilization; and 3) salt-related velocity anomalies. Along the southwestern margin only a limited number of faults can be observed with relatively low angles and minimum vertical displacements.

Basement has not been penetrated in the central part of the Broome Platform. However, Top basement horizon can be interpreted with reasonable confidence by following a continuous high-amplitude reflection from both the northeastern and southwestern margins of the platform. In the northwest portion of the platform, the horizon dips gently inwards from both margins to define a central northwest-striking syncline with a wavelength of approximately 100 km, and depth in TWT ranging from ~0.9 s in the northeast to ~1.3 s in the axis (Map 1). The syncline appears to terminate around 30 km southwest of Theia 1 and becomes a ramp dipping towards the southwestern margin. However, interpolation of Top basement carries uncertainties due to the sparsity of seismic data in this area. Overall, the horizon gradually deepens towards the McLarty 1 area (~1.3 s in TWT) before reaching the shallow eastern margin of the platform (~1.2 s).

Munro Arch

No basement rocks have been intersected in the Munro Arch. The only well drilled in this area (Pegasus 1) intersected 75 m of the upper part of the Early Ordovician Nambeet Formation which directly overlies the basement elsewhere in the basin. This interval and its lateral extension on seismic sections (Fig. 19) corresponds to a package of moderately continuous flat-lying strata between strong reflectors above 1.4 s and a chaotic zone below 1.65 s. The calibration indicates a reasonable placement of Top basement horizon at 1.65 s below the flat-lying section.

Top basement becomes difficult to interpret towards the west because of the sparseness and poor quality of the seismic data, leading to an arbitrary correlation with the Willara Sub-basin. In comparison, the data to the north are of reasonable quality and show that the horizon generally shallows towards the Broome Platform with a fault present around 10 km north of the currently defined tectonic element boundary (Fig. 19b). This fault dips towards the south-southwest and has a vertical offset of around 100 ms at Top basement level (Map 1). This fault is herein interpreted as the southeast extension of the ABFZ, based on similar orientation and displacement for Top basement and the lower part of the basin fill. However, such fault correlations cannot be guaranteed due to the limitation of the current seismic grid. The extrapolation of Top basement shows that the horizon maintains a similar depth (~1.8 to 2 s) from the Munro Arch to the Willara Sub-basin, and gently ramps up towards the Broome Platform.

Top Nambeet Formation (Appendix 3, Maps 5–9)

The lowermost sedimentary unit of the southern Canning Basin is the Nambeet Formation named after the Nambeet 1 well less than 5 km southwest from Samphire Marsh 1 where it was first intersected (Playford et al., 1975). In Samphire Marsh 1 it consists of 775 m of thinly laminated grey-green shale alternating with some limestone and sandstone interbeds (Johnstone, 1961). This unit contains Early Ordovician faunas, overlies mid-Cambrian granitic basement (Haines et al., 2018) at 2015 m and is unconformably overlain by the Permo-Carboniferous Grant Group above 1240 m.

Willara Sub-basin

In the southern Willara Sub-basin, the Nambeet Formation in Samphire Marsh 1 corresponds with a zone of relatively low-amplitude continuous reflectors that differs from a series of high-amplitude reflectors at this stratigraphic level in Calamia 1 (Fig. 15). The differences in seismic character of the Nambeet Formation between these wells is related to the local loss of certain intervals: erosional removal of the upper interval of shale and limestone in Samphire Marsh 1 vs southwards thinning of the lower interval of the formation in Calamia 1. The southwards thinning on seismic profiles is more pronounced around Munro 1, which intersected mainly limestone and sandstone with a thickness of about 90 m on the footwall of a fault block. The significant difference in the Nambeet Formation thickness from the hangingwall to footwall of the fault implies syndepositional movement during the Early Ordovician. Despite the differences in seismic character, Top basement horizon can be correlated between these wells and is interpreted to deepen towards the northeast in the Willara Sub-basin.

The Nambeet Formation in Willara 1, about 761 m thick from 3142 m to total depth, can be divided into two units based on lithology and wireline log characteristics (Johnson, 1966b). The upper unit (3142 to 3410 m) mainly consists of an alternation of shales and carbonates, and is calibrated to a zone of high-amplitude continuous southwest-dipping reflectors (Fig. 12). The lower unit includes a monotonous sequence of thinly bedded and interlaminated shale, sandstone and minor limestone (3410 m to total depth; Johnson, 1966b) and corresponds to a much less reflective zone below 1.9 s. Both units in Willara 1 can be correlated across the nearest fault although they become thinner towards the north within the ABFZ. The bottom of the lower unit is tentatively interpreted at about 2.2 s (Fig. 12; approximately 4100 m, ~200 m below total depth of the well).

Leo 1 penetrated the much thinner Nambeet Formation (66.5 m) overlying low-grade metasedimentary basement (Command Petroleum N.L. 1989), creating some difficulties in tracing the interval in this area. This intersection of mainly limestone, shale and siltstone exhibits a relatively strong reflection which is similar only to the upper unit in Willara 1. The lack of the lower seismic unit in Leo 1 indicates that the lower Nambeet Formation unit thins or is absent towards the northeast across the ABFZ. The upper unit may be more laterally extensive with variable thickness along the northern margin of the Willara Sub-basin. The top Nambeet Formation generally follows the structural trend of Top basement, deepening from less than 1000 m in the southwest of the sub-basin, to ~3400 m 10 km southwest of Willara 1, then stepping up across the ABFZ (Fig. 12; Maps 7, 8).

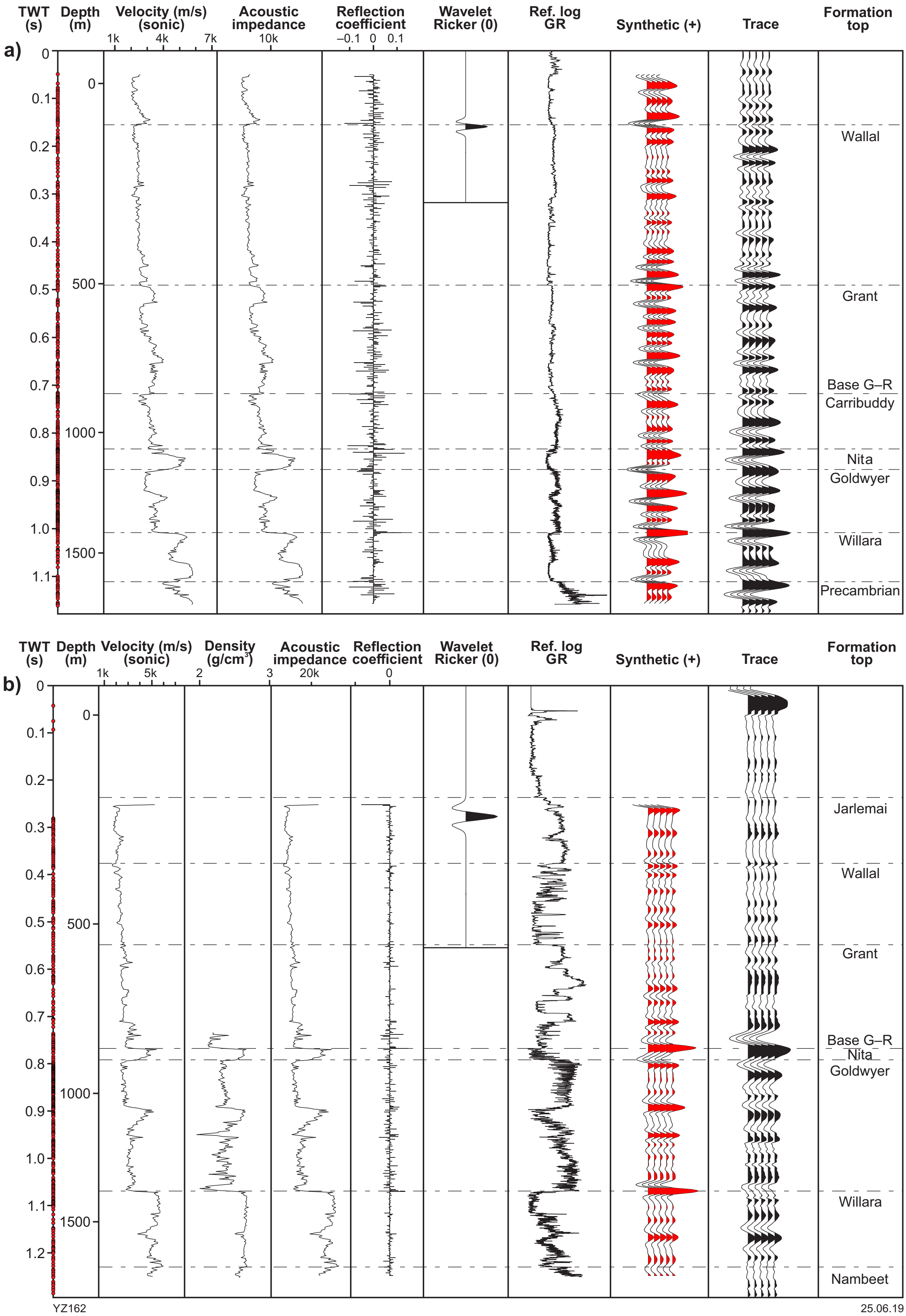

Figure 9. Synthetic seismograms for: a) Parda 1; b) Sharon Ann 1 on the Broome Platform

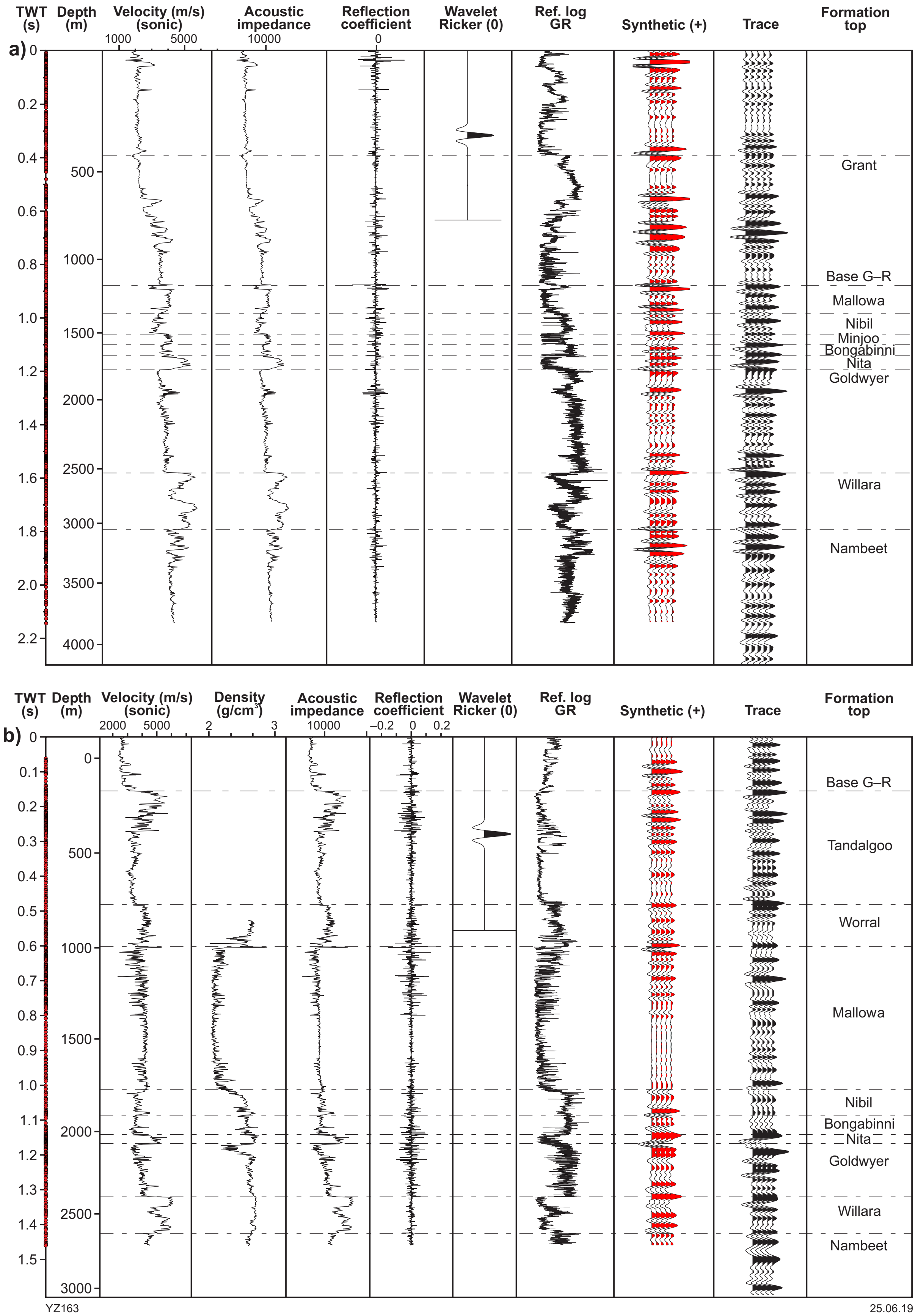

Figure 10. Synthetic seismograms for: a) Willara 1; b) Pegasus 1 in the Willara Sub-basin and Munro Arch, respectively

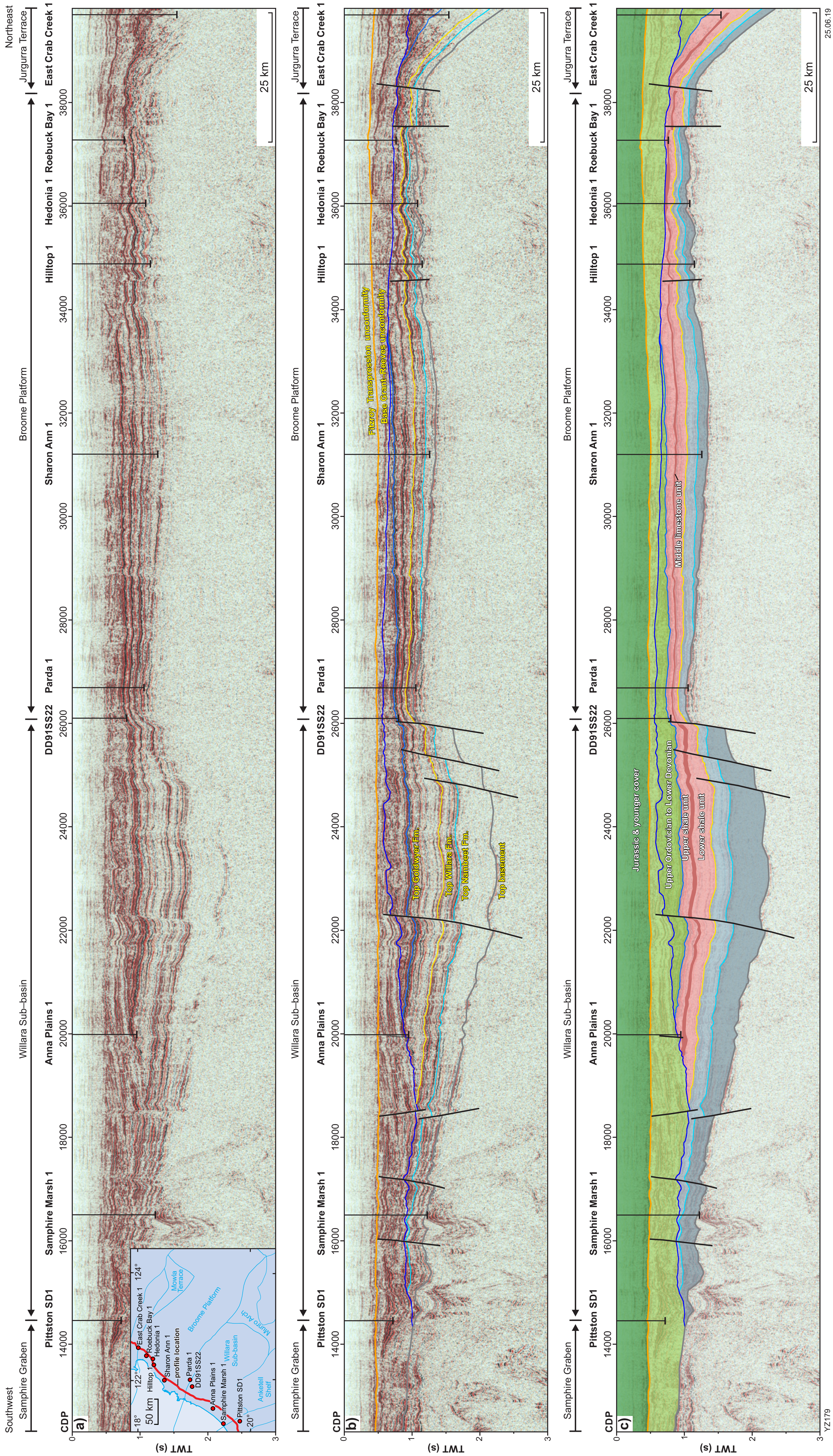

Figure 11. Southwest–northeast seismic interpretation from Pittston SD 1 to East Crab Creek 1

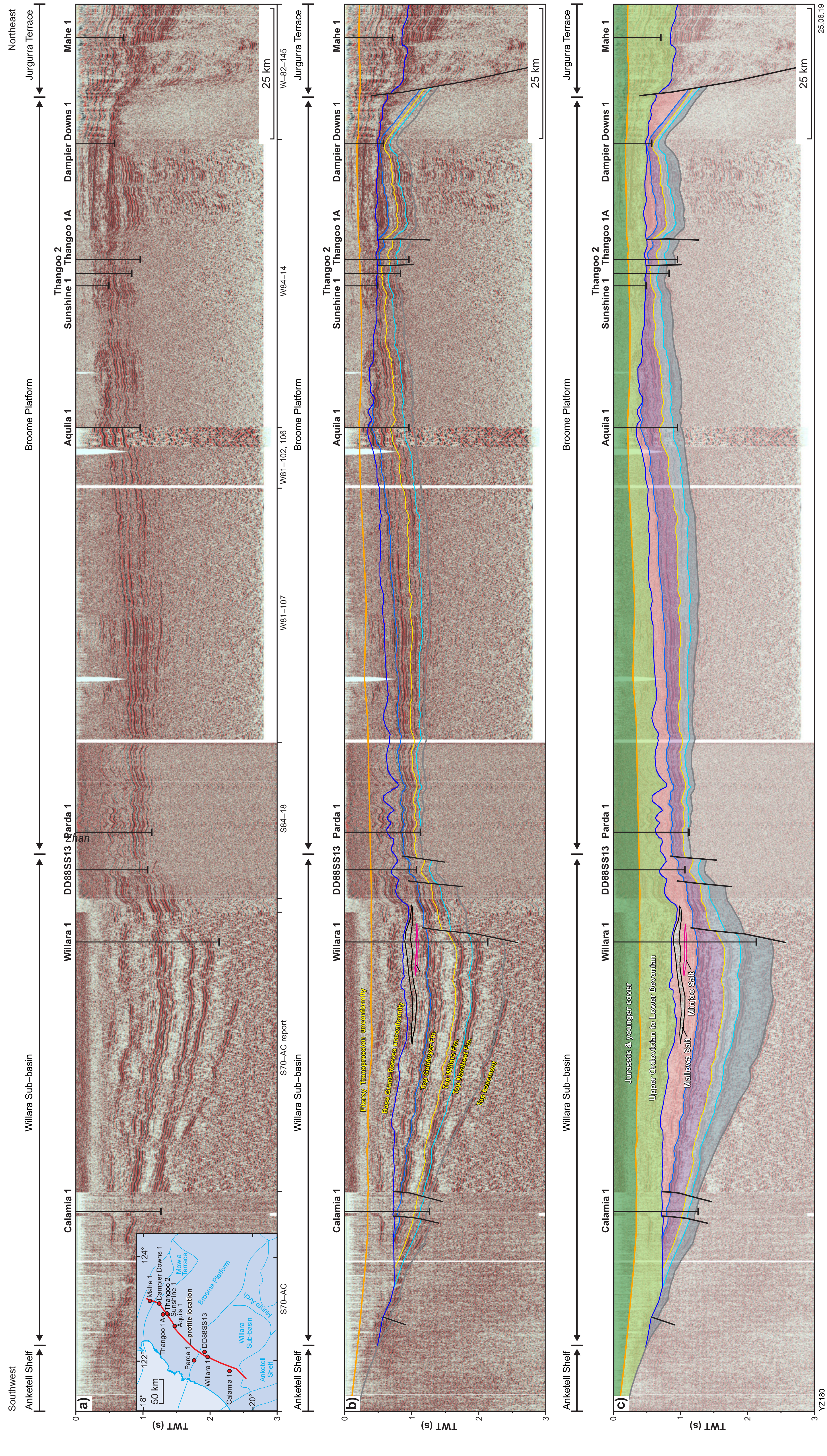

Figure 12. Southwest–northeast seismic interpretation from Calamia 1 to Mahe 1

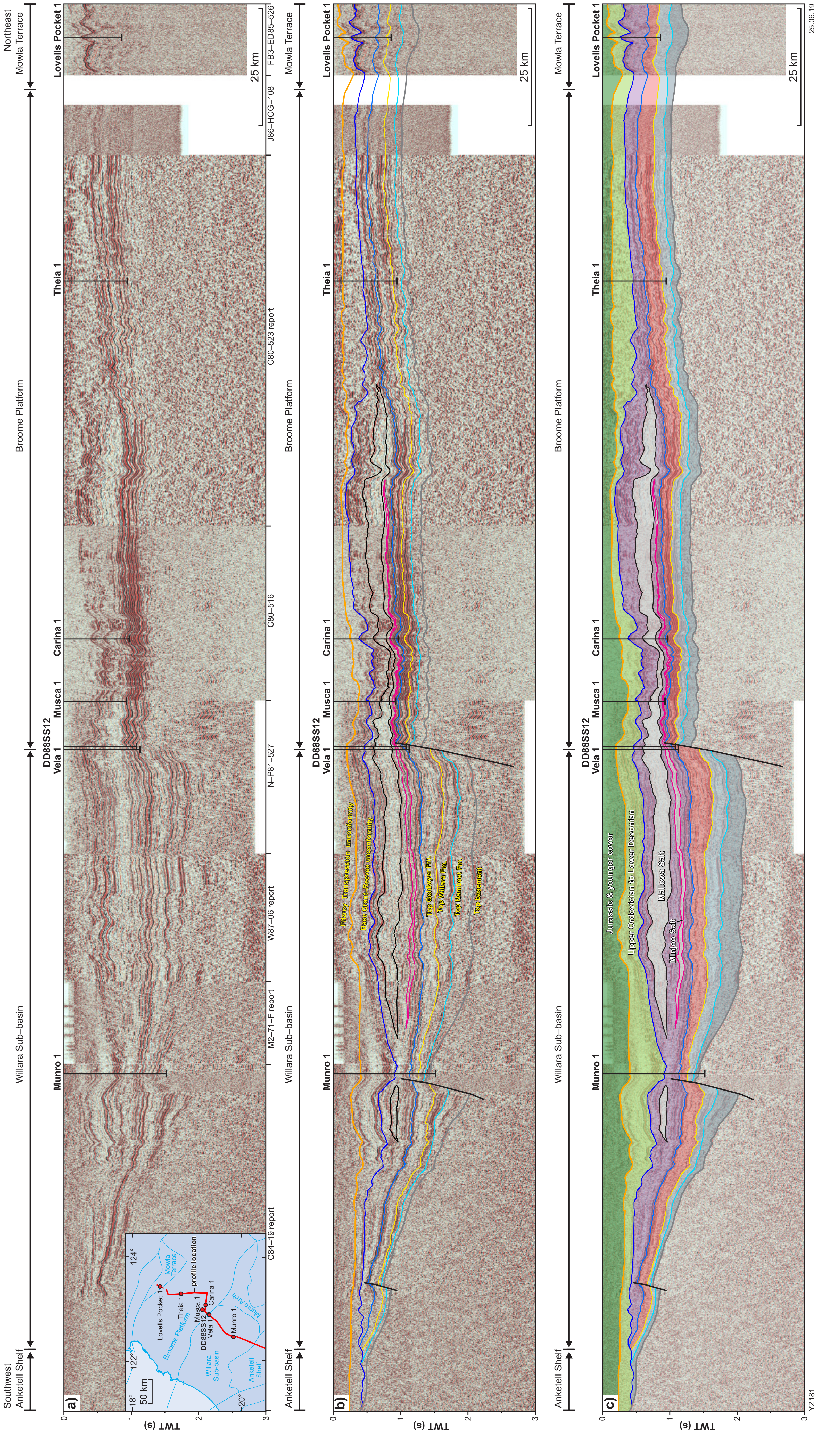

Figure 13. Southwest–northeast seismic interpretation from Munro 1 to Lovells Pocket 1

Broome Platform

The Nambeet Formation continues to shallow northwards from the ABFZ to the Broome Platform. Near the middle of the platform, Sharon Ann 1 reached a total depth in the upper Nambeet Formation (top at 1768 m; Figs 9b, 20). The formation is estimated to be approximately 300 m thick at this location based on the interpretation of Top basement at 1.34 s (Fig. 11; Map 9). The top Nambeet Formation shows a relatively flat-lying seismic event extending from Sharon Ann 1 to the ABFZ, as opposed to the southwestwards shallowing Top basement interpretation for the same profile (Fig. 11). Thus the Nambeet Formation enclosed within these horizons has a wedge-shaped geometry, and is interpreted to be absent along the southwestern margin of the Broome Platform. This is consistent with the absence of Nambeet Formation in Parda 1 (Fig. 20), which bottomed in early Cambrian low-grade metasediments (Haines et al., 2018; previously interpreted as Precambrian basement gneiss and schist in Williams, 1965) below the Willara Formation. The Canning Coastal seismic profile (Fig. 17) shows the Nambeet Formation appearing to onlap the basement about 15 km south of Sharon Ann 1, indicating that lack of deposition across a basement high, rather than post-depositional erosion, best explains the missing Nambeet Formation. The structure maps (Maps 7–9) indicate areas where the Nambeet Formation is absent along the southwestern margin of the platform near the ABFZ, and then thickens towards the centre of the platform.

Highly variable thicknesses of the Nambeet Formation have been encountered along the northeastern margin of the Broome Platform, for example 338 m thick in Hilltop 1, 32.4 m in Goldwyer 1 and 241 m in Hedonia 1 within a radius of less than 15 km (Fig. 20). Normore and Dent (2017) indicated a similar variation of thickness between Thangoo 1A (151.5 m) and Thangoo 2 (288 m) with the lower part of the package absent in the former well. The reason for the significant changes in the thickness within a short distance is difficult to identify from the seismic data as it is compromised by poor quality. It may be related to faults (e.g. Fig. 12), which appear to be more intensive in this area than elsewhere on the platform, creating compartmentalization and small pocket-like depocentres, or irregular basement topographic settings, but uncertainty remains regarding these variations in thickness.

In the central part of the platform, McLarty 1 intersected the Nambeet Formation at 2341 m, which is about 600 m deeper than in Edgar Range 1 (1754 m). These depth variations are visible on the seismic profiles, showing that the top Nambeet Formation horizon generally shallows towards the northern margin of the Broome Platform (Figs 11–13). In addition, this shallowing trend is common in all the Lower to Middle Ordovician horizons. These horizons define a series of small-scale folds, which were possibly related to salt withdrawal or compressional movement before the Permian, but may also be artefacts caused by erroneous velocity and/or static corrections in seismic processing.

Munro Arch

The only partial penetration of the Nambeet Formation on the Munro Arch, 75 m at Pegasus 1, consists of interbedded sandstone and claystone. The upper boundary is difficult to identify as the formation is lithologically similar to the overlying Willara Formation (Franks, 1989; Fig. 19). The minor contrast in the lithology generates a less pronounced reflector at the top Nambeet Formation, and is calibrated to a zero amplitude from a negative trough above, to a positive peak below based on synthetic seismograms (Fig. 10b). Because of the poor-quality seismic profiles in the Munro Arch area, the interpretation for the top Nambeet Formation horizon has a relatively low level of confidence. Nevertheless, a southwards-deepening trend can be interpreted on the seismic profiles, dipping from 2600 m near the ABFZ to 3600 m at the southeastern margin.

Waukarlycarly Embayment

The study area encompasses the northwestern extension of the Waukarlycarly Embayment (Fig. 1), the main sedimentary package of which is of uncertain age due to the lack of well control and its isolation from other tectonic units. The package interpreted as pre-Permian (‘probably Ordovician’ in Zhan, 2018) is tentatively identified as the Nambeet Formation based on similar truncations in the southwestern Willara Sub-basin near Samphire Marsh 1. Mapping indicates this interval is fault bounded and thickens towards the main depocentre of the Waukarlycarly Embayment, reaching up to 1500 m in the south-southeast corner of the study area (Map 9).

Top Willara Formation (Appendix 3, Maps 10–14)

The Willara Formation (Playford et al., 1975; McTavish and Legg, 1976) has a type section in Willara 1 between 2610 m and 3142 m, where the formation rests conformably on the Nambeet Formation and is conformably overlain by the Goldwyer Formation. The Willara Formation consists of interbedded sandy and silty limestone, dolomite, siltstone, with a sandstone unit at the base. Based on conodont faunas, the Willara Formation is of Early Ordovician age with local extension into the Middle Ordovician (Playford et al., 1975; Smith et al., 2013).

Willara Sub-basin

The Willara Formation can be subdivided into three units in Willara 1 based on shale content (Johnson, 1966b): 1) an upper interval (2610–2704 m) dominated by limestone with minor shale beds; 2) a middle interval (2704–2890 m) containing interbedded limestone and shale, with the latter becoming dominant below 2765 m; and 3) a lower interval (2890–3142 m) of predominantly limestone with minor amounts of shales. These three lithological intervals do not strictly correspond to three seismic reflection packages when the well is calibrated to seismic profiles via sonic logs, possibly due to the low seismic resolution at this level. Instead, two distinctive packages can be observed on the seismic profile (Fig. 12): 1) an upper package showing high-amplitude alternating reflectors from 2610 to 2850 m; and 2) a lower package exhibiting reduced amplitude and low-frequency reflectors. The upper package may be related to multiplicative reflections from the interface between the overlying thick shaley Goldwyer Formation and the underlying limestone within the Willara Formation.

Overall, such subdivision of the Willara Formation on the seismic data can only be achieved on a few lines, and it is difficult to systematically interpret the interface between the upper and lower seismic packages. Both seismic packages shallow towards the southwest with the lower package pinching out in the middle of the Willara Sub-basin.

Within the ABFZ, only Leo 1 fully penetrated the Willara Formation. At this location, the formation can be divided into upper (1948–2066 m) and lower (2115–2253 m) limestone units separated by a middle unit of thinly interbedded shale and limestone. Again, the boundaries between these units are gradational and difficult to trace laterally on the seismic profiles. Only the top interface with the Goldwyer Formation exhibits continuous high-amplitude reflections. Constrained by well intersections, the Willara Formation is shown to have significant changes in thickness, ranging from ~200 to 800 m, across the ABFZ (Map 14). This variation is most likely attributed to syndepositional movement along the fault zone during the Early Ordovician.

In the southern part of the Willara Sub-basin, the Willara Formation has been intersected in Calamia 1 and Munro 1, both showing a similar sequence of predominantly limestone. This sequence, as indicated from the well completion reports, could be individually subdivided into several lithological units based on clastic content, although such units are difficult to correlate between the wells. The seismic profile across Calamia 1 (Fig. 15) shows that the Willara Formation, which lies below a relatively strong reflector, can be divided into two units; the upper ~40 ms shows weak reflection and the lower ~40 ms is a continuous high-amplitude zone. Both units are displaced by a series of southwest-dipping faults. The top Willara Formation deepens towards the northeast from less than 1000 m along the southern margin to ~2700 m near Munda 1 in the centre of the Willara Sub-basin (Map 13). The horizon is truncated by the overlying base Permian succession about 8 km to the southwest of Calamia 1 (Fig. 15). The truncation points are generally evident on the northeast-trending seismic profiles and can be traced in a northwest direction towards the offshore Canning Basin. Here the horizon is characterized by a strong reflector between an overlying near transparent zone that lacks internal reflection, and an underlying zone of high-amplitude alternating reflectors (Fig. 21). The Willara Formation is interpreted to have been completely eroded near the current southwest boundary of the Willara Sub-basin, and approximately ~50 km northwest of the coastline (Maps 10–14).

Broome Platform

Well intersections of the Willara Formation are more common on the Broome Platform than in the Willara Sub-basin because of shallower burial depths in the former area. The top Willara Formation exhibits significant responses on wireline logs (e.g. wireline logs of Sharon Ann 1 in Fig. 9b). In the downhole direction, these responses include a sharp decrease in the gamma ray, an abrupt decrease in delta-T on the sonic log representing increase in velocity, a rapid jump in density from ~2.45 g/cm^3 to ~2.66 g/cm^3, and a sudden increase in resistivity. These characteristics on wireline logs reflect a lithological change from mostly shale above to the underlying limestone unit of the upper Willara Formation. On seismic profiles, the top Willara Formation horizon is characterized by a continuous high-amplitude peak which is similar to that in the Willara Sub-basin (Figs 11–13). The internal signatures of the formation are marked by multiple strong reflectors which are parallel to the top horizon in some places, such as the area between Thangoo 2 and Damper Downs 1, 30 km southwest of Twin Buttes 1. These reflectors are possibly generated by the interbedding of shale and sandstone units that separate the Willara Formation into several informal members. However, these members show varying seismic wavelengths, leading to difficulties in regional correlation of the members. The top Willara Formation horizon generally parallels the top Nambeet Formation, shallowing towards the northern margin of the Broome Platform and deepening from the coastal area to the southeast part of the platform (Map 13). It varies in depth from 1000 m around Thangoo 1 and Olympic 1, to 2000 m near McLarty 1. On average, the total thickness of the formation on the platform is thicker than the underlying Nambeet Formation, ranging from ~600 m (about 20 km southwest of Theia 1) to ~200 m (southwest margin of the platform; Map 14).

Munro Arch

The only Willara Formation intersection in the Munro Arch (288 m in Pegasus 1) indicates an interval of predominantly limestone interbedded with calcareous siltstone and sandstone. The bottom part of the formation is transitional with the Nambeet Formation, marked by an increasing volume of sandstone (Exploration Logging Australia Ltd, 1988). The top of the formation shows the same responses on wireline logs as those on the Broome Platform, such as sharp downhole increase in velocity and density. These responses determine the upper surface of a high acoustic impedance interval which can be calibrated to a peak, given a zero phase and normal SEG polarity, on the seismic profile through the well at ~1.3 s (Figs 10b, 15). As the base of the formation is less prominent on seismic sections, the Willara Formation interval is difficult to map across the arch, and is inferred to range between 250 and 500 m in thickness in this area (Map 14).

Top Goldwyer Formation (Appendix 3, Maps 15–19)

The Goldwyer Formation, named after Goldwyer 1 well, is present over a large area of the southern Canning Basin and lies between the underlying Willara Formation and the overlying Nita Formation. The type section for the Goldwyer Formation is in Thangoo 1A between 848 and 1060 m (Pudovskis,1960; Elliott, 1961), with additional reference sections in Solanum 1 on the Barbwire Terrace and CRAE mineral exploration drillhole DD87SS7 in the ABFZ nominated by Haines (2004). These sections comprise predominantly dark-grey calcareous shales and commonly include an informal middle limestone member between upper and lower shale units. The Goldwyer Formation, mainly deposited in an open marine to intertidal environment (Forman and Wales, 1981; Haines, 2004), is dated to the Middle Ordovician based on graptolites and conodonts (Gilbert-Tomlinson, 1961; McTavish and Legg, 1972; Nicoll, 1993). Due to high concentrations of marine algae, the Goldwyer Formation is commonly interpreted to have excellent source rock potential (Foster et al., 1986; Edwards et al., 1997) and has total organic carbon (TOC) levels up to 6% on the Barbwire Terrace (Ghori, 2013). Thus this formation has been one of the most intensively studied and is often a primary or secondary objective for petroleum drilling activities in the southern Canning Basin. Recently full core recovery in Theia 1 showed the lower shale unit has high porosity (~9.5%) and TOC (~3.8%), good permeability, high wet mud gas readings, fluorescence, and associated hydrocarbon odour (Finder Exploration, 2016; Normore et al., 2018).

The upper boundary of the Goldwyer Formation is marked by a distinct inflection in both gamma ray and acoustic logs from low readings in the lower part of the overlying Nita Formation to high readings in the upper part of the Goldwyer Formation (Figs 9, 10). The wireline signatures revert to low readings below the lower boundary between the Goldwyer and Willara Formations. These prominent characteristics reflect the lithological variation at formation scale and allow for consistent placement of the formation boundaries along with biostratigraphic constraints (Haines, 2004) across the Willara Sub-basin and Broome Platform areas. On seismic profiles, the top and base boundaries are commonly interpreted as an amplitude trough above a relatively thick transparent zone and a peak below this zone, respectively.

Willara Sub-basin

The thickest intersection of the Goldwyer Formation in the Willara Sub-basin, 736 m in Willara 1 (Johnson, 1966b; Haines, 2004), comprises predominantly calcareous shale with thin beds of limestone (e.g. 2250–2255 m, 2480–2500 m). The Goldwyer Formation is calibrated to 1.18 s to 1.59 s on the seismic section through this well (Fig. 12). Both the synthetic (Fig. 10a) and seismic reflection profiles (Figs 11–13) show several strong reflectors such as the peaks at 1.27 s and 1.52 s within the transparent zone. The strong reflectors correspond to the tops of comparatively thick interbeds of limestone. Away from Willara 1, these intraformational strong reflectors can also be observed on seismic lines to the northwest and southeast (Figs 12, 17). These similar seismic signatures indicate that the limestone interbeds probably have wide distributions in the Willara Sub-basin. However, it remains uncertain as to whether they can be laterally correlated or represent different limestone units that interfinger with each other. The Goldwyer Formation presently has a maximum burial depth of ~2000 m, approximately 15 km southeast of Willara 1, and generally shallows from northeast to southwest across the Willara Sub-basin (Map 18). A prominent truncation of the top Goldwyer Formation is observed near Anna Plains 1, about 10 km northeast of the point of complete erosion of the formation on the coastal seismic line (Fig. 11). Both the top Goldwyer and Willara Formations were truncated by the overlying base Permo-Carboniferous succession. The complete section of Goldwyer Formation to the northeast of the erosional boundary varies from ~900 m thick southeast of Willara 1 to ~200 m about 50 km southwest of Munro 1 (Map 19).

Within the ABFZ, the thickness of the Goldwyer Formation (Map 19) decreases from the southwest to the northeast as indicated by the complete intersections of 736 m in Willara 1, 294 m in Leo 1, 229 m in DD86SS3 and 137 m in Great Sandy 1. The seismic profiles show that the thickness variation is not related to a gradual thinning, but is characterized by discrete decreases in thickness as the formation is displaced by the series of faults within the zone (e.g. Fig. 17). Due to the thickness differences across the faults, syndepositional fault movement is interpreted as continuous from the deposition of the underlying Willara and Nambeet Formations to the Goldwyer Formation, even though each individual formation does not necessarily thicken towards the fault plane in the hangingwall (Figs 11–13).

Broome Platform

In the coastal area of the Broome Platform, the Goldwyer Formation is characterized on the seismic profiles by two relatively thick zones of weak reflection and a middle highly reflective unit (Fig. 11). These intervals correlate to two informal shale members interbedded with a middle limestone member (34 m thick in Parda 1, 59 m in Sharon Ann 1, 31 m in Goldwyer 1; Haines, 2004) based on wireline log signatures. The upper shale unit and middle limestone member shallow up and are truncated by Permian strata around Hedonia 1.

With wells constraints provided by Aquila 1, Thangoo 2 and Dampier Downs 1, a subparallel seismic profile about 50 km east of the Canning Coastal deep crustal seismic line shows a similar intraformational limestone unit and erosion of the formation towards Thangoo 2 (Fig. 12). The top Goldwyer Formation deepens and forms a small-scale asymmetrical trough between Thangoo 2 and Dampier Downs 1 with folds developed at either side of the structure. The trough is bounded by a near-vertical northwest-striking fault and is split by a parallel fault, with both faults appearing to not propagate into the Permo-Carboniferous strata (Fig. 12). Other faults are also observable in the trough, although not correlated between seismic sections due to their minimal displacements. The displacements along the two interpreted faults in the Lower to Middle Ordovician section are uncertain to some extent. They possibly have reverse and strike-slip components and indicate deformation that is post-Goldwyer Formation but prior to the Permian.

The seismic characteristic of the Goldwyer Formation changes from three units in the coastal area (two weak reflection zones and a middle prominent unit in Fig. 12) to a package of strong reflectors around Theia 1 and farther southeast (Fig. 22a). The change in seismic response indicates lithological variation shown as a higher percentage of limestone at Looma 1, Canopus 1 and Pictor 1 in comparison to the wells in the coastal area. In the southeast part of the Broome Platform, the Goldwyer Formation maintains a relatively uniform thickness from the southern margin of the platform towards the centre, and then thickens towards the northern margin (Map 19). The top Goldwyer Formation is interpreted to deepen from the northern margin of the platform to the Mowla and Barbwire Terraces through either dipping or downthrown faults (Map 18).

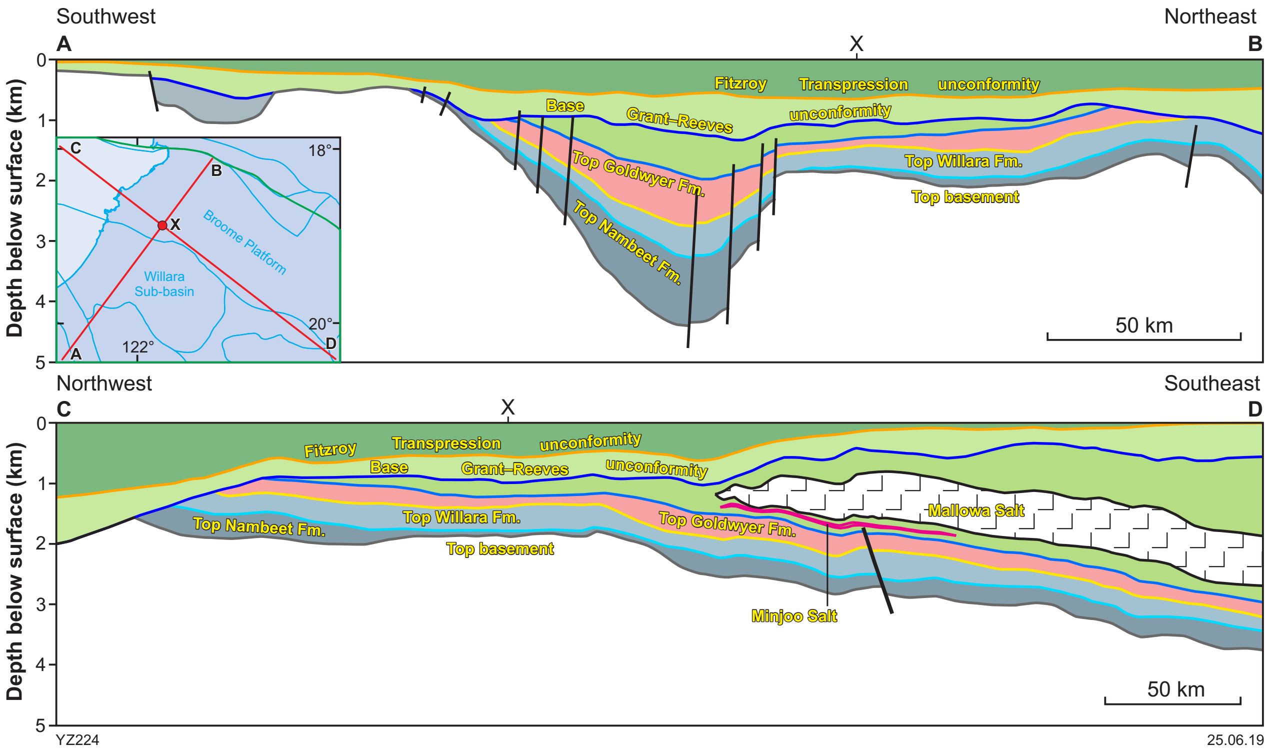

Figure 14. Interpreted geological sections in southwest–northeast (top) and northwest–southeast (below) directions

Munro Arch

In the southeast of the study area, the top Goldwyer Formation appears to be continuously deepening from both the Willara Sub-basin and Broome Platform across the Munro Arch with an average depth of ~2400 m in the middle of the arch (Fig. 19b). There is no indication of a large-scale anticline between the Willara and Kidson Sub-basins. The thickness of the Goldwyer Formation does not seem to be influenced by the Munro Arch, ranging from ~300 m in the east near Pegasus 1 to ~600 m in the west (Map 19).

Top and base of Minjoo and Mallowa Salts (Appendix 3, Maps 20–37)

Two evaporate intervals, Minjoo and Mallowa Salts (Fig. 3), have been intersected within the Upper Ordovician to lower Silurian Carribuddy Group mainly in the southern Canning Basin. The Mallowa Salt is the upper and thicker evaporite interval within the Carribuddy Group. Foster and Williams (1991) interpreted a Late Ordovician to earliest Silurian age for the Mallowa Salt, based on the identification of early land plant spores assigned to *Tetrahedraletes medinensis* in mudstone interbeds in core from mineral exploration drillhole BHP Gingerah Hill 1. The formation was defined by Lehmann (1984) with the name derived from Mallowa Native Well (No. 32 on the Canning Stock Route; coordinates: 22°24'32.40"S, 124°35'2.40"E). It replaced the earlier informal ‘Carribuddy Unit B’ of Koop (1966a,b). Lehmann (1984) nominated a type section in Kidson 1 between 2967 and 3501 m, an interval containing mainly halite with minor dolomite, siltstone and claystone. Within the study area, the maximum intersected section is 800.5 m in potash exploration drillhole BHP Brooke 1, with other thick intersections including 788.5 m in Pegasus 1 and 767 m in McLarty 1. Based on drillcore examination, Cathro et al. (1992) recognized two types of cycles (Table 1) one of which (Type 2) was interpreted as incomplete and lacked lower dolomite and anhydrite portions. The bulk of the Mallowa Salt is composed of repeatedly stacked Type 2 cycles.

Table 1. Two types of cycles showing lithological and mineralogical composition of the Mallowa Salt (Cathro et al., 1992)

Type 1 cycle (2–15 m thick)	*Type 2 cycle (1–4 m thick, interpreted as incomplete Type 1 cycle)*
Terrigenous mudstone (top) Banded halite with variable, upwardly increasing clay content Clear, coarsely crystalline halite Massive to laminated anhydrite Dolomite (base)	Terrigenous mudstone (top) Banded halite with variable, upwardly increasing clay content Clear, coarsely crystalline halite (base)

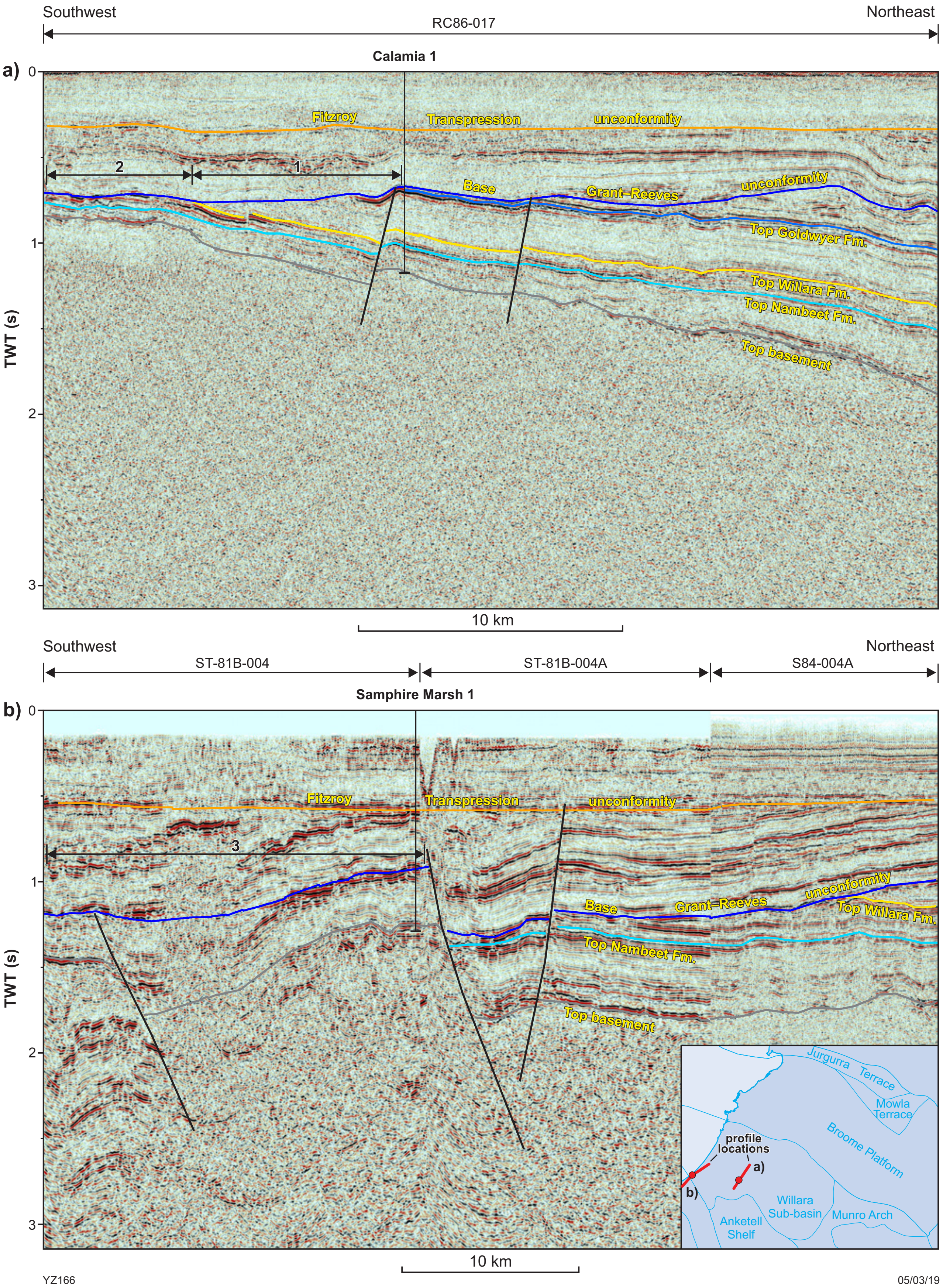

Figure 15. **Seismic interpretation across: a) Calamia 1; b) Samphire Marsh 1 in the Willara Sub-basin, showing a series of faults and the erosional contacts between the Permian and Lower to Middle Ordovician sections. The marked 1, 2 and 3 portions of the Base Grant–Reeves unconformity are amalgamated on maps with the tops of the Goldwyer, Willara and Nambeet Formations, respectively, to delineate the lateral extent of the remnant Ordovician sections**

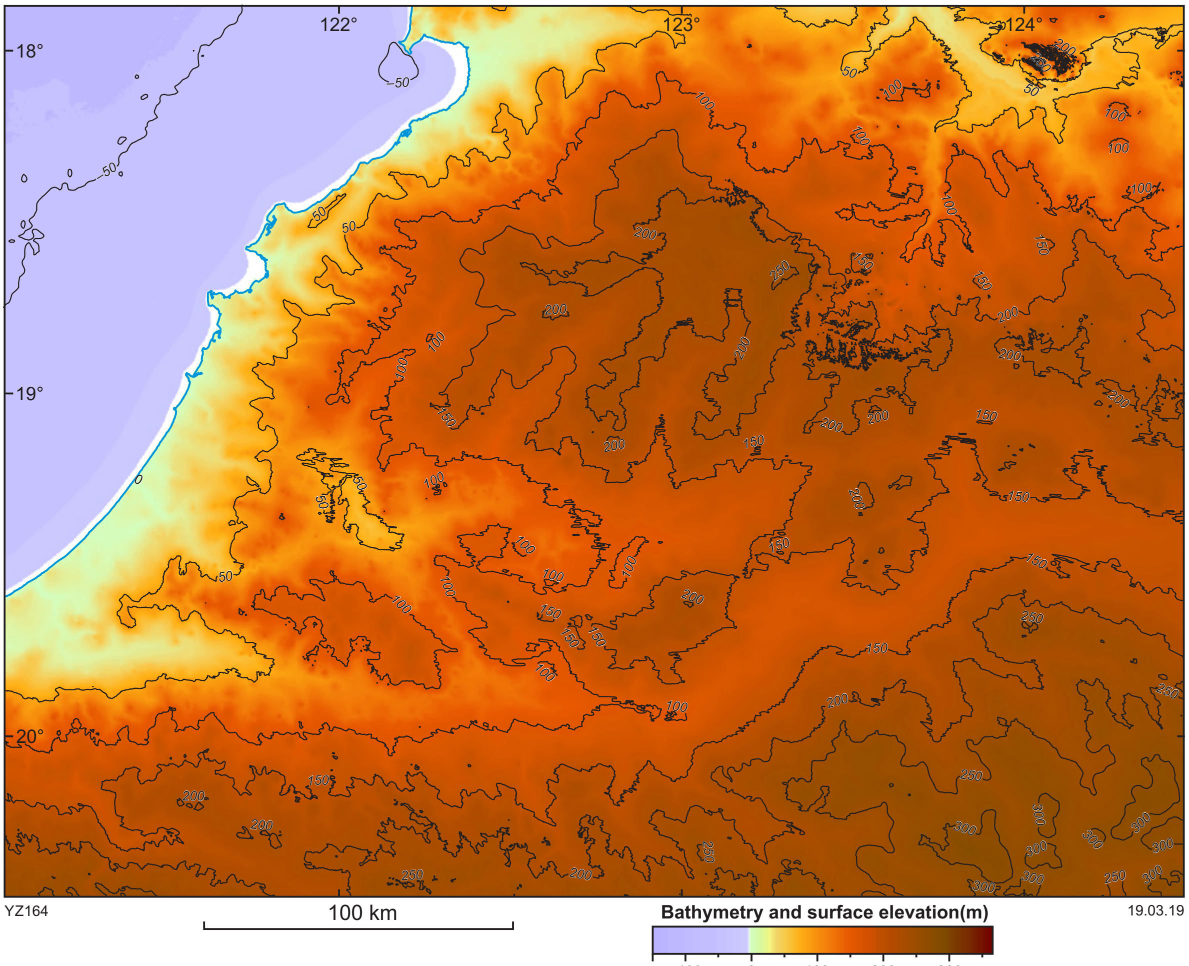

Figure 16. Map of elevation onshore and water depth offshore (Geoscience Australia, 2006; Whiteway, 2009)

The Minjoo Salt was defined by Lehmann (1984) and was named after Minjoo Native Well (No. 35 well near the Canning Stock Route; coordinates: 22°13'1.20"S, 125° 2'60.00"E) to replace the earlier informal 'Carribuddy Unit D' of Johnson (1966a). The type section nominated by Lehmann (1984) is the interval from 3905 to 4071 m in Kidson 1 and comprises mainly halite with a few interbeds of claystone and dolomite, and a minor component of anhydrite. The separation of the Minjoo Salt from the Mallowa Salt was interpreted (Edwards, PB, 2019, written comm.) to be caused by the intercalation of silty material, thus no substantial difference exists between the salt units. Haines (2009) indicated that the halite beds in some wells show regular cyclicity and a pronounced thickening upwards trend to the top of the Minjoo Salt. The author also indicated that the contacts with the underlying Bongabinni Formation and overlying Nibil Formation are conformable and gradational.

Seismic characteristics and distribution

As the Mallowa Salt predominantly consists of thick halite with near-constant acoustic impedance, the salt interval on legacy seismic profiles often correspond to a thick transparent zone that separates the Lower to Middle Ordovician strata from the overlying Silurian to Devonian section (e.g. right portion of Fig. 23a). Within the inner part of the salt deposition, this zone can also be laterally extended to a package of chaotic weak-amplitude reflection (near Pegasus 1 on Fig. 23a) with a series of continuous parallel reflectors in some places on the reprocessed profiles (the southernmost part of Fig. 23a). Based on well correlations, the Mallowa Salt in a west–east direction (Fig. 23b) exhibits similar alternating signatures, containing subtle intraformational continuous reflectors in the west, a featureless zone in the middle, and a relatively bulky package lacking internal reflections in the east. The intraformational reflectors are interpreted to be associated with salt cyclicities, and are mapped as parts of the salt (Map 37). Small-scale faults are probably present within the salt interval (e.g. Fig. 22b) but are difficult to correlate between profiles due to the ductile nature of the salt and scarcity of data.

In general, the Mallowa Salt is characterized by a relatively flat-lying thick sheet over the Ordovician succession. The salt sheet displays a number of localized distortional features (e.g. Fig. 22), most of which are located along the present-day margin of the salt. The current salt edge loosely follows the contours of Top basement horizon (Figs 12, 13), indicating that the salt was deposited and preserved in topographically low areas. This is consistent with well penetrations in the relatively deep part of the study area, including the northeastern Willara Sub-basin,

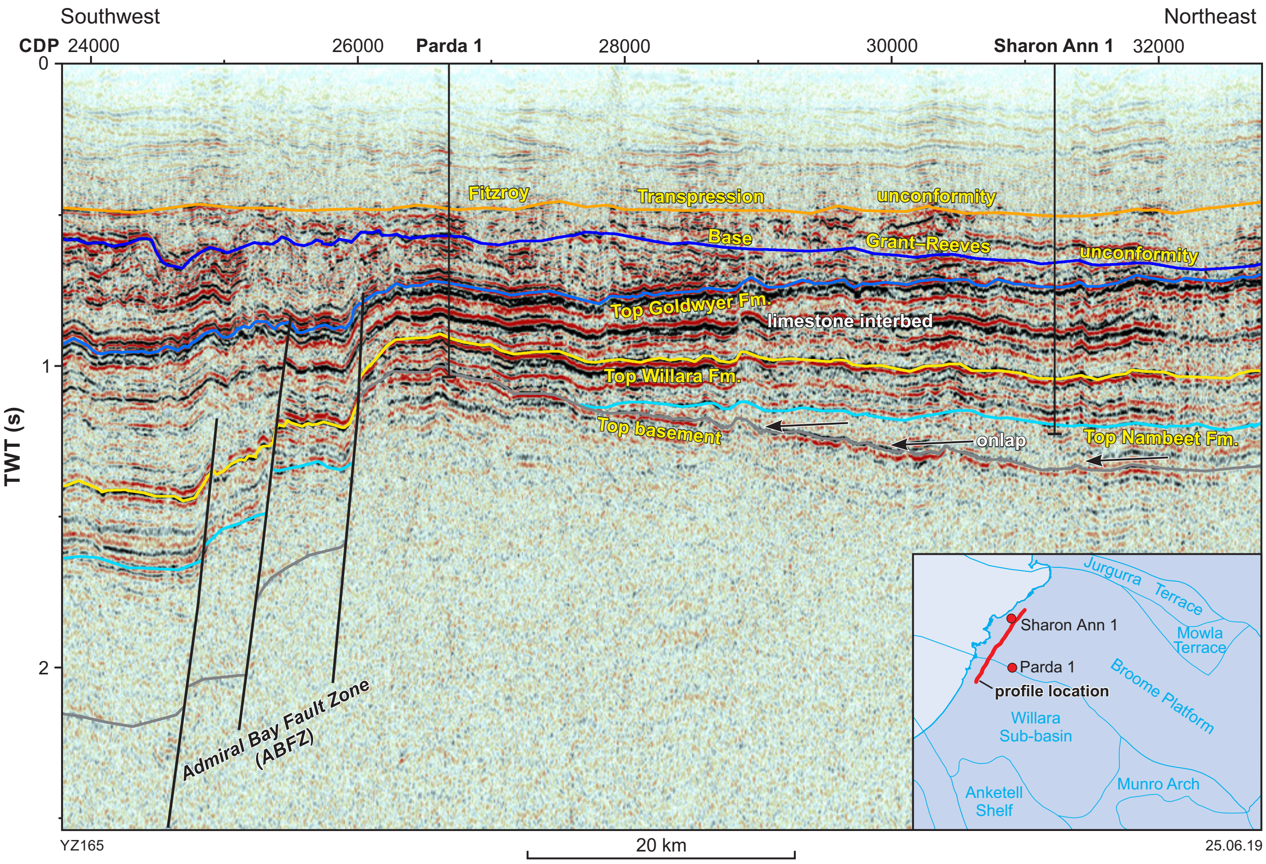

Figure 17. Seismic interpretation across the ABFZ, showing faults downstepping towards the southwest, multiplicative refection below the Top basement on the Broome Platform, and onlapping signatures within the Nambeet and Willara Formations

southeastern Broome Platform and the Munro Arch. Based on well intersections and a general thick transparent zone on seismic profiles, the Mallowa Salt is mainly present in the northeast of the Willara Sub-basin, the southeast part of the Broome Platform and across most of the Munro Arch with a thickness up to 950 m south of the Munro Arch (Map 37). Near the current margins of the Mallowa Salt, the top and base horizons of the salt are interpreted to follow the curvature of those sections and merge towards the periphery of the southern Canning Basin. The seismic interpretation of the salt being absent in the northeastern flank of the Broome Platform and northwestern part of the Willara Sub-basin (Fig. 4) is supported by lack of salt preservation in the almost entirely cored Carribuddy Group in Theia 1 (Finder Exploration, 2016; Normore et al., 2018), and absence of the Carribuddy Group in Anna Plains 1 (Davies and Dorsch, 1988), respectively.

The Minjoo Salt has mainly been intersected around the southeastern part of the transition area between the Broome Platform and Willara Sub-basin, as well as in Willara 1 in the deepest part of the sub-basin. The apparent lack of this formation in other deep wells may be related to 1) non-deposition, 2) salt dissolution and mobilization, or 3) failure to recover salt where the interval is very thin, disseminated, or dissolved due to the use of unsaturated drilling mud. The seismic interpretation of the top and base of the Minjoo Salt is mainly based on the interpolation of formation tops at well intersections and is considered as somewhat arbitrary on many seismic profiles mainly due to its thinness. Assuming the limited reported intersections of the Minjoo Salt (seven wells including one which bottomed in this interval; see Appendix 1) provide a true indication of its distribution in the study area, this unit is restricted in lateral distribution and is less than 80 m thick, most of which is halite. Such thin intervals will be less than one seismic wavelength (120 m) based on an approximate seismic frequency of 35 Hz and velocity of 4200 m/s for salt (see synthetic seismogram of Willara 1 in Fig. 10a). Therefore, even though the Minjoo Salt is within the seismic resolution (30 m as a quarter of the wavelength), it is still too thin to produce a bulky non-reflective zone separating the enclosing formations.

Although the interpretation is of low confidence, the Minjoo Salt appears to deepen towards the southeast and presumably extends through the Munro Arch and to the Kidson Sub-basin, with a thickness of up to 100 m near the east margin of the Willara Sub-basin (Map 28). The assumption of salt deposition across the Munro Arch is based on the horizons of the Lower Ordovician and Top basement showing that the ‘arch’ structurally transitions from the Willara to Kidson Sub-basins, instead of being an anticline separating the two sub-basins. The continuity of salt between Willara 1 and Vela 1 (Map 28) is also uncertain due to imaging limitations and the scarcity of seismic data, although it is assumed to be continuous as mapped along the deep part of the Willara Sub-basin.

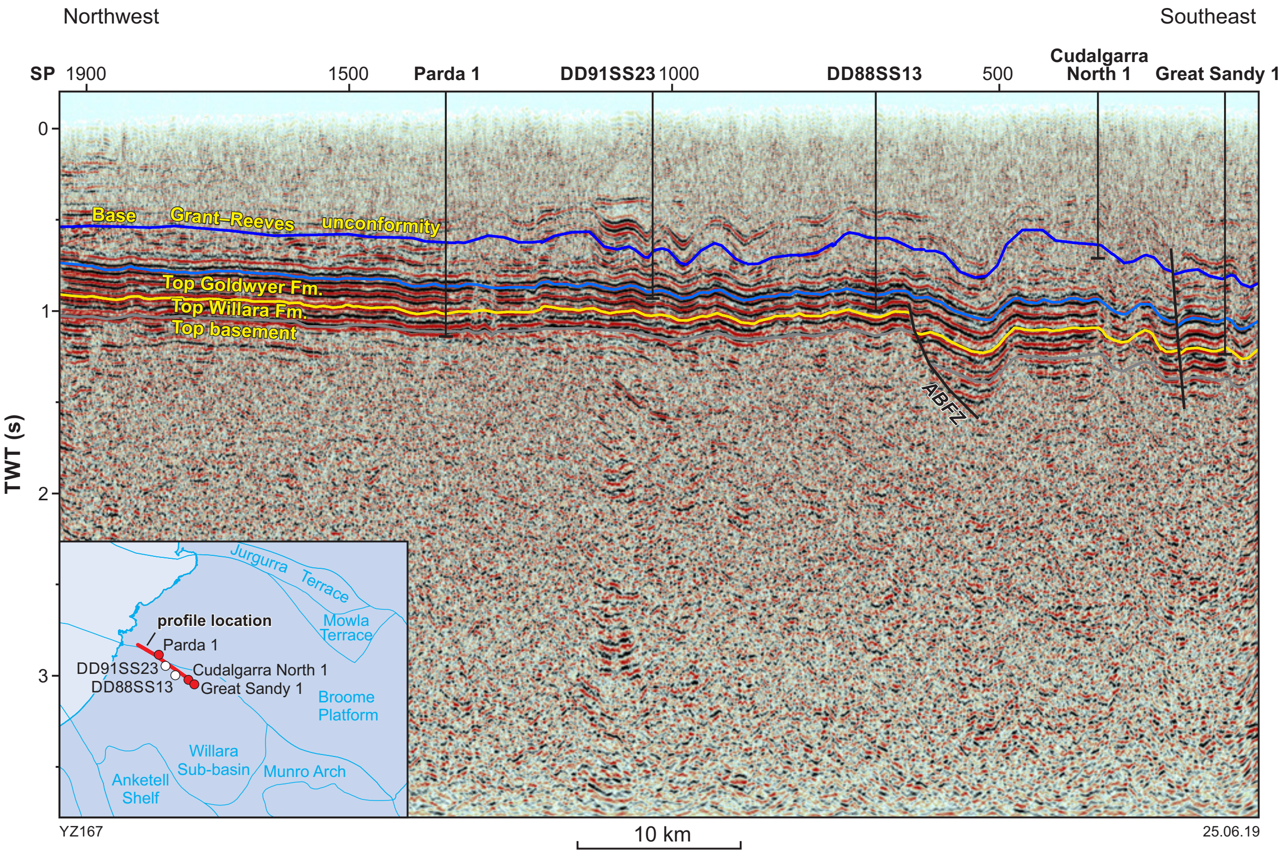

Figure 18. Seismic interpretation from Parda 1 to Great Sandy 1, showing a relatively shallow basement reflector and thin Lower to Middle Ordovician section in the Broome Platform

Salt deposition

Salt deposition in the southern Canning Basin is interpreted to relate to a ~30 Ma interval of global glaciation and a basinwide tectonic movement during the Late Ordovician to early Silurian. Williams (1991) suggested that the depositional cycles of the Mallowa Salt were in agreement with Milankovitch orbital cycles during the Late Ordovician to early Silurian glaciation. The overall cooling event (e.g. Frakes et al., 1992; Page et al., 2007) includes seven glacial maxima of which four occurred in the Late Ordovician and three in the Llandovery (Munnecke et al., 2010) with several second- or third-order warm periods. The cooling was the dominant force driving paleoclimate change, the abrupt extinction in the end-Ordovician (e.g. Sheehan, 2001), seawater chemistry, marine sedimentation, and other effects. During glacial intervals, the rising volume of ice resulted in a drop of sea level, the effect of which may explain the shallowing-upwards trend in the Middle to Upper Ordovician Canning Basin strata noted by Haines (2004) whereby subtidal facies transitioned upwards through zones of increasing energy and decreasing water depth.

The sea-level drop could eventually lead to subaerial exposure in structurally high areas, blocking the southern Canning Basin from open marine access and creating a hypersaline environment (Fig. 24). Such subaerially exposed barriers between open marine and restricted environments with salt deposition can be found on a much smaller scale along the present-day Western Australian coast, e.g. Hutt Lagoon near Port Gregory separated by a barrier from the Indian Ocean, and Pink Lake in the Goldfields–Esperance region isolated from the Southern Ocean (Mernagh, 2013). Within restricted settings, evaporation of a 1 km column of seawater can only produce about 14 m of evaporites including gypsum, anhydrate, halite, in that order of precipitation (Lugli, 2009). Thus multiple influxes of seawater into the basinal area would be required to build up massive salt intervals (a maximum thickness of 313 m for the Minjoo Salt in Patience 2 and 800 m for the Mallowa Salt in BHP Brooke 1; Haines, 2009). The gradational nature of the contacts between salt cycles and overlying strata might be related to brine dilution by seawater overflows and re-precipitation by evaporation. During those influxes, at least the upper part of the salt bed would dissolve until a saturated state was reached at the bottom part of the brine pool where the solubility was low. After each seawater influx, the net evaporation would lead to re-precipitation of salts from solution onto the sea floor as a new cycle of evaporites, followed by clastic/carbonate sedimentation at the top of the cycle (Table 1).

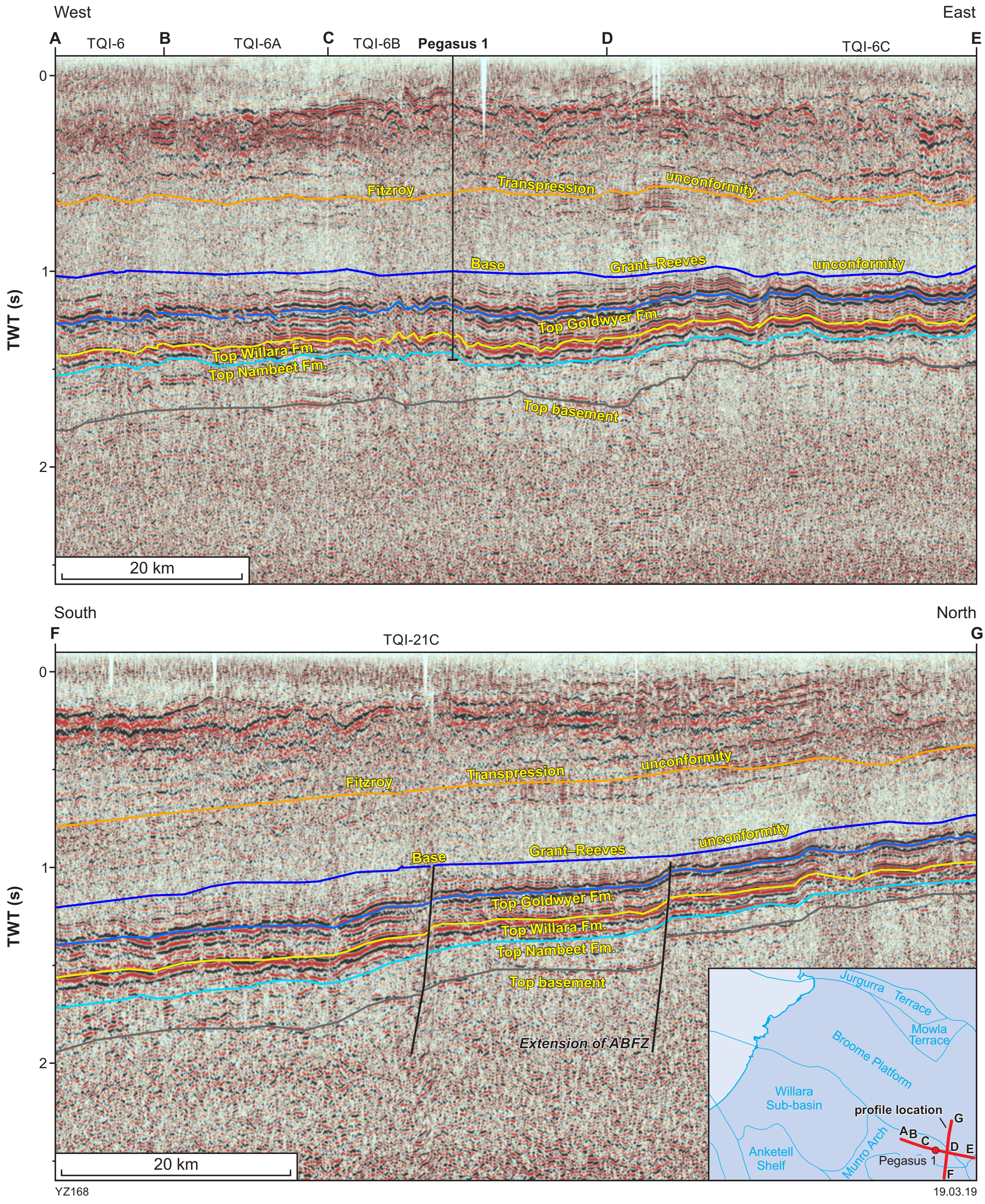

Figure 19. Seismic interpretation across Pegasus 1 on the Munro Arch: a) west–east; b) south–north

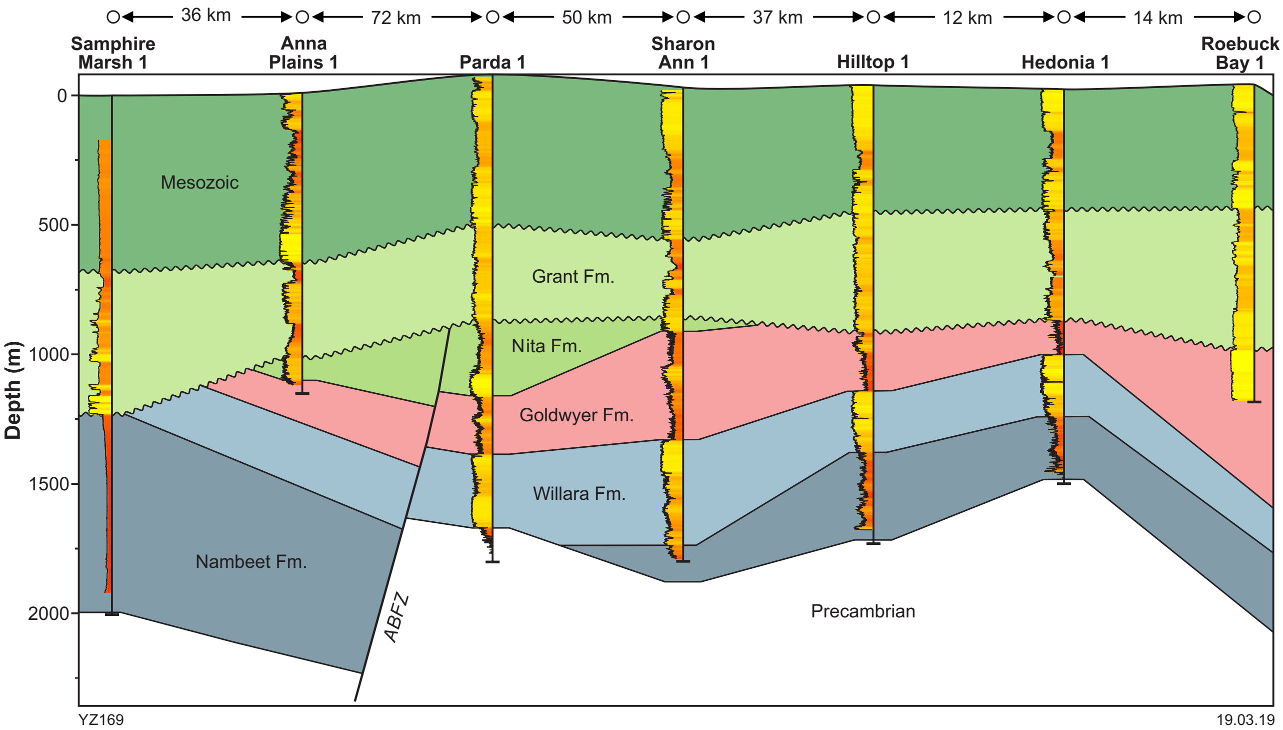

Figure 20. Well correction from Samphire Marsh 1 to Roebuck Bay 1 along the coastal area

In addition to global glacio-eustatic sea-level changes, a change of structural style is interpreted to have contributed to the creation of the salt in the southern Canning Basin during the Late Ordovician to early Silurian. Interpretation of the Willara Sub-basin and Broome Platform (Figs 11–13; Zhan, 2017) suggests that:

1. An erosional contact is present below the base Grant Group progressively removing an increasing thickness of Ordovician rocks towards the northern margin of the Broome Platform, as seen in well correlations from Sharon Ann 1 to Hedonia 1 in the coastal part of the basin

2. From the centre of the Broome Platform, the Lower to Middle Ordovician succession below the top Goldwyer Formation is interpreted to thin or pinch out towards the southern margin of the platform, although it retains a relatively uniform thickness or slightly thickens towards the northern margin. For example, the Nambeet Formation is absent at Parda 1 in the south although it is about 240 m thick in Hedonia 1 in the north (plate 1 of Haines, 2004). This suggests that prior to erosion beneath the Grant Group, a considerable thickness of Ordovician to Silurian succession was present near the northern margin of the platform.

Based on the amount of erosion, a regional structural event is interpreted to have occurred to uplift the southern Canning Basin, particularly the Jurgurra–Barbwire Terraces, northern margin of the Broome–Crossland Platforms and the present-day offshore and nearshore portions of the Broome Platform – Willara Sub-basin (Fig. 24). In the absence of this tectonic event, it would be difficult to explain the current basin configuration, as the southern Canning Basin succession would continue deepening towards the northeast thus no restricted depression would have formed. Apart from global sea-level changes discussed above, the regional tectonic uplift of the sea floor along the northwest-striking belt and the offshore/nearshore area possibly controlled the barrier between open marine and restricted evaporite deposition within the southern Canning Basin.

Salt structural configuration

Due to their thickness, the salts are expected to have influenced the structure of younger strata via post-depositional salt dissolution and mobilization. Historically, the presence of salt tectonics has been related to its buoyancy, such that overlying dense sediments sink into the less-dense fluid-like salt layer and displace the salt upwards to form diapirs (Jackson, 1995, 1997). The dominant force driving salt flow has subsequently been revised to differential loading, which includes gravitational loading, displacement loading and thermal loading (Hudec et al., 2007; Jackson and Hudec, 2017). Such forces were probably present and influenced the Minjoo and Mallowa Salts in the Canning Basin. For example, after salt deposition and eventual burial to over 1000 m, multiple contractional and extensional events could exert sufficient gravitational and displacement loadings to mobilize the salt. In addition, the relatively high geothermal gradient along the Broome and Crossland Platforms (Ghori, 2013) would result in thermal intra-salt convection facilitating salt tectonics by expanding the salt volume and decreasing its diffusivity and viscosity (Jackson and Hudec, 2017). In other words, these factors could trigger salt movements at any stages after the salt deposition. However, given the poor quality and paucity of the seismic data, large-

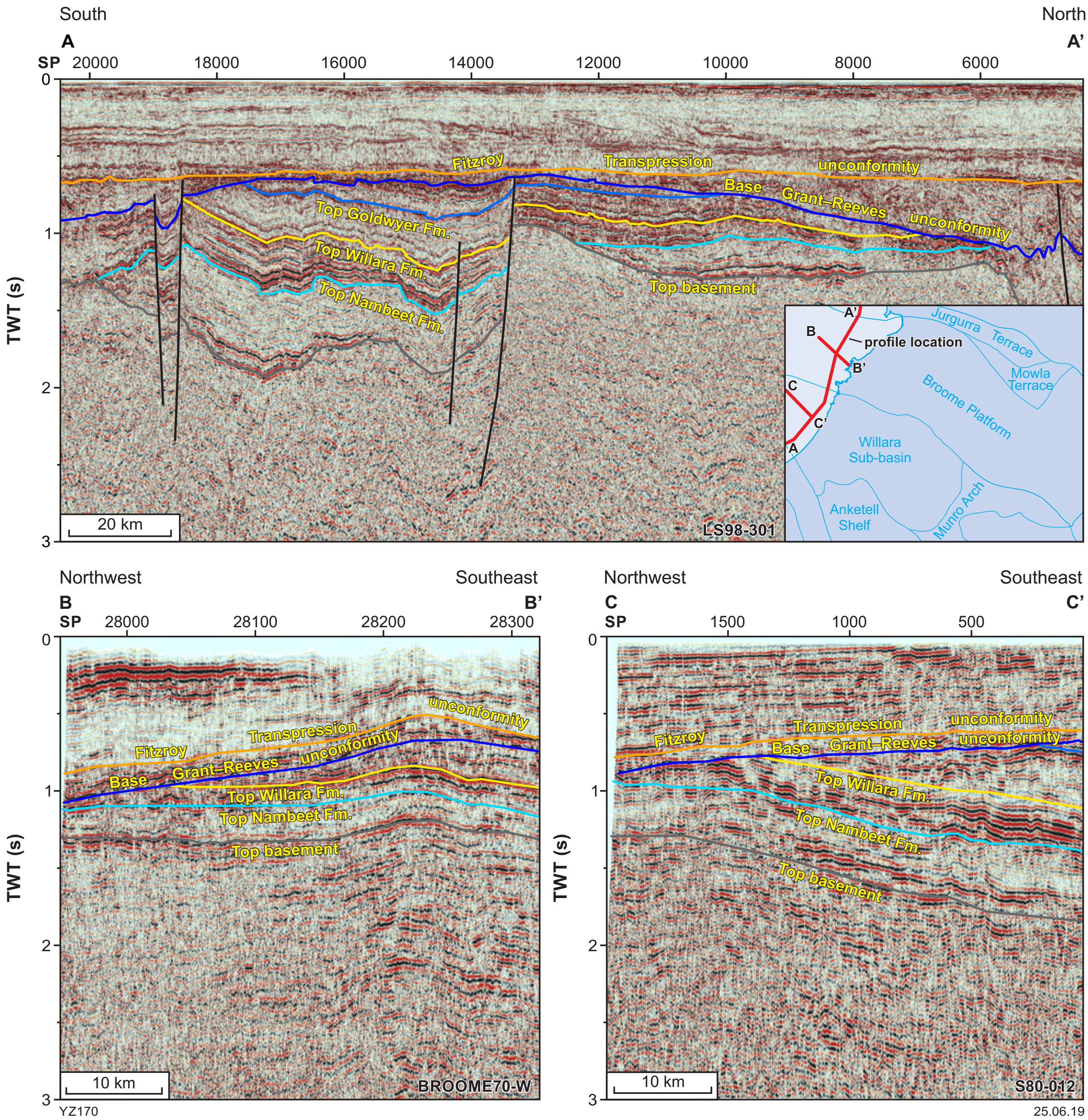

Figure 21. Seismic interpretation in the offshore area, showing a relatively thick Lower to Middle Ordovician section near the coast (A–A') and thinning trend towards the northwest (B–B' and C–C')

scale structures of mobilization, such as salt domes and diapirs, are not observed in the study area but are present on the southern margin of the Fitzroy Trough north of the study area.

Dissolution affected not only the geometry of the salt units, but also the successions above, evident in the area around the salt margins. Good-quality seismic profiles in these areas (e.g. Figs 22, 25) show small-scale anticline features above the salt intervals, commonly interpreted as the result of salt dissolution (e.g. Geary and Robbie, 1989). Initially, localized salt dissolution created depressions or mini-basins into which varying thicknesses of sediments were deposited (Fig. 26). A subsequent phase of salt dissolution resulted in the collapse of the overlying sediments, leaving thicker sediments within the infilled depressions as turtle structures (Jenyon, 1986; Romine et al., 1994; SRK Consulting Pty Ltd, 1998; Thomas, 2000). The early researchers also described these features as 'sombrero structures' and related them to underlying faults and fractures that allowed formation waters to migrate into the salt formation. The mechanism might be more complex, in that faults in the overlying succession may also act as conduits for the fluids responsible for dissolution (e.g. Fig. 22b). Conversely, it may also be the case that salt withdrawal occurred first and resulted in the fault displacement in the overlying section.

The relationship between faults and fluid migration remains uncertain due to insufficient constraints associated with the poor quality and paucity of the current dataset.

The collapse after salt dissolution could have occurred at any stage during the depositional history of the southern Canning Basin, as the interpretation of the exact withdrawal time is highly dependent on the quality of seismic data. Near the current southern margin of the salt units in the Willara Sub-basin, a seismic profile (Fig. 25) shows that the Permian strata were strongly deformed compared to the underlying Ordovician and overlying Mesozoic strata. This implies that the deformation was probably related to Triassic to Jurassic salt dissolution, rather than compressional movements affecting the Permian section. Otherwise, the Ordovician would be folded with similar geometry. An Early Cretaceous phase of salt deformation can also be inferred from the right part of the seismic profile (Fig. 5) where both the Permian and most of the Mesozoic successions exhibit a small-scale syncline but with different magnitude. This indicates that salt was originally deposited in this particular area, but was mobilized during the Triassic to Jurassic event and dissolved after the Jurassic.

The timing of the two withdrawal events discussed above possibly corresponds to the Triassic to Jurassic Fitzroy Transpression and the Early Cretaceous breakup movement. With those two events observable on the seismic profiles, it could be speculated that multiple phases of salt dissolution occurred, including the tectonic movement related to the prolonged Alice Springs Orogeny, and events after the Early Cretaceous. These major tectonic movements could initiate faults and fractures that allowed circulation of water during the dissolution process (Fig. 26). The brine sourced from the near margin

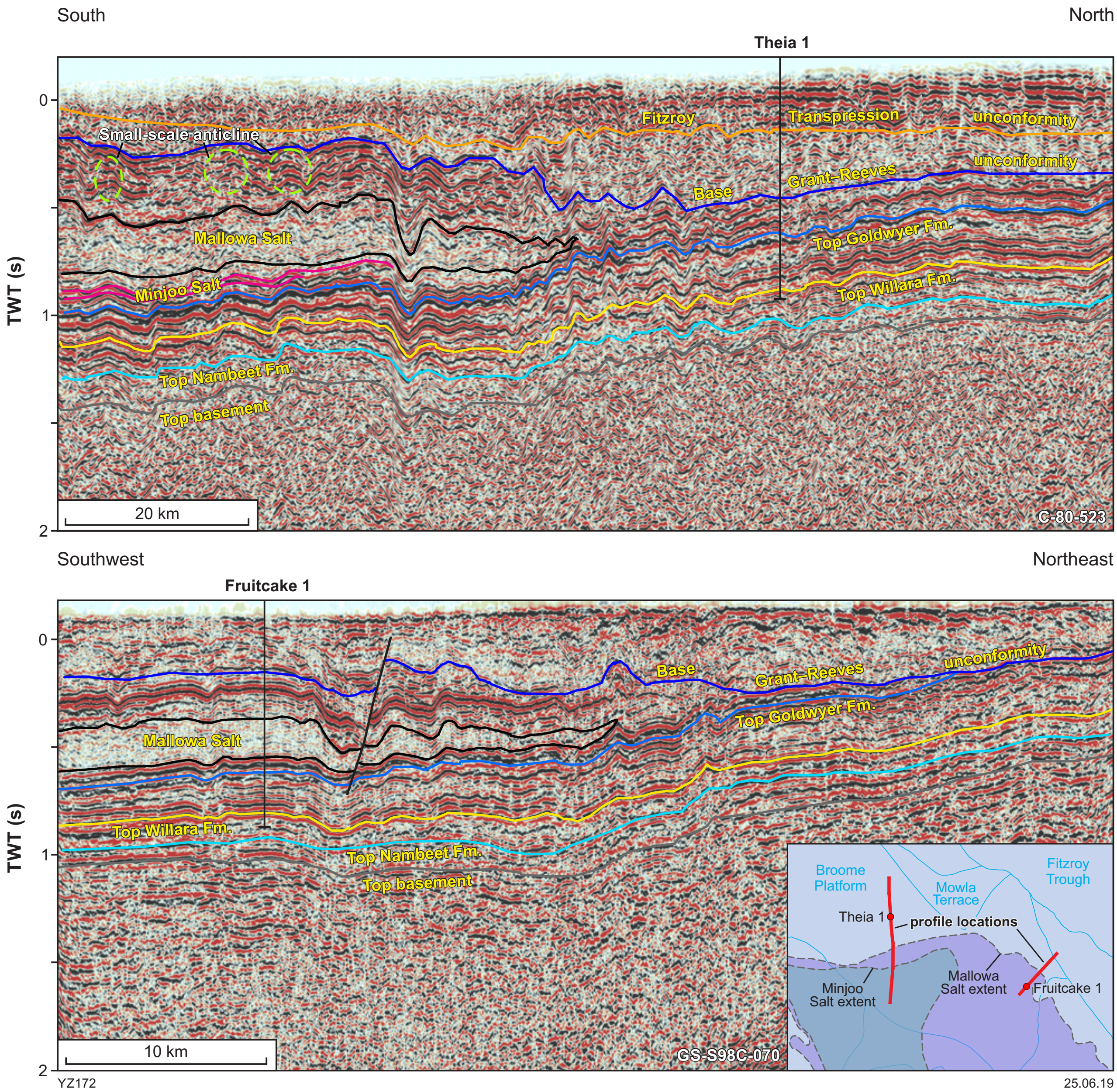

Figure 22. Seismic interpretation around the present-day salt margins showing salt collapse and probable fault connectivity

dissolution could be pushed upwards to the surface via fault connectivity and formation pressure, but probably flowed directly into the open sea, when present, or transported to the sea along with rainfall runoff in the early stages of dissolution. However, during late stages or in modern times, the brine reaching the surface probably became stranded in various catchment systems developed over the southern Canning Basin. Such hypersaline water might have re-precipitated salt and provided an input to modern salt lakes, such as Lakes Waukarlycarly, Auld, Dora and others (Fig. 27). However, the link to modern salt lakes, as well as details of dissolution stages, is difficult to interpret on current seismic profiles due to the limitation in data quality and quantity.

Base Grant–Reeves unconformity (Appendix 3, Maps 38–42)

The Base Grant–Reeves unconformity is a well-established seismic horizon in the Canning Basin due to sufficient well penetrations (Mory, 2010). This basinwide erosive surface lies either below the Permo-Carboniferous Grant Group in the southern Canning Basin, or below the Carboniferous Reeves Formation in the northern Canning Basin. This is because the Reeves Formation does not extend south of the Fitzroy Trough; sections previously included into the Reeves Formation (Mory, 2010) are now placed within the Grant Group (Backhouse and Mory, 2019, written

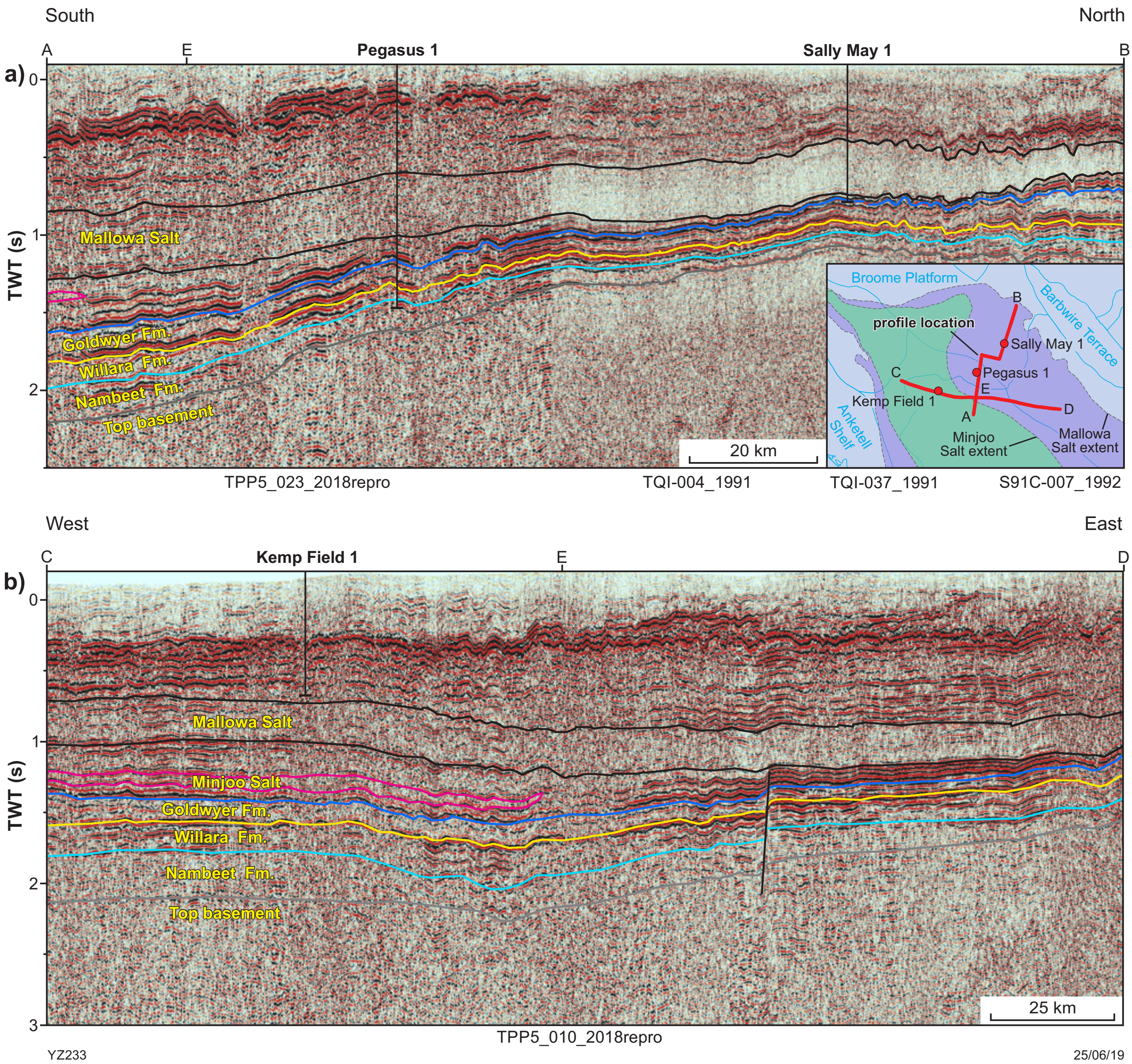

Figure 23. Seismic interpretation within the inner area of the salt deposition: a) south–north direction; b) west–east direction

comm., June; Fig. 3). The Grant Group was named after Grant Range in the middle of the Fitzroy Trough, and was previously known as 'Grant Range Beds' (Woolnough, 1933) and 'Grant Formation' (Guppy et al., 1952; Playford et al., 1975). The group has been lithostratigraphically subdivided into three units based on outcrop data: Betty, Winifred, and Carolyn Formations (Crowe and Towner, 1976), or locally into Hoya, Calytrix and Clianthus Formations from well data (Redfern, 1991; Apak and Backhouse, 1998). The group is a fluvial to marine glacigene succession of mainly sandstone, with lesser siltstone, diamictite, conglomerate and shale. It is overlain by the Poole Sandstone and due to its unconformable base is underlain by units of different ages and lithology across the Canning Basin. The Grant Group is assigned an early Permian to late Carboniferous age based on palynomorphs (Mory, 2010; Backhouse and Mory, 2019, written comm., June). Overall, the Base Grant–Reeves unconformity is widespread, being encountered in all petroleum wells and mineral drillholes in the Willara Sub-basin, Broome Platform and Munro Arch.

Within the study area, the strata underlying the Grant Group vary in age and lithology (Fig. 11), ranging from Early Ordovician Nambeet Formation in Samphire Marsh 1, to the Late Ordovician to early Silurian Carribuddy Group and Worral Formation and locally the Devonian section, reflecting the amount of pre-Permian erosion in different areas. In addition, the variation in strata beneath the Grant Group affects the signature of the unconformity on wireline logs (gamma ray, acoustic velocity, bulk density, and others). For example, the gamma ray varies from relatively low readings in the Grant Group to high readings in the more shaly Goldwyer Formation at Goldwyer 1 and Hedonia 1, but changes in the opposite direction at Darriwell 1 and Juno 1 which intersected the evaporitic Carribuddy Group directly below the Grant Group.

Willara Sub-basin

The Base Grant–Reeves unconformity is best constrained in the Willara Sub-basin with over 30 wells intersecting this horizon. The depth of the unconformity ranges from 781 m in BHP Brooke 1 in the east to 1344 m at Juno 1 in the middle of the sub-basin, corresponding to about 0.45 to 1 s on seismic sections based on velocity survey data or sonic logs. In the coastal part of the sub-basin, the horizon deepens from 0.6 s around the ABFZ to 1 s about 20 km northeast of Samphire Marsh 1 (Fig. 11; Zhan, 2017). The change in thickness of the Grant Group in this area is apparently caused by subsequent erosion at a shallow level which is discussed in the Fitzroy Transpression unconformity. The Lower Ordovician package deepens and thickens to the northeast of the area of truncation by the Base Grant–Reeves unconformity. The unconformity between the Permian and Lower Ordovician is clearly angular, and can be interpreted with a high level of confidence (Fig. 11).

The signature of the Base Grant–Reeves unconformity is less prominent in the middle part of the sub-basin (e.g. Figs 15, 28a), where the salt units were presumably deposited, but later dissolved, particularly around the current salt margins. However, the angular contact can be amplified to a degree by flattening the horizon under which reflectors are truncated (Fig. 28b). The lower part of the Grant Group is mostly characterized as high-amplitude reflections with a time thickness of around 200 ms. Compared with the Lower Ordovician horizons, the overall trend of the Base Grant–Reeves unconformity dips more gently towards the north near the southwestern margin of the Willara Sub-basin (Figs 15, 28). This trend is similar to that along the northeastern margin of the sub-basin, where the unconformity gradually shallows towards the ABFZ (Map 41).

Broome Platform

The Base Grant–Reeves unconformity is apparently not displaced by the ABFZ near the southern margin of the Broome Platform (Fig. 11). Instead, the horizon gradually shallows to the north from ~700 ms in the Willara Sub-basin to ~600 ms over the Broome Platform near the southern coastal area. Moreover, depth variation across the ABFZ becomes minimal in the southeast, especially between the platform and Munro Arch. To the south of the Jurgurra Terrace, the Base Grant–Reeves unconformity gently deepens northwards in contrast to the shallowing top horizons of the Lower Ordovician (Figs 11, 12). Thus the older strata are more deeply eroded in this direction, leading to partial or even complete removal of units in some areas, for example the absence of the Goldwyer Formation in Olympic 1.

The seismic interpretation of the unconformity to the south of the Mowla and Barbwire Terraces becomes difficult because of the scarcity and poor quality of seismic data, although the horizon is believed to shallow up from ~400 to 200 m based on well intersections (e.g. 289 m in Crystal Creek 1, 367 in Robert 1). Overall the base of the Grant Group generally shallows inland and is less affected by faults compared with the underlying Lower Ordovician horizons (Map 41).

Munro Arch

The only well in the Munro Arch, Pegasus 1, intersected the Base Grant–Reeves unconformity at 410 m, corresponding to a strong reflector below a set of parallel and relatively strong reflection zones (Fig. 19). This signature is locally used to interpret the unconformity which can be correlated to the wells and seismic profiles in the southeast of the Broome Platform. Similar to the rising trend onto the platform, the Base Grant–Reeves unconformity generally shallows up from the Willara Sub-basin to the Munro Arch, as demonstrated by comparing the unconformity depth of 781 m in BHP Brooke 1 with 410 m in Pegasus 1 (Map 41).

Fitzroy Transpression unconformity (Appendix 3, Maps 43–46)

The Fitzroy Transpression unconformity was related to a significant tectonic event that helped shaped the current topography of the onshore Canning Basin. Rattigan (1967) and Smith (1968) identified a series of en echelon, easterly trending anticlines and synclines, as well as numerous northerly trending faults from outcrop in the northern

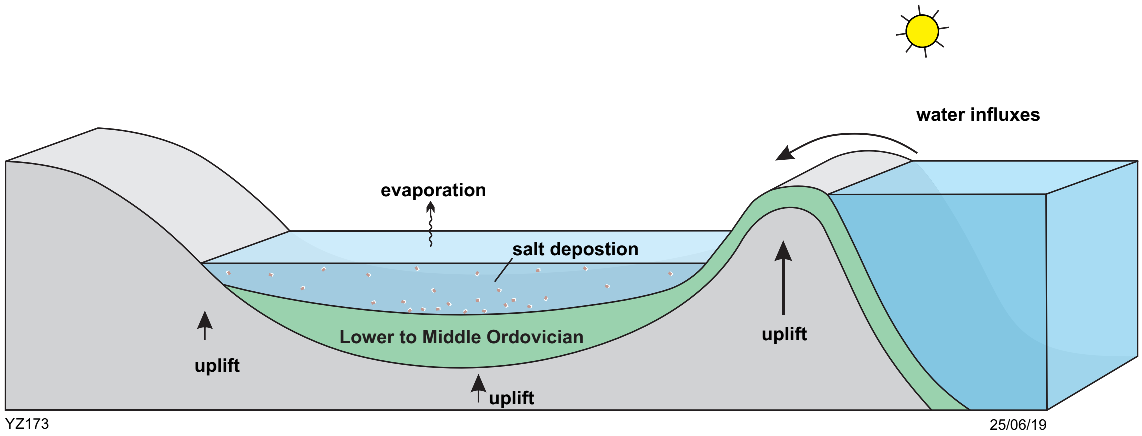

Figure 24. Schematic diagram for salt deposition showing a separation of the southern Canning Basin from the north via differential uplift to create a hypersaline environment in the south

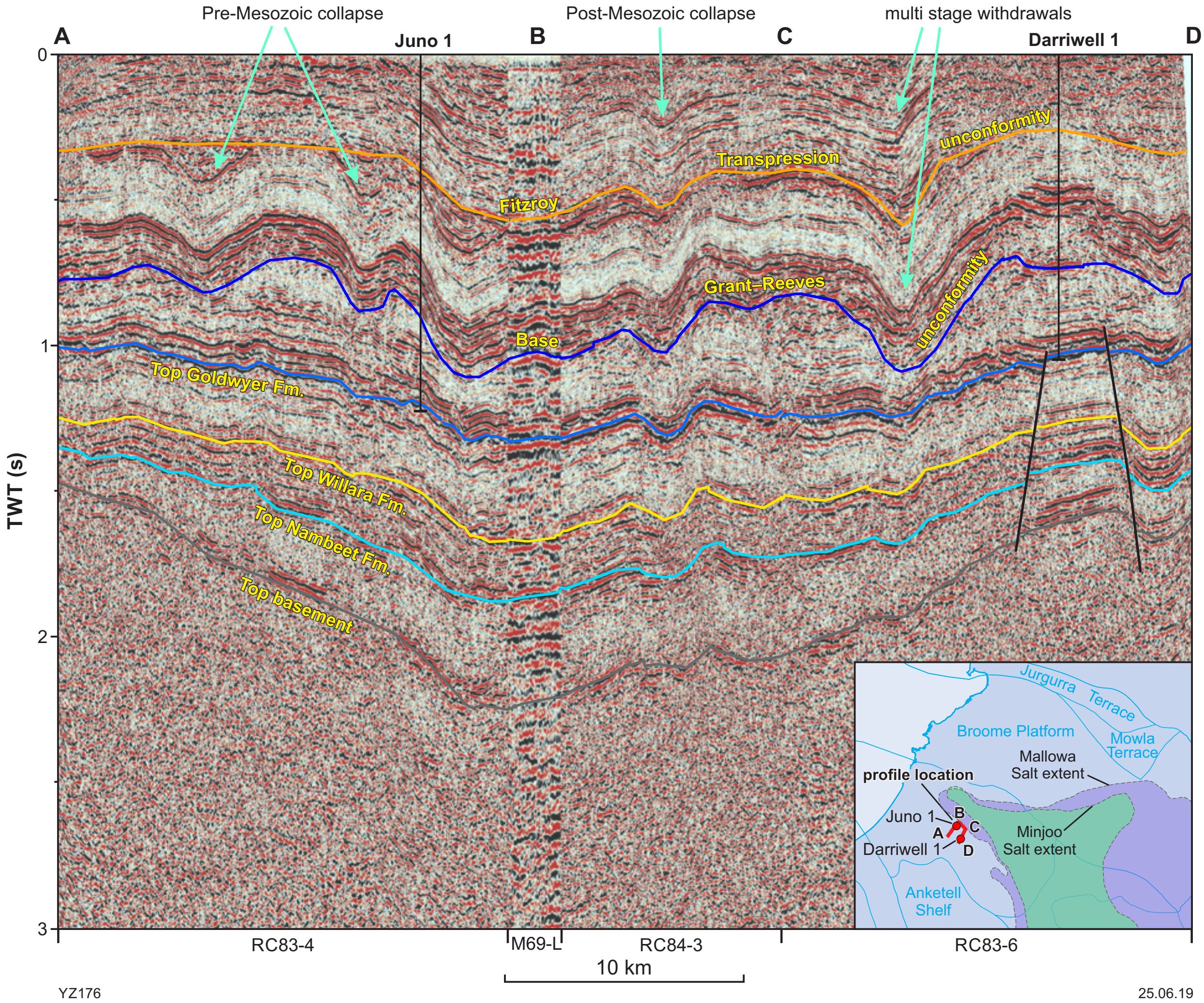

Figure 25. Salt withdrawal and associated structures within the post-salt section beyond the present-day salt margin: 1) the deformed Permian section near Juno 1, overlain by flat-lying Mesozoic, indicates Triassic to Jurassic salt removal after the deposition of the Permian Grant Group; 2) the downwards fold from Mesozoic to Ordovician sections in the centre of the profile suggests possible compressional event; 3) the deformation near Darriwell 1 that is less intense in the Mesozoic section than the Permian implies at least two stages of salt movement in the same area

Canning Basin, and suggested a tectonic event involving right-lateral wrenching movement in an easterly direction during the Mesozoic (Fitzroy Transpression of Kennard et al., 1994). Erosion after the wrenching produced an angular unconformity that is mostly at the base of Jurassic strata (Zhan and Mory, 2013). Although it remains unclear whether the wrenching impacted the southern Canning Basin, a depositional break between the Middle Jurassic and Permian has been identified throughout the drillholes in the southern part of the basin (Mory, 2010), suggesting regional influence of the wrench movement.

Even in the northern Canning Basin, the stratigraphic gap between the topmost eroded sequence of the Lower to Middle Triassic and the first deposited sediment of the Middle Jurassic is too long to indicate a precise age for the Mesozoic wrenching movement. However, data from outside the Canning Basin may help dating of the movement. For example, for the Canning Basin SEEBASE project, Frogtech Geoscience (2017) inferred a Late Triassic to Early Jurassic time span for the event based on similar features in:

1. the Browse Basin, where potentially equivalent movement was from c. 228 to 190 Ma (Struckmeyer et al., 1998)
2. the Petrel Sub-basin, where the syninversion Malita sequence was dated as Late Triassic to Early Jurassic (Colwell and Kennard, 1996)
3. the north of the Woodroffe Thrust (Musgrave Province adjacent to southeastern Canning Basin) where recent (U–Th)/He thermochronology analysis on zircon suggested a c. 215 Ma-aged exhumation event (Quentin de Gromard et al., 2017) that was probably related to, and propagated from the Canning Basin.

Within the study area, the Canning Coastal seismic profile (Zhan, 2017) reveals that the base of the Jurassic strata corresponds to an angular unconformity mostly at ~500 ms (approximately 650 m in depth: Zhan, 2018). The Mesozoic succession above is characterized by a package of parallel flat-lying seismic reflectors that locally truncate the underlying Permian section, such as in the south of the Willara Sub-basin. This unconformity gently shallows up from the centre of the Broome Platform to the northern margin of the platform where it is ~400 ms (equivalent to ~500 m; Map 45).

Based on well penetrations, the Fitzroy Transpression unconformity generally shallows in a southeast direction inland where the Jurassic and younger succession becomes difficult to identify on the reflection data. This is due to the increasing lack of fold coverage upwards at near surface level. As a result of insufficient quality, the interpretation of the Fitzroy Transpression unconformity is largely based on well data across most of the inland area. The maps of the unconformity (Maps 43–46) show no apparent segmentation of this horizon by the ABFZ or other faults. This indicates less tectonic movement subsequent to the formation of the base Grant Group and top horizons of Lower Ordovician and basement. The Fitzroy Transpression unconformity maintains a similar depth (~500 to 600 m) from the Broome Platform to Willara Sub-basin along the coast (Fig. 11). The horizon gradually shallows southeastwards (e.g. 231 m in BHP Brooke 1 and 85 m in Pegasus 1) before the Permian succession outcrops farther inland as indicated on the bedrock geology map (GSWA, 2010; Map 46). It deepens from the near shore (~600 m) to offshore areas (over 1000 m; Fig. 21) along the strike of the Canning Basin tectonic elements.

Discussion and conclusion

The major faults and key stratigraphic horizons in the Broome Platform, Willara Sub-basin and Munro Arch areas have been interpreted and mapped, through the integration of petroleum wells, mineral drillholes, seismic profiles, and surface geological mapping, to enhance the geological understanding of the southern Canning Basin. This study incorporates recently acquired open-file seismic datasets to provide an updated regional understanding of structural features and tectonic evolution of the Willara Sub-basin and surrounds. It presents supporting interpreted regional seismic lines and structural maps ranging from Top basement to the Mesozoic Fitzroy Transpression unconformity.

Most of the northwesterly striking faults, including the ABFZ, displace the Ordovician succession and terminate below the Base Grant–Reeves unconformity. The thickness of the Ordovician succession varies from the hangingwall to footwall with a maximum difference estimated at over 2000 m across the ABFZ. These faults evidently represent the initial phase of subsidence producing a northwest-striking depression. In comparison, other faults oblique to the northwest-striking set, mostly east to east-northeasterly oriented, displace the Ordovician to Permian strata, but terminate below the Fitzroy Transpression unconformity. They do not appear to lead to the thickness variations especially in the Ordovician succession. These easterly oriented faults are interpreted to be much younger than the northwest-striking faults and most likely formed during Permian extension. It should be noted that detailed correlation of faults is hindered by the current spacing of seismic profiles and a denser grid of good-quality data is needed for clear delineation of the faults.

The horizons interpreted in this study can be categorized into three groups: 1) tops of the basement and Ordovician units; 2) tops and bases of the Minjoo and Mallowa Salts; and 3) angular unconformities at the bases of Permian and Jurassic strata. These horizons are selected for interpretation based on petroleum prospectivity, seal significance and geological implications.

Group 1 (Appendix 3, Maps 1–19)

The first group of horizons includes the tops of basement, Nambeet, Willara and Goldwyer Formations, which, apart from Top basement, are conformable. Generally, these horizons deepen northeastwards into the Willara Sub-basin and reach maximum depth just south of the ABFZ. Across this fault zone, the horizons are all significantly displaced with up to three major faults upstepping the horizons towards the northeast (Figs 11–13, 17). Both the amount of throw and the number of the faults diminish towards the southeast and the structure probably changes to a southwest-dipping monocline between the Crossland Platform and Kidson Sub-basin farther to the southeast (e.g. Map 4). Towards the northeast, the horizons slightly deepen inwards from either margins of the Broome Platform such that the middle is a northwest-striking syncline of approximately 100 km wavelength. Farther north these horizons either plunge northeastwards, as indicated on the Canning Coastal seismic profile, or downstep via faults (e.g. Dampier, Collins, Dummer Range Faults) onto the Jurgurra, Mowla and Barbwire Terraces. These areas are not discussed in the current study, although they are planned to be mapped after systematic correlation and interpretation for the north Canning Basin including the Fitzroy Trough.

The seismic interpretation shows that the Lower Ordovician units exhibit stratigraphic thinning trends from the Willara Sub-basin towards the Anketell Shelf – Wallal Platform, as well as basement-onlapping patterns within the Nambeet and Willara Formation along the southern margin of the Broome Platform (Fig. 17). These seismic characteristics indicate that the initial phase of the basin subsidence was followed by gradual expanding of the accommodation space from the Early to Middle Ordovician. This gradual expansion indicates a possible sag configuration for the initial phase of basin development, eventually leading to a rifting phase focused on the ABFZ.

The Lower Ordovician units were progressively eroded by the Base Grant–Reeves unconformity towards the southern margin of the Canning Basin along the Anketell Shelf – Wallal Platform (Fig. 11). Such truncations are also evident along the northern margin of the Broome Platform, where the Ordovician sections from Nita to Willara Formations were increasingly eroded as indicated by the absence of the Goldwyer Formation in Olympic 1. This erosion can be further interpreted between the two margins as shown by the angular contact beneath the base Grant Group. In consideration of the higher thermal maturity of the Ordovician with respect to the overlying Permian section (Ghori, 2013; Zhan, 2017), the erosion indicates that the study area was probably subject to a regional uplift movement following deposition of the Middle Ordovician strata.

Group 2 (Appendix 3, Maps 20–37)

The second group of horizons includes the tops and bases of two Upper Ordovician to lower Silurian salt intervals, the Minjoo and Mallowa Salts. Interpretation of the Minjoo Salt, which is mostly intersected around the southeast part of the study area between the Broome Platform and Willara Sub-basin, bears a high degree of uncertainty due to its thinness and the poor quality of seismic profiles at this level. The presence of the Minjoo Salt between Willara 1 and Vela 1 is assumed to be continuous and mapped along the deeper part of the Willara Sub-basin. It appears to thicken towards the southeast and presumably extends across most of the Munro Arch, based on correlation with wells in the Kidson Sub-basin (Haines, 2009) and the arch itself being a transitional tectonic element, instead of an elevated unit of basement high. In comparison, the well intersections of the Mallowa Salt are much thicker and interpretation from seismic data carries a relatively high level of confidence (e.g. Fig. 22). It is generally characterized on seismic profiles as a relatively flat-lying transparent sheet covering the Lower to Middle Ordovician succession. It is probably present in the relatively deep part of the study area, including the northeastern Willara Sub-basin, southeastern Broome Platform and most of the Munro Arch. Some discontinuous salt pillows may exist as residuals after several stages of dissolution near the present-day salt margins.

The deposition of both salt intervals was probably linked to two factors: sea-level and tectonic changes. A series of well-documented glaciation events during the Late Ordovician – early Silurian possibly led to sea-level drops with consequential subaerial exposure in the southern Canning Basin. The restricted environment with multiple episodes of sea water influx enabled evaporation and precipitation to build up massive salt intervals with thicknesses of up to 313 m for the Minjoo Salt and 800 m for the Mallowa Salt (in Patience 2 and BHP Brooke 1, respectively, based on Haines, 2009; Fig. 24). The change in tectonic regime is interpreted to have occurred after the Middle Ordovician and is expressed by the regional uplift discussed in Group 1 above. The uplift resulted in elevation of the southern Canning Basin, especially along the northern margin of the Broome–Crossland Platforms and the offshore/nearshore part of the study area, and allowed a transition from open marine to restricted evaporite deposition after the deposition of the Middle Ordovician succession.

Large-scale salt diapirs or domes are not observed on the current dataset in the study area. Nevertheless, seismic profiles indicate that multiple episodes of salt dissolution may have occurred to form ‘sombrero’ or ‘turtle’ structures in the overlying strata. These deformational structures indicate that the original salt deposits were beyond the current salt margins, and thus once covered a larger area in the southern Canning Basin (Fig. 25). It is also interpreted that the dissolution might be associated with faults and fractures in both underlying and overlying successions that act as conduits for migrating water into the salt formation (Fig. 26). The collapse after salt dissolution led to small-scale synclines filled with younger strata, and occurred multiple times, of which two episodes (Triassic to Jurassic and Early Cretaceous) are observed on the current seismic dataset. The current interpretation also allows speculation that the brine might migrate to the surface during late stages or in modern times, and part of the brine could be stranded in restricted inland areas and re-precipitated in modern salt lakes, such as Lake Auld and Lake Dora.

It is also noted that the deformational structures related to salt movement mainly occurred around the salt margins, but a greater portion of the salt has remained undeformed in the southern Canning Basin. This lack of deformation is difficult to reconcile with a thick overburden, and the many post-early Silurian tectonic movements that could have triggered salt movement. The Lower to Middle Ordovician sections below the salt intervals are reasonably well imaged on seismic profiles, which is in stark contrast to bottomless reflection for subsalt sections in general due to its extreme difference in impedance from clastic or carbonate rocks. The exceptions in both salt deformation and processing difficulties are interpreted to relate to the salt cyclicities, as noted by Cathro et al. (1992) and Haines (2009), which can potentially reduce the salt ductility and normalize its impedance to the level of the enclosing formations. As salt intervals provide an effective seal for petroleum reservoirs, the lack of salt movement increases the likelihood that any subsalt structural or stratigraphic traps remain unbreached.

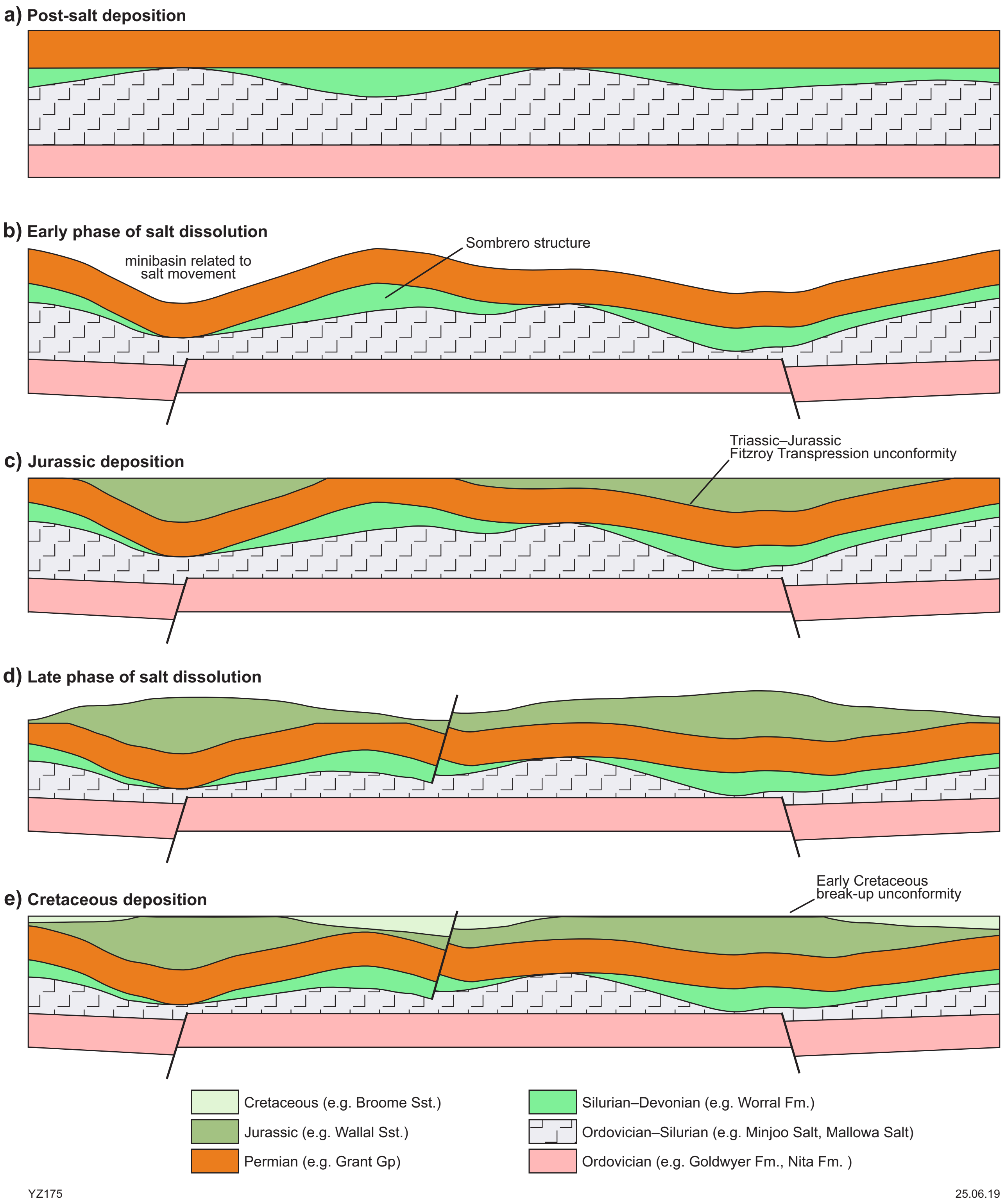

Figure 26. **Schematic diagram illustrating salt dissolution in the southern Canning Basin (modified from Jenyon,1986; Romine et al., 1994; SRK Consulting Pty Ltd, 1998). The minibasins could be generated at different times and filled with different stratigraphic units than indicated, depending on when the salt was dissolved**

Figure 27. Modern salt lakes in the southern Canning Basin

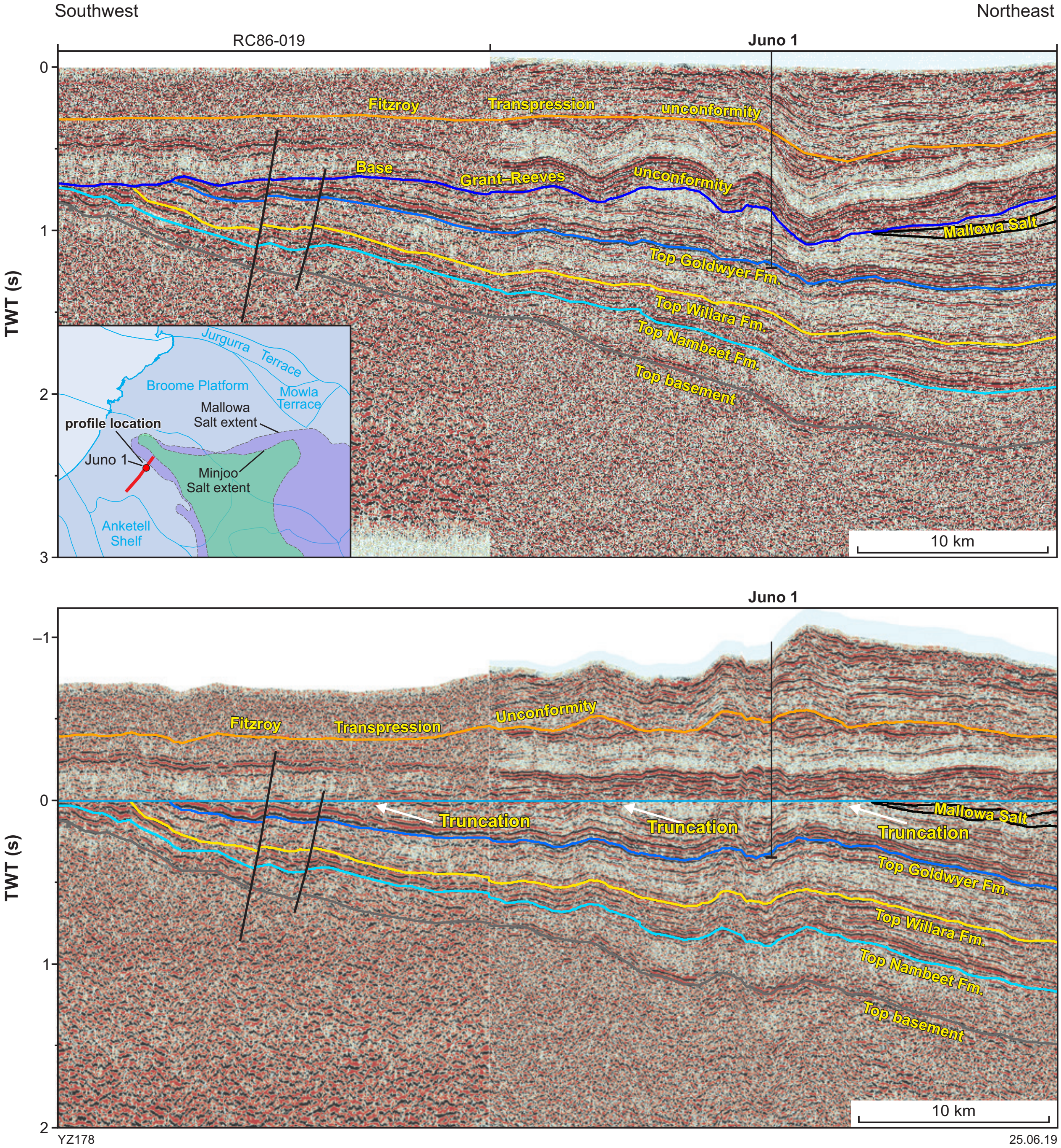

Figure 28. **Seismic interpretation in the area affected by salt movements: a) normal TWT profile; b) profile flattened to the Base Grant–Reeves unconformity**

Such traps could be charged with hydrocarbons sourced from prospective Ordovician strata, such as the Bongabinni (Haines, 2009), Goldwyer (Edwards et al, 1997; Haines, 2009; Ghori, 2013) and Nambeet Formations (Normore and Dent, 2017), in the southern Canning Basin.

Group 3 (Appendix 3, Maps 38–46)

The third group of horizons comprises two major angular unconformities: base of the Grant–Reeves and base of Jurassic strata. The lower discontinuity indicates a regional-scale tectonic movement across the Canning Basin and can be interpreted with a relatively high level of confidence, except in the area where salt dissolution has highly distorted the truncated reflectors below the unconformity. The horizon only subtly follows the structural trend of the basement, relatively deep in the Willara Sub-basin and shallow over the Broome Platform, and is much less faulted than Top basement. The unconformity generally shallows towards the southeast along the strike of these tectonic units. The depth of the Base Grant–Reeves unconformity varies gently across the northern margin of the Broome Platform, either slightly ramping up or dipping towards the northeast, as opposed to the more pronounced deepening trend of the Group 1 horizons.

The upper unconformity (Fitzroy Transpression unconformity) at the base of the Jurassic section is related to a wrenching movement which generated a series of en echelon, easterly trending anticlines and synclines, as well as numerous northerly trending faults during the Mesozoic in the northern Canning Basin (e.g. Rattigan, 1967; Zhan and Mory, 2013). Subsequent erosion produced a basinwide angular unconformity extending to the southern Canning Basin. The unconformity is interpreted at the bottom of parallel seismic reflectors, typically at ~500 ms in the coastal area. This horizon does not reflect the basin subdivisions as it undergoes limited depth variation across the boundaries. The Fitzroy Transpression unconformity generally shallows in a southeast direction towards the inland where the Jurassic and younger successions become difficult to identify on the reflection data, and the horizon is largely interpolated from well intersections across most of the inland area. Both unconformities deepen towards the offshore Roebuck Basin, with the lower cutting down to Top basement northwestwards and along strike from the Willara Sub-basin and Broome Platform. Overall, both unconformities are more flat lying and are less affected by faults when compared to Group 1 horizons. It can be inferred from the lateral extent and thickness trends of the overlying packages that the depocentre shifted from the current inland to offshore from the Paleozoic to Mesozoic. The depositional axis might have rotated multiple times, noticeably northwesterly oriented in Ordovician, westerly in the Permian and northeasterly in the Mesozoic.

Acknowledgement

The author acknowledges the constructive comments and suggestions from Darryl Kingsley, Peter Edwards, Lynn Pryer and Julian Mather.

References

Apak, SN and Backhouse, J 1998, Re-interpretation of the Permo–Carboniferous succession, Canning Basin, Western Australia, *in* The Sedimentary Basins of Western Australia 2 *edited by* PG Purcell and RR Purcell: The Petroleum Exploration Society of Australia Symposium, Perth, Western Australia, p. 683–694.

BHP-Utah Minerals International Asia Pacific Division 1988, CR6294 Annual report Gingerah Hill, Western Australia; BHP Minerals Limited, Exploration Department: Geological Survey of Western Australia, Statutory mineral exploration report, A27334.

Buru Energy 2011a, 2011 Athos 2D seismic survey – operations report; Buru Energy: Geological Survey of Western Australia, Statutory petroleum exploration report, S10755A2, 14p.

Buru Energy 2011b, 2011 Commodore East 2D seismic survey – operations report; Buru Energy: Geological Survey of Western Australia, Statutory petroleum exploration report, S10757A2, 14p.

Cathro, DL, Warren, JK and Williams, GE 1992, Halite saltern in the Canning Basin, Western Australia, a sedimentological analysis of drill core from the Ordovician–Silurian Mallowa Salt: Sedimentology, v. 39, p. 983–1002.

Colwell, JB and Kennard, JM 1996, Petrel Sub-basin study, 1995–1996: Australian Geological Survey Organisation, Record 1996/40, 122p.

Command Petroleum N.L. 1989, EP164 Leo 1 Final well report; Command Petroleum N.L.: Geological Survey of Western Australia, Statutory petroleum exploration report, W3368A2, 275p.

Copp, IA 1994, Depth to base Phanerozoic map of Western Australia: Explanatory Notes: Geological Survey of Western Australia, Record 1994/9, 14p.

Crowe, RWA and Towner, RR 1976, Definitions of some new and revised rock units in the Canning Basin: Geological Survey of Western Australia, Record 1976/24, 22p.

Davies, B and Dorsch, C 1988, Final well report Anna Plains 1, Canning Basin, Western Australia; Sydney Oil Company (Canning) Pty, Ltd for EP 142 (S) Joint Venture: Geological Survey of Western Australia, Statutory petroleum exploration report, W3233 A2, 173p.

Dayboro Geophysical 2010, Final report 2010 2D Seismic Data Reprocessing EP465 Western Australia; Global International (Australia) Pty Ltd: Geological Survey of Western Australia, Statutory petroleum exploration report, P6465A1.

Dennison, RG 1964, Canning Basin Preliminary seismic report on the Parda Basin reconnaissance seismic survey project 133; West Australian Petroleum Pty Limited: Geological Survey of Western Australia, Statutory petroleum exploration report, S166A1V1.

DownUnder Geosolutions 2013, 2D land seismic reprocessing report: Geological Survey of Western Australia, Statutory petroleum exploration report, P6443A7, 52p.

DownUnder Geosolutions 2015, 2D land seismic data processing, Canning Basin — processing report: Geological Survey of Western Australia, Statutory petroleum exploration report, S10808 A2, 32p.

Edwards, DS, Summons, RE, Kennard, JM, Nicoll, RS, Bradshaw, J, Bradshaw, M, Foster, CB, O'Brien, GW and Zumberge, JE 1997, Geochemical characteristics of Palaeozoic petroleum systems in northwestern Australia: APPEA Journal, v. 37, p. 351–377.

Elliott, RML 1961, New and amended formation names (Appendix 7), *in* Thangoo No. 1 and No. 1A wells, Western Australia *compiled by* V Pudovskis and SP Willmott: Bureau of Mineral Resources, Geology and Geophysics, Canberra, Petroleum Search Subsidy Acts Publication No. 14, p. 37–43.

Exploration Logging Australia Ltd 1988, Final Well Report, Pegasus No. 1, Onshore Canning Basin, Western Australia; Amoco Australia Petroleum: Geological Survey of Western Australia, Statutory petroleum exploration report, W3338A2V1, 199p.

Farrelly, JJ 1988, Pegasus No. 1 geological well report; A: Geological Survey of Western Australia, Statutory petroleum exploration report, S3338A3, 309p.

Finder Exploration 2016, Theia-1 well completion report, Volume 2 – derivative data; Finder Shale Pty Ltd: Geological Survey of Western Australia, Statutory petroleum exploration report, W20663A2, 40p.

Flavelle, AJ 1974, Canning Basin gravity surveys, 1953–1962: Bureau of Mineral Resources, Geology and Geophysics, Record 1974/181, 74p.

Flavelle, AJ and Goodspeed, MJ 1962, Fitzroy and Canning Basins reconnaissance gravity surveys, Western Australia 1952–60 (Record 1962/105 edition): Bureau of Mineral Resources, Geology and Geophysics, 46p.

Forman, DJ and Wales, DW 1981, Geological evolution of the Canning Basin, Western Australia: Bureau of Mineral Resources, Geology and Geophysics, Bulletin 210, 91p.

Foster, CB, O'Brien, GW and Watson, ST 1986, Hydrocarbon source potential of the Goldwyer Formation, Barbwire Terrace, Canning Basin, Western Australia: APEA Journal, v. 26, p. 142–155.

Foster, CB and Williams, GE 1991, Late Ordovician – Early Silurian age for the Mallowa Salt of the Carribuddy Group, Canning Basin, Western Australia, based on occurrences of *Tetrahedraletes medinensis* Strother and Traverse 1979: Australian Journal of Earth Sciences, v. 38, p. 223–228.

Frakes, LA, Francis, JE and Syktus, JI 1992, Climate modes of the Phanerozoic: The history of the Earth's climate over the past 600 million years: Cambridge University Press, Glasgow, UK, 274p.

Franks, PC 1989, Petrography, X-ray diffraction analysis and diagenesis of 10 sidewall cores, Nambeet, Willara, Nita and Carribuddy Formations, Pegasus No. 1 Well, Canning Basin, Australia; Amoco Production Company: Geological Survey of Western Australia, Statutory petroleum exploration report, W3338A3.

Frogtech Geoscience 2017, Canning Basin SEEBASE study and GIS data package: Geological Survey of Western Australia, Report 182, 297p.

Geary, GC 1988, Calamia 1 well completion report, EP 231, Western Australia; Oil Company of Australia NL: Geological Survey of Western Australia, Statutory petroleum exploration report, W3245 A2, 240p.

Geary, GC and Robbie, SM 1989, Darriwell 1 well completion report, EP 231, Western Australia; Oil Company of Australia NL: Geological Survey of Western Australia, Statutory petroleum exploration report, W3337 A2 V1, 247p (open).

Geological Survey of Western Australia 2010, Atlas mosaic of 1:250 000 geological series map images, Western Australia, June 2010 update: Geological Survey of Western Australia, digital data layer.

Geological Survey of Western Australia 2017, 1:500 000 tectonic units of Western Australia, 2017: Geological Survey of Western Australia, <www.dmp.wa.gov.au/ebookshop>.

Ghori, KAR 2013, Petroleum geochemistry and petroleum systems modelling of the Canning Basin, Western Australia: Geological Survey of Western Australia, Report 124, 33p.

Gilbert-Tomlinson, J 1961, Preliminary report on Lower Palaeozoic fossils of Samphire Marsh No. 1, *in* Samphire Marsh No. 1 Well, Western Australia *compiled by* MH Johnstone: Bureau of Mineral Resources, Geology and Geophysics, Canberra, Petroleum Search Subsidy Acts Publication No. 5, p. 29–36.

Guppy, DJ, Lindner, AW, Rattigan, JH and Casey, JN 1952, The stratigraphy of the Mesozoic and Permian sediments of the Desert Basin, Western Australia, *in* XIX International geological congress (Gondwana Symposium): Alger, p. 107–114.

Haines, PW 2004, Depositional facies and regional correlations of the Ordovician Goldwyer and Nita Formations, Canning Basin, Western Australia, with implications for petroleum exploration: Geological Survey of Western Australia, Record 2004/7, 45p.

Haines, PW 2009, The Carribuddy Group and Worral Formation, Canning Basin, Western Australia: stratigraphy, sedimentology, and petroleum potential: Geological Survey of Western Australia, Report 105, 60p.

Haines, PW, Wingate, MTD and Kirkland, CL 2013, Detrital zircon U–Pb ages from the Paleozoic of the Canning and Officer Basins, Western Australia: implications for provenance and interbasin connections, *in* The Sedimentary Basins of Western Australia IV *edited by* M Keep and SJ Moss: Petroleum Exploration Society of Australia; West Australian Basins Symposium, Perth, 18 August 2013, 19p.

Haines, PW, Wingate, MTD, Zhan, Y and Maidment, DW 2018, Looking beneath the Canning Basin: new insights from geochronology, seismic and potential-field data, *in* GSWA 2018 extended abstracts: promoting the prospectivity of Western Australia: Geological Survey of Western Australia; Record 2018/2, p. 30–33.

Hocking, RM 1994a, Basin subdivisions of Western Australia, *in* Subdivisions of Western Australian Neoproterozoic and Phanerozoic sedimetary basins: Geological Survey of Western Australia, Record 1994/4, Plate 1.

Hocking, RM 1994b, Subdivisions of Western Australian Neoproterozoic and Phanerozoic sedimentary basins: Geological Survey of Western Australia, Record 1994/4, 85p.

Hudec, MR and Jackson, MPA 2007, Terra infirma: understanding salt tectonics: Earth Science Reviews, v. 82, p. 1–28.

Iasky, RP, Middleton, MF and Taylor, DD (compilers) 1991, Canning Basin — top Ordovician: Geological Survey of Western Australia, 1:1 000 000 seismic subsurface time structure map.

Jackson, MPA 1995, Retrospective salt tectonics, *in* Salt Tectonics: a Global Perspective *edited by* MPA Jackson, DG Roberts and S Snelson: AAPG Memoir vol. 65, p. 1–28.

Jackson, MPA 1997, Conceptual breakthroughs in salt tectonics: A historical review, 1856–1993; Report of Investigations, 246: The University of Texas at Austin, Bureau of Economic Geology, 51p.

Jackson, MPA and Hudec, MR 2017, Salt tectonics: principles and practice: Cambridge, Cambridge University Press, 514p.

Jenyon, MK 1986, Salt tectonics: Elsevier Applied Science Publishers, New York, USA, 191p.

Johnson, NEA 1966a, Kidson No. 1 well completion report; West Australian Petroleum Pty Ltd: Geological Survey of Western Australia, Statutory petroleum exploration report, W244 A1 (unpublished).

Johnson, NEA 1966b, Willara No. 1 well completion report; West Australian Petroleum Pty Limited: Geological Survey of Western Australia, Statutory petroleum exploration report, W214 A1 (unpublished).

Johnstone, MH 1961, Samphire Marsh 1 well completion report, *in* Samphire Marsh No. 1 well, Western Australia, of West Australian Petroleum Pty Limited: Bureau of Mineral Resources, Petroleum Search Subsidy Acts Publication 5, p. 1–9.

Johnstone, MH 1966, Samphire Marsh 1: Geological completion report; West Australian Petroleum Pty Limited: Geological Survey of Western Australia, Statutory petroleum exploration report, W 101 A1, 33p.

Kennard, JM, Jackson, MJ, Romine, KK, Shaw, RD and Southgate, PN 1994, Depositional sequences and associated petroleum systems of the Canning Basin, WA, *in* The Sedimentary Basins of Western Australia *edited by* PG Purcell and RR Purcell: Petroleum Exploration Society of Australia, West Australian Basins Symposium, Perth, p. 657–676.

Kingsley, DR and Russell, TG 1989, A geohistory study of EP164 southwest Canning Basin Western Australia, Geological Survey of Western Australia, Statutory petroleum exploration report, S6164 R1 A12, 266p.

Koop, WJ 1966a, Appendix 1, Sahara No. 1 well, stratigraphic nomenclature, *in* Summary of data and results, Canning Basin, Western Australia, Sahara No. 1 well of West Australian Petroleum Pty Limited: Bureau of Mineral Resources, Canberra, ACT, Petroleum Search Subsidies Act, Publication 80, p. 1–19.

Koop, WJ 1966b, Regional stratigraphy of the South Canning Basin; West Australian Petroleum Pty Limited: Geological Survey of Western Australia, Statutory petroleum exploration report, G105 A1, 12p.

Lehmann, PR 1984, The stratigraphy, palaeogeography and petroleum potential of the Lower to lower Upper Devonian sequence in the Canning Basin, *in* The Canning Basin, WA *edited by* PG Purcell: Geological Society of Australia and Petroleum Exploration Society of Australia; Canning Basin Symposium, Perth, Western Australia, 27 June 1984, p. 253–275.

Lugli, S 2009, Evaporites, in Encyclopedia of Paleoclimatology and Ancient Environments *edited by* V Gornitz: Springer, Dordrecht, The Netherlands, p. 321–324.

McTavish, RA and Legg, DP 1972, Middle Ordovician correlation: conodont and graptolite evidence from Western Australia: Neues Jahrb. Geologie und Palaontologie Monatshefte, v. V8, p. 465–474.

McTavish, RA and Legg, DP 1976, The Ordovician of the Canning Basin, Western Australia, *in* The Ordovician System *edited by* MG Bassett: University of Wales Press and National Museum of Wales; Palaeontological Association symposium, Birmingham, UK, September 1974; Proceedings, p. 447–478.

Mernagh, TP 2013, A Review of Australian Salt Lakes and Assessment of their Potential for Strategic Resources: Geoscience Australia, Record 2013/39.

Mory, AJ 2010, A review of mid-Carboniferous to Triassic stratigraphy, Canning Basin, Western Australia: Geological Survey of Western Australia, Report 107, 130p.

Mory, AJ and Haines, PW 2013, A Paleozoic perspective of Western Australia, *in* The Sedimentary Basins of Western Australia IV *edited by* M Keep and SJ Moss: Petroleum Exploration Society of Australia; West Australian Basins Symposium, Perth, 18 August 2013, 25p.

Moyes, CP 1972, Munda No. 1 well completion report; West Australian Petroleum Pty Limited: Geological Survey of Western Australia, Statutory petroleum exploration report, W655 A2, 17p.

Munnecke, A, Calner, M, Haper, DAT and Servais, T 2010, Ordovician and Silurian sea-water chemistry, sea level, and climate: a synopsis: Palaeogeography, Palaeoclimatology, Palaeoecology, v. 296, no. 3–4, p. 389–413.

Nicoll, RS 1993, Ordovician conodont distribution in selected petroleum exploration wells, Canning Basin, Western Australia: Australian Geological Survey Organisation, Record 1993/17, 136p.

Normore, LS and Dent, LM 2017, Petroleum source potential of the Ordovician Nambeet Formation, Caning Basin: evidence from petroleum well Olympic 1: Geological Survey of Western Australia, Report 169, 20p.

Normore, LS, Dent, LM and Symonds, AK 2018, Theia 1, Canning Basin: Geological Survey of Western Australia, Digital Core Atlas Series.

Page, A, Zalasiewicz, J, Williams, M and Popov, L 2007, Were transgressive black shales a negative feedback modulating glacioeustasy in the Early Palaeozoic Icehouse?, *in* Deep-Time Perspectives on Climate Change: Marrying the Signal from Computer Models and Biological Proxies *edited by* M Williams, AM Haywood, FJ Gregory, and DN Schmidt: The Geological Society of London; Special Publication, p. 123–156.

Playford, PE, Cope, RN, Cockbain, AE, Low, GH and Lowry, DC 1975, Chapter 2. Phanerozoic, *in* The geology of Western Australia: Geological Survey of Western Australia, Memoir 2, p. 223–432.

Pudovskis, V 1960, Thangoo No.1A Geological Completion Report; West Australian Petroleum Pty Limited: Geological Survey of Western Australia, Statutory petroleum exploration report, W94A1, 34p.

Quentin de Gromard, R, Howard, HM, Kirkland, CL, Smithies, RH, Wingate, MTD and Jourdan, F 2017, Post-Giles Event evolution of the Musgrave Province constrained by (multi-method) thermochronology, *in* GSWA 2017 Extended abstracts: promoting the prospectivity of Western Australia: Geological Survey of Western Australia, Record 2017/2, p. 42–47.

Quilty, JH 1960, Canning Basin aeromagnetic reconnaissance survey, WA 1954: Bureau of Mineral Resources, Geology and Geophysics, Records 1960/11, 21p.

Rattigan, JH 1967, Fold and fracture patterns resulting from basement wrenching in the Fitzroy Depression, Western Australia, *in* Proceedings of the Australasian Institute of Mining and Metallurgy: v. 223, p. 17–22.

Rea, D 2014, Commodore West 2D seismic survey EP 471 and EP390R1 – operations report; Buru Energy: Geological Survey of Western Australia, Statutory petroleum exploration report, S10801A3, 231p.

Redfern, J 1991, Subsurface facies analysis of Permian-Carboniferous glaciogenic sediments, Canning Basin, *in* Gondwana 7 Proceedings *edited by* H Ulbrich and A Rocha-Campos: University of Sao Paulo, p. 349–363.

Romine, KK, Southgate, PN, Kennard, JM and Jackson, MJ 1994, The Ordovician to Silurian phase of the Canning Basin WA, *in* The Sedimentary Basins of Western Australia *edited by* PG Purcell and RR Purcell: Petroleum Exploration Society of Australia, Western Australian Branch; West Australian Basins Symposium, Perth, 1994, p. 677–696.

Royal Resources Exploration, Inc 1985a, Juno 1 final well report: Geological Survey of Western Australia, Statutory petroleum exploration report, W 2872 A3, 41p (open).

Royal Resources Exploration, Inc 1985b, Woods Hills 1 final well report: Geological Survey of Western Australia, Statutory petroleum exploration report, W2710 A2, 106p (open).

Rudge, T 2011, Commodore East 2011 seismic survey interpretation report 390 R2; Buru Energy Limited: Geological Survey of Western Australia, Statutory petroleum exploration report, S10757A4, 30p.

Schroder, RJ, Miller, A and Shakespeare, D 1986, 1984 Anna Plains seismic survey interpretation report EP 142(S), Canning Basin; Sydney Oil Company: Geological Survey of Western Australia, Statutory petroleum exploration report, S2696A3, 36p.

Sheehan, PM 2001, The Late Ordovician mass extinction: Annual Review of Earth and Planetary Sciences, v. 29, p. 331–364.

Smith, JG 1968, Tectonics of the Fitzroy wrench trough, Western Australia: American Journal of Science, v. 266, p. 766–776.

Smith, TE, Edwards, DS, Kelman, AP, Laurie, JR, le Poidevin, S, Nicoll, RS, Mory, AJ, Haines, PW and Hocking, RM (compilers) 2013, Canning Basin biozonation and stratigraphy - Chart 31: Geoscience Australia, <https://d28rz98at9flks.cloudfront.net/65648/Canning_Basin.pdf>.

SRK Consulting Pty Ltd 1998, Canning Basin Project, 1998, Report prepared for Shell Development Australia: Geological Survey of Western Australia, Statutory petroleum exploration report, S10372 (unpublished).

Struckmeyer, HIM, Blevin, JE, Sayers, J, Totterdell, JM, Baxter, K and Cathro, DL 1998, Structural evolution of the Browse Basin, North West Shelf; new concepts from deep seismic data, *in* The Sedimentary basins of Western Australia *edited by* PG Purcell and RR Purcell: Petroleum Exploration Society of Australia, p. 345–367.

Taylor, DD, Middleton, MF and Luck, GR (compilers) 1991, Onshore Canning Basin — base Grant Group: Geological Survey of Western Australia, 1:1 000 000 seismic subsurface time structure map.

Thomas, P 2000, Seismic interpretation report Survey S98C Permit EP353, Canning Basin (1998 Great Sandy 2D Seismic Survey); Shell Development (Australia) Pty Ltd: Geological Survey of Western Australia, Statutory petroleum exploration report, S10372, 128p.

Towner, RR and Gibson, DL 1983, Geology of the onshore Canning Basin, Western Australia: Bureau of Mineral Resources, Geology and Geophysics, Bulletin 215, 51p.

Veevers, JJ and Wells, AT 1961, The geology of the Canning Basin: Bureau of Mineral Resources, Geology and Geophysics, Bulletin 60, 323p.

Wells, AT 1960, Explanatory notes Mount Bannerman 4-mile sheet: Australia Bureau of Mineral Resources: Geological Survey of Western Australia.

Whiteway, T 2009, Australian Bathymetry and Topography Grid, June 2009: Geoscience Australia, viewed 2 October 2016, <www.ga.gov.au/metadata-gateway/metadata/record/gcat_67703>.

Williams, CT 1965, Parda No. 1 well completion report; West Australian Petroleum Pty Limited: Geological Survey of Western Australia, Statutory petroleum exploration report, W198A1, 48p.

Williams, VA and Harvey, RH 1989, Report on the Admiral Bay project ELs 04/265-268, 04/302-303,04/311-317, 04/319-323, 04/504-516, 45/601-603, 45/639-644, Canning Basin, WA; CRA Exploration Pty, Limited: Geological Survey of Western Australia, Statutory mineral exploration report, A28951, 98p.

Williams, GE, 1991, Milankovitch-band cyclicity in bedded halite deposits contemporaneous with Late Ordovician–Early Silurian glaciation, Canning Basin, Western Australia: Earth and Planetary Science Letters, 103 (1991), p143-155

Woolnough, WG 1933, Report on aerial survey operations in Australia during 1932: Australia Commonwealth Parliamentary Paper 2164, 83p.

Zhan, Y 2017, Canning Coastal seismic survey — an overview of the Canning Basin: Geological Survey of Western Australia, Record 2017/5, 29p.

Zhan, Y 2018, A seismic interpretation of the southwestern Canning Basin, Western Australia: Geological Survey of Western Australia, Report 178, 34p.

Zhan, Y and Mory, AJ 2013, Structural interpretation of the northern Canning Basin, Western Australia, *in* The Sedimentary Basins of Western Australia IV *edited by* M Keep and SJ Moss: Petroleum Exploration Society of Australia; West Australian Basins Symposium, Perth, 18 August 2013, 18p.

APPENDICES

The Appendices are available on the accompanying zip file

1. Summary of key horizons for petroleum wells and mineral drillholes

2. Available seismic surveys in the Broome Platform, Willara Sub-basin and Munro Arch area

3. Maps from seismic interpretation

1. TWT to Top basement
2. Average velocity to Top basement
3. Depth below MSL to Top basement
4. Depth below surface to Top basement
5. TWT to top Nambeet Formation
6. Average velocity to top Nambeet Formation
7. Depth below MSL to top Nambeet Formation
8. Depth below surface to top Nambeet Formation
9. Isopach map of Nambeet Formation
10. TWT to top Willara Formation
11. Average velocity to top Willara Formation
12. Depth below MSL to top Willara Formation
13. Depth below surface to top Willara Formation
14. Isopach map of Willara Formation
15. TWT to top Goldwyer Formation
16. Average velocity to top Goldwyer Formation
17. Depth below MSL to top Goldwyer Formation
18. Depth below surface to top Goldwyer Formation
19. Isopach map of Goldwyer Formation
20. TWT to top Minjoo Salt
21. Average velocity to top Minjoo Salt
22. Depth below MSL to top Minjoo Salt
23. Depth below surface to top Minjoo Salt
24. TWT to base Minjoo Salt
25. Average velocity to base Minjoo Salt
26. Depth below MSL to base Minjoo Salt
27. Depth below surface to base Minjoo Salt
28. Isopach map of Minjoo Salt
29. TWT to top Mallowa Salt
30. Average velocity to top Mallowa Salt
31. Depth below MSL to top Mallowa Salt
32. Depth below surface to top Mallowa Salt
33. TWT to base Mallowa Salt
34. Average velocity to base Mallowa Salt
35. Depth below MSL to base Mallowa Salt
36. Depth below surface to base Mallowa Salt
37. Isopach map of Mallowa Salt
38. TWT to Base Grant–Reeves unconformity
39. Average velocity to Base Grant–Reeves unconformity
40. Depth below MSL to Base Grant–Reeves unconformity
41. Depth below surface to Base Grant–Reeves unconformity
42. Isopach map of Grant Group
43. TWT to Fitzroy Transpression unconformity
44. Average velocity to Fitzroy Transpression unconformity
45. Depth below MSL to Fitzroy Transpression unconformity
46. Depth below surface to Fitzroy Transpression unconformity

Based on integration of petroleum wells, mineral drillholes, seismic profiles, and surface geological mapping, this study aims to delineate the regional structural elements and map the key stratigraphic horizons, including Top basement, tops of key Lower Ordovician formations, tops and bases of two salt intervals (Mallowa and Minjoo Salts), and two pronounced unconformities (Base Grant–Reeves Formation and the Fitzroy Transpression unconformities). The depth of these horizons and the thicknesses of the key formations contribute to an intuitive understanding of the structural framework and petroleum prospectivity within the Broome Platform, Willara Sub-basin and Munro Arch.

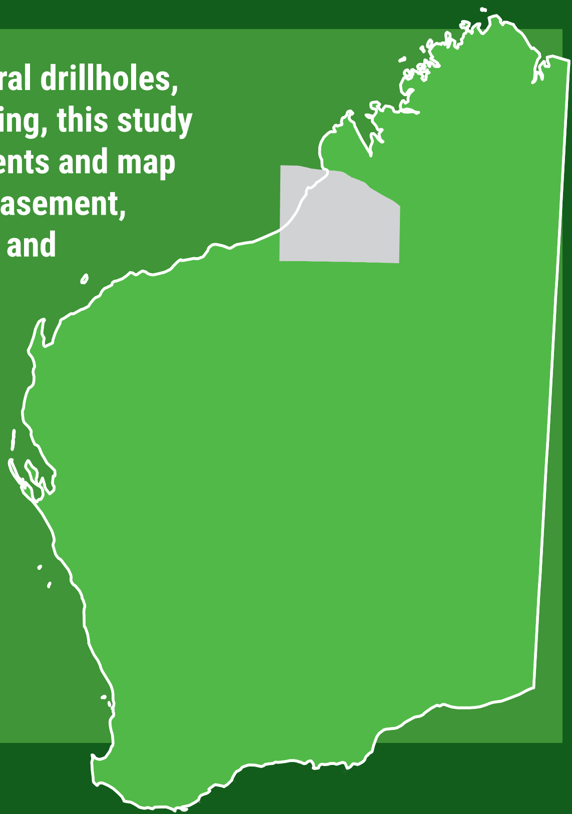

ZHAN

A SEISMIC INTERPRETATION OF THE BROOME PLATFORM, WILLARA SUB-BASIN AND MUNRO ARCH OF THE CANNING BASIN, WESTERN AUSTRALIA

REPORT 193

Further details of geoscience products are available from:

Information Centre
Department of Mines, Industry Regulation and Safety
100 Plain Street
EAST PERTH WA 6004
Phone: (08) 9222 3459   Fax: (08) 9222 3444

www.dmp.wa.gov.au/GSWApublications